WASHINGTON STATE HIGHWAY DEPARTMENT RESEARCH PROGRAM REPORT **17.1**

PAVEMENT RESPONSE AND EQUIVALENCIES FOR VARIOUS TRUCK AXLE-TIRE CONFIGURATIONS

RESEARCH PROJECT

Y-1441

NOVEMBER 1974

PREPARED FOR
WASHINGTON STATE HIGHWAY COMMISSION
IN COOPERATION WITH
U.S. DEPARTMENT OF TRANSPORTATION
FEDERAL HIGHWAY ADMINISTRATION

RONALD L. TERREL
SVENG RIMSRITONG

DEPARTMENT OF CIVIL ENGINEERING
UNIVERSITY OF WASHINGTON

TECHNICAL REPORT STANDARD TITLE PAGE

1. Report No.	2. Government Accession No.	3. Recipient's Catalog No.

4. Title and Subtitle	5. Report Date
Pavement Response and Equivalencies For Various Truck Axle-Tire Configurations	November, 1974
	6. Performing Organization Code
7. Author(s)	8. Performing Organization Report No.
Ronald L. Terrel/S. Rimsritong	---
9. Performing Organization Name and Address	10. Work Unit No.
Department of Civil Engineering University of Washington Seattle, Washington	11. Contract or Grant No. Y-1441
	13. Type of Report and Period Covered
12. Sponsoring Agency Name and Address	
Washington Department of Highways Olympia, Washington	14. Sponsoring Agency Code

15. Supplementary Notes

Study was conducted in cooperation with the Federal Highway Administration.

16. Abstract

There are indications that many trucks now have front axle loads approaching the maximum allowable for single axles which increases the potential for pavement damage.

This report is intended to be a State-Of-The-Art approach to answer several pertinent questions from a theoretical study based on hypothetical pavements and loads, but based on reasonable material characteristics and pavement behavior from previous research. The results are a series of relationships based on pavement life which can be used to determine any number of "equivalencies." These equivalencies can be used to compare the destructive effects of various sizes of single and dual tires, axle loads, pavement thicknesses, speed and temperatures.

The general nature of this report provides a wide range of conditions for comparison on a relative basis.

17. Key Words	18. Distribution Statement
asphalt pavement, equivalencies, wheel load, tire contact pressure, speed and temperature.	

19. Security Classif. (of this report)	20. Security Classif. (of this page)	21. No. of Pages	22. Price
unclassified	unclassified	52	

Form DOT F 1700.7 (8-69)
HWY FORM 341-004 6/72

TABLE OF CONTENTS

TABLE OF CONTENTS (continued)

CHAPTER I

INTRODUCTION AND OBJECTIVES

Increased traffic, together with changes in allowable operating procedures for trucks, have created the potential for rapid deterioration of the highway system. Moreover, new truck and tire designs are resulting in increasing loads on single-tired axles. These factors may have accelerated wear-out of pavements. Thus a need exists for determining the relative destructive effect of these factors.

Most of the past studies and literature deal only with relationships between dual tired single axle and dual tired tandem axles. Therefore, this study is to examine relative destructive effect of the single tire versus dual tires and especially between wide single tire (super single, floatation) and conventional dual tires. There are indications that many trucks now have front axle loads approaching the maximum allowable (18,000 lbs. in Washington) for single axles. The fact that these are on single tires increases the potential for pavement damage.

Confirmation of increased damage can ultimately come only from observation of pavement performance under known traffic conditions. Alternatively, one could construct test pavements with a range of variables and using suitable instrumentation, could measure relative behavior under varying truck loading. This approach probably has a reasonable chance of success for determining actual stress-strain values which can then be used to calculate relative destructive potential. These relative values can then be translated into an "equivalency" value or rating for each situation. Before one embarks on such a comprehensive and expensive study, however, much can be learned from a theoretical study based on hypothetical pavements and loads, but based on reasonable material characteristics and pavement behavior from previous research.

This report is intended to be a "state-of-the-art" approach to answer several pertinent questions using current technology. The results are a series of relationships based on pavement life. One can then use them to determine any number of "equivalencies" of relating variables based on a certain set of conditions.

Basic variables considered in this study include:

1. Wheel load,
2. Tire contact pressure and width,
3. Thickness and nature of pavement layers, and
4. Speed of vehicle,
5. Pavement temperature.

A three-layer pavement structure with an asphalt concrete surface, AC, untreated aggregate base, UTB, and natural soil subgrade were selected for this study. Multilayered elastic theory is used to compute structural behavior.

The deflections, stresses, and strains are computed by using the Chevron n-layer computer program. The location of critical values in the pavement structure under single wheel loading is shown in Figure 1. The horizontal tensile strain at the bottom of the asphalt treated layer, ε_h and the vertical compressive strain at the top of the subgrade, ε_v are examined in determining the maximum number of load applications to failure. Under dual wheel loading, the location in the pavement structure where these critical strains are maximum is shown in Figure 2. Two conditions are checked under various wheel loads. The maximum strains, especially in the thin pavement layers, can occur directly under one of the dual wheels rather than midway between them.

The maximum number of load applications, N, are determined from the criteria developed from laboratory fatigue tests on asphalt to minimize pavement cracking from repeated loading and from the criteria developed from that of Shell to minimize surface rutting caused by over stressing the subgrade.

Based on the maximum number of the standard axle load applications, fatigue and rutting equivalencies are established. These equivalencies can be used to compare the destructive effects of various sizes of single and dual tires, and various axle loads.

The effects of changes in the level of temperature and variation in vehicle speeds on the fatigue and rutting in terms of the maximum number of load applications are also examined. The average pavement temperatures during summer and winter of various depths of asphalt concrete are selected from an assumed pavement temperature profile based on weather records. The modulus of elasticity for each individual depth corresponding to each temperature is determined from laboratory test data. The load durations of various speeds on a selected path are calculated. The modulus corresponding to each load duration is determined from the stress duration vs. resilient modulus relationship developed from laboratory tests.

The maximum number of load applications at various pavement temperatures and speeds can be used to compare the relative destructive effects of various speeds and seasonal changes on pavement.

CHAPTER II

THEORETICAL BACKGROUND

The original purpose of a pavement was to protect the subgrade from excessive deformation under traffic. Consequently, vertical displacement or strain at the surface of the subgrade is a critical factor. Selection of pavement thickness by conventional procedures ensures that an allowable strain at this point is not exceeded.

Also, under moving traffic, the upper layers flex or bend with each load application. Critical tensile strain occurs at the bottom of the asphalt layer and, if this strain is excessive, the surface will fail through cracking.

Elastic Theory Constants and Assumptions

The materials used in flexible pavement construction are essentially of four categories:

1. Bituminous bound
2. Cement bound
3. Unbound aggregate - non-cohesive soil
4. Cohesive subgrade soil

All these materials are in reality non-homogeneous, anisotropic non-linear and non-elastic and their properties are to some extent time dependent and are affected by changes of environment such as temperature and moisture content.

At the present time, the layered elastic theory, which is relatively simple, promises to be a reasonable approach for design purposes. The successful use of this method for predicting stress and strains in a road structure depends primarily on how well the modulus of elasticity or its equivalent, and Poisson's ratio, under conditions appropriate to

the particular analysis are known. This is because stresses in a layered system depend on the ratio of elastic modulus between one layer and its neighbor while strains being calculated from stresses depend also on the actual value of modulus at the point concerned.

Elastic modulus, E, is the rate at which a material develops strength when strained. For the purpose of this study, it is the stress divided by the strain under simple axial loading. In the road, the materials are seldom strained more than 1%, so the moduli at low strains are those in which we are interested.

Poisson's ratio, ν, is an elastic constant that is difficult to reliably evaluate for most pavement materials. For an ideal isotropic, cylindrical specimen of material subjected to a uniform principal stress state, Poisson's ratio is obtained by dividing the lateral strain by the axial strain. Variation in Poisson's ratio does not greatly affect vertical stresses but has a significant effect on horizontal stresses particularly near the surface and so it merely shifts the plots horizontally in a rigid manner with no decrease in scatter of the data (1).

The general assumptions of elastic layer theory are:

1. The materials are linear elastic, isotropic and homogeneous.
2. The load is applied uniformly distributed over a circular area.
3. The interfaces between layers are either completely "rough" or "smooth," the former being the more normally assumed condition.

In addition to the well-known basic assumptions on which the classical elasticity theory is based, the following simplifying assumptions are made in all of the stress analyses:

1. The tire-pavement surface contact pressure is assumed to be uniform and equal to the tire pressure wherever contact pressures have not been experimentally determined. Thus, the contact area is computed by means of the tire pressure and the wheel load, and is assumed to be circular.
2. Stresses under dual tires and tandem axles are computed on the assumption of the validity of the principle of superposition in stress analysis.
3. It is assumed that no surface shear stresses are induced at the contact between the tire and pavements.

Material Characteristics

In general, asphalt materials are visco-elastic and therefore their stress-strain characteristics are dependent on both time of loading and temperature. At short loading times, the stiffness approaches a constant value which, under this condition, is analogous to a modulus of elasticity (2). In addition to the environmental factors, the stiffness also depends on the mix variables such as aggregate type and grading, bitumen type and content, degree of mix compaction and the resulting air void content.

For accurate values of stiffness, measurements should be made at the appropriate values of temperature, time and stresses. A number of experimental methods have been developed to describe the relationship between stress and strain for asphalt mixes (3). Two of these methods, the dynamic complex modulus and the modulus of resilient deformation,

are similar. The concept and definition of the dynamic complex modulus for asphalt concrete has been presented by Papazian (25). Seed, Chan, and Lee (24) developed the background and the concept of the modulus of resilient deformation. The stiffness modulus is another concept developed by Deacon (26) for describing the relationship between stress and strain for asphalt mixes in repeated load beam flexure.

The tests mentioned above are expensive, complicated and, therefore, may not be available for different pavement design agencies. For this reason, and in order to effectively evaluate the modulus or strength properties of the paving materials, researchers have often attempted to correlate these properties to some standard or conventional tests. It should be recognized that these correlations should be used for estimating only when actual test data are not available.

One of the more useful as well as convenient methods for estimating resilient modulus of asphalt treated mixtures is based on the stiffness concept of Van der Poel. By this method the stiffness or resilient modulus of pure asphalts can be estimated from nomographs. The penetration and ring and ball softening point of the asphalt in the mix are needed as input for this estimate.

Heukelom and Klomp (27) extended the work of Van der Poel to estimate the stiffness of asphalt treated mixtures. In addition to the penetration and ring and ball softening point data, the volume concentration of the aggregate, C_v, must be determined. Heukelom and Klomp's semi-empirical equation for mixture stiffness is reliable for mixtures with approximately 3% air voids. Subsequently, Van Draat and Sommer modified this relationship to include the effects of different air voids.

For asphalt-bound materials, stiffness is defined by the relation (8):

$$S\ (t,T) = \frac{\sigma}{\varepsilon}$$

where

$S(t,T)$ = Mixture stiffness at a particular temperature and time of loading and σ,ε = applied stress and strain, can be used and either measured directly or estimated.

The subgrade is defined as the soil prepared to support the pavement and is sometimes called "basement soil" or "foundation soil." The design thickness of the pavement is strongly influenced by the design strength assigned to the subgrade. This subgrade strength can be measured directly or estimated from tests on the subgrade soil. Three tests frequently used to determine the strength or modulus of subgrade soils are:

1. The resilient modulus test using repeated load triaxial apparatus.
2. The California bearing ratio (CBR) test.
3. The repeated plate load test.

For untreated materials such as the subgrade, a measure of stiffness termed the resilient modulus can be determined from a simple repeated load triaxial compression test defined as:

$$M_R = \frac{\text{Repeated Axial Stress}}{\text{Recoverable Axial Strain}}$$

Such techniques are described in Appendix C of Reference (4). However, this equipment is not always available or convenient to use.

A widely used method of estimating subgrade modulus, E_s, is the relationship between subgrade CBR and dynamic modulus developed by Heukelom and Foster (5).

$$E = 1500 \text{ CBR (in psi)}$$

The repeated-plate load test (6) is another method that can be used to estimate the subgrade modulus.

For untreated granular materials, the same type of test can be used to determine a stiffness modulus. That modulus is dependent on the applied stresses

$$E_R = K\theta^n$$

where: $\theta = \sigma_1 + \sigma_2 + \sigma_3$ (sum of principal stresses)

K & n = the material constants

Alternatively, one can make use of the procedure suggested originally by the Shell (7) investigators wherein the stiffness of the granular layer is proportional to the stiffness of the underlying material, i.e.,

$$(E_{gran}) = F(E_{subgrade})$$

where F is a function of the stiffness of both the subgrade and the asphalt-bound layer varying from 1 to 4 (1). Environmental influence must be considered when the response of untreated materials is assessed. Accordingly, proper water contents (or soil suction) as well as the effects of freezing and thawing should be reflected in stiffness measurements.

Structural Analysis and Evaluation

To permit estimation of the potential for fatigue distress requires an estimation of the stress and deformations resulting from moving wheel loads on realistic representations of pavement structures. As noted by a number of researchers (Barksdale and Hicks; Deacon; Terrel; Havens, Deen and Southgate; and Witczak), the assumption of the pavement responding as a layered elastic system appears reasonable at this time. Computer solutions are available (CHEV 5L, BISTRO or BISAR and GCP-1) to facilitate determination of the stresses. Typical results from a specific analysis are shown in Figure 3 for the horizontal tensile strains on the under side of asphalt concrete. This is a reasonable fatigue damage determinant.

When using such solutions for material response characteristics that depend on stress, it is necessary to use an iterative type of solution as indicated in Figure 4 for pavement section containing a granular material (9).

Distress in Pavement Structure

For convenience, the various distress mechanisms have been grouped into three categories (10) which either by themselves or in combination can lead to a reduction in pavement serviceability with time. The three distress modes (i.e., fracture, distortion and disintegration) have been listed in Table 1 and various manifestations as well as distress mechanisms have been included for asphalt pavements. Moreover, the distress mechanisms have been subdivided into those caused by both traffic and non-traffic associated factors.

It has been indicated (11) that the most frequently occurring mode of distress in asphalt highway pavements in the United States is fatigue cracking associated with traffic loads.

Fatigue has been defined as the phenomenon of fracture under repeated or fluctuating stress having a maximum value generally less than the tensile strength of the material. It appears that stiffness plays a predominant role in determining the fatigue behavior of asphalt mixes and maximum principal strain is a major determinant of fatigue crack initiation. Poorest fatigue results are from the base and base course type mixes with low binder contents and, unfortunately, it is the layer consisting of these mixes which normally carry the highest tensile strains (2). Factors affecting the stiffness and fatigue behavior of asphalt mixtures are shown in Table 2 (10).

For comparatively thin asphalt bound layers the controlled strain mode of loading is more appropriate. The controlled-stress mode of loading will only be approached in pavements containing comparatively thick (greater than 6"), stiff sections of asphalt concrete.

Fatigue behavior of asphalt concrete can be represented by an equation of the form

$$N_f = K \left[\frac{1}{\varepsilon_{mix}} \right]^n$$

where

N_f = stress applications to failure

ε_{mix} = tensile strain repeatedly applied to the mix

K,n = constants depending on mixture characteristics, n depends on mixture stiffness and ranges from 2 to 6.

In practice, pavements are subjected to a range of loadings; accordingly, a cumulative damage hypothesis is required since fatigue data are usually determined from the results of simple loading tests. One of the simplest of such hypotheses is the linear summation of cycle ratios. This cumulative damage hypothesis states that fatigue failure occurs when

$$\sum_{i=1}^{i} \frac{n_i}{N_i} = 1$$

where:

n_i = number of applications at strain level i

N_i = number of applications to cause failure in simple loading at strain level i.

Fatigue life prediction under compound loading becomes a determination of the time at which this sum reaches unity.

Permanent Deformation

Structural failure of a flexible pavement may be defined as a state in which repeated application of a specified wheel load results in ever-increasing plastic deformations of the pavement surface. A pavement should be considered structurally adequate for certain wheel loads if the depth of rut caused by repeated application of that wheel load reaches a final value which does not increase with further load applications.

Of course, a flexible pavement may be inadequate and become unserviceable if the rut depth exceeds a certain limit. Normally, it is to be expected that the safety factors against structural failure will be of such magnitude that pavements remain serviceable for the specified number of load repetitions.

Observations indicate that the phenomenon of structural failure of flexible pavements is governed by the relative resilience or compressibility of the subgrade soil with respect to the shear strength of the pavement structure. In the case of a relatively weak, compressible subgrade and a strong, well-compacted, but thin pavement structure, structural failure occurs essentially through punching shear. Rutting is then due primarily to compression and distortion of the subgrade soil.

On the other hand, in the case of a relatively firm, incompressible subgrade and a poorly compacted or generally weak pavement structure, as well as in the case of any subgrade supporting a very thick pavement structure, failure phenomena may resemble more the phenomenon of general shear of an incompressible soil under a footing. Rutting is then caused primarily by distortion or shear deformation of the pavement structure. Of course, all possible combinations of the two extreme types of phenomena occur in intermediate cases.

It is of interest to note that there apparently exists a critical subgrade stress level beyond which the rutting is extended into the subgrade soil. If the vertical stresses on the subgrade never exceed the critical level, ruts are formed primarily by shear deformations in the pavement structure. This finding justifies the selection of limiting subgrade stress or strain as one of the major design criteria in flexible pavement design.

From an examination of stresses and deformations (using elastic theory) in pavements designed (10) according to CBR procedures, and those at the AASHO road test, the pavement will carry the corresponding load repetitions without excessive permanent deformation as long as the vertical compressive strain at the surface does not exceed the values shown as follows:

Weighted Load Applications	Compressive Strain At Surface of Subgrade (in/in x 10^{-4})
10^5	10.5
10^6	6.5
10^7	4.2
10^8	2.6

Environmental Effects

Because the response of asphalt-bound materials is dependent on temperature, distributions of temperature within layers containing such materials should be determined.

Pavement temperatures can be computed from weather data. That is done by solving the heat conduction equation by numerical technique, such as finite-difference procedure or finite-element procedure, or by closed-form techniques as presented by Barber (28). Alternatively, a representative temperature can be estimated by the procedure suggested by Havens, Deen and Southgate or by Witczak.

Temperature stresses can often be as high as load stresses, as has been shown in numerous studies, particularly in rigid pavements, where temperature stresses are due to curling, warping, expansion or contraction. Those same types of stresses are present in asphalt concrete pavements. They are tensile or compressive stresses due to increase or decrease in the general level of temperature and bending stresses due to temperature differential within the pavement structure itself.

The tensile or compressive stresses due to general or seasonal changes in the level of temperature, as are the resulting changes in material properties, notably asphalt stiffness. The bending stresses,

on the other hand, are due to diurnal or daily temperature cycles or variations.

CHAPTER III

COMPUTATIONS

Input Variables and Pavement Material Selection

Various wheel loads and tire widths to be considered as input variables in the computer analysis were suggested by the Washington State Highway Department as shown in Table 3.

Assuming that tire-pavement surface contact pressure is uniform and equal to the tire pressure and the contact area is circular, various tire pressures have been calculated by dividing wheel load by a tire contact area. These values are tabulated in Table 4.

Several thicknesses of pavement structure have been selected: 3", 6" and 9.5" of asphalt concrete surface on 8" untreated base. The subgrade layer is assumed to be semi-infinite.

The types of material in each layer of the pavement structure selected for this study are based on the availability of the laboratory and field test data in combination with those common in Washington. They are Class "B" wearing course, untreated aggregate base and the natural undisturbed clay type soil.

Estimate of Material Parameters

Asphalt Concrete

The major factor influencing the modulus of the asphalt treated layer is the temperature. A temperature vs. dynamic modulus relationship for class "B" wearing course (mean density is equal to 149.9#/ft.^{3}) is developed from Washington State University Test Track data and is shown in Figure 5 (14). From this figure, a modulus of 400,000 psi has been selected for an average temperature of 68.5^{o}F, and the Poisson's ratio is assumed as 0.3.

Untreated Base

The modulus of the untreated base is sensitive to density, gradation, and confining stress. A relationship between resilient modulus and bulk stress has been developed from laboratory tests by using repeated load triaxial compression test (15). The effect of bulk stress on the modulus is shown in Figure 6. The central curve on this figure is used to check for the modulus required by stress conditions during the iterative computational procedure. As shown in Figure 6, a range of modulus has established on either side of this curve so that any modulus used for computation that lies within this range is considered to be acceptable. The untreated base modulus used for computation is assumed to be from 1 to 3 times the value for underlying material (16). Poisson's ratio is taken as 0.4 (17).

Subgrade

A relationship between repeated plate load stress and subgrade modulus has been developed from laboratory test data (18) and shown in Figure 7. As in the case of untreated base, this curve is used to check for the modulus required by calculated stress conditions. A range of modulus has also been established. An average modulus of 6500 psi has been selected for the subgrade and varied but little for all calculations. Poisson's ratio is taken as 0.45 (17).

Calculation Procedure

The Chevron 5L computer program (19) was used to calculate the strains and deflections, under the application of a single circular load with a uniformly distributed pressure, at several depths within each layer and at several radial distances from the axis of the loaded area. The effect of the dual load on any point is then determined manually by linear superposition of the effects of each of the loads at the point in

question. The application of superposition implies linear response and, thus, the utilization of this principle is an approximation of the dual load.

Figure 8 illustrates the cross-sectional geometry (thickness) of the assumed pavement structure, input variables, and material parameters as used in the computer analysis. The untreated base layer which is 8 inches has been divided into three sublayers for convenience during the stress-modulus matching procedure for each iteration.

In order to eliminate many variables, some of them have been assumed to remain constant for all computations as noted in Figure 8. Additional input variables such as the depths and radial distances where strains and deflections being considered are summarized in Figure 9.

Summary

The computational procedure includes several iterative steps. For a particular computation, these can be summarized as follows:

1. Select thickness of each layer.
2. Estimate modulus and Poisson's ratio for each layer.
3. Select wheel load and contact area (radius of circular area of contact with pavement).
4. Select points for calculation of stresses, strains, and displacements. These will usually include depths ranging from the surface downward at least into the subgrade. Points are selected radially from the center of load sufficiently far to include the adjacent dual tire (if any). Preliminary calculations indicated that tires at the opposite end of the axle from those under consideration do not contribute significantly.

5. Following computer calculation, appropriate values are selected from the printout and compared to the material behavior, i.e., Figs. 6 and 7. If the required moduli are not within the given range, they are adjusted and the computations repeated until required agreement is attained. When dual tires are utilized, the additive values are used for this comparison so that maximum values are always considered.
6. When agreement is attained, the final iteration is used as being representative of that combination of load and pavement response.
7. The above steps are repeated for each combination of load, tire width, pavement thickness, etc.

Comparison With Experimental Data

Pavement response computed according to the above procedure is entirely theoretical, although input variables and computation techniques are reasonably acceptable. In order to gain confidence that computed values are reasonable, they were compared to data from several test roads where instrumentation permitted actual measurement of pavement response. Although nearly impossible to select identical conditions, pavements similar to those assumed in this study were found in the San Diego Test Road (20), Brampton, Ontario Test Road (21), and the WSU Test Track (14). These comparisons are summarized in Table 5.

Results

For various sizes of single and dual tires and various wheel loads, the relationships between various thicknesses of asphalt concrete and the maximum subgrade compressive strains, surface deflections, subgrade

deflections and radial tensile strains are shown in Appendix A, from Figs. A1 to A24. These four types of response have been selected for analysis in the following section.

In addition to the response for actual wheel loads as originally selected, interpolated values were determined for axle loads of 18, 20, 22 and 24 kips. Maximum horizontal tensile strains for these axle loads as well as maximum vertical compressive strains are shown in Appendix B, Figs. B1 to B8.

CHAPTER IV

EQUIVALENCY DETERMINATION

Although behavior has been established for both strain and deflection, as shown in Appendices A & B, strain criteria appear to be more suitable at this time. Surface deflection is often a good indicator of pavement behavior changes, but in itself it cannot be readily related to performance over a wide range of conditions. Therefore, the main concern will be with radial tensile strain on the bottom of asphalt concrete layers as it relates to fatigue cracking or failure. In addition, vertical compressive strain on the subgrade is examined with respect to its relationships to limiting rutting in the pavement structure.

Fatigue

Laboratory testing of asphalt paving mixtures have been tested over a wide range of conditions with reasonable success. In addition, an engineering estimate can be made as to the predicted life of a pavement with respect to initial fatigue cracking. Accordingly, a typical fatigue curve representing mixtures similar to class B has been selected for this project (22) and is shown in Appendix C, Fig. C1.

Also included in Appendix C are plots showing the expected number of load application to failure for the various combinations of wheel load, tire size, axle load, and pavement thickness. These are shown in Figs. C2 - C5 and provide a convenient means of transferring computed tensile strain values (Figs. B1 - B4) to number of load applications.

A complete and reasonably convenient summary of all these data is shown in Fig. 10. In this figure, the relative number of applications of a particular load or combination of loads can be determined. As a basis for comparison in establishing Fig. 10, a "standard" condition was

defined as an 18-kip axle load with 10-inch wide dual tires on a pavement with 6 inches of asphalt concrete. Thus, this point on Fig. 10 has an equivalency equal to unity. With the data normalized in this manner, any two points can be compared (divided) directly using the relative equivalencies on the vertical scale.

Rutting

Permanent deformation or rutting of asphalt pavements and the engineer's ability to predict it are less well-defined than for fatigue. This limitation results from the more complex nature of the problem. Current research is well underway to providing a solution, but for the purposes of this study, the data developed by Shell (7) is used. This approach is based on the fact that if the vertical stress or strain at the top of the subgrade is limited to some specific value, permanent deformation in the form of rutting will not occur in the overlying layers. From field measurements compared to multi-layer elastic theory, strain was found to be the better indicator. A general relationship was developed with respect to the level of traffic as shown in Appendix D, Fig. D1.

Using the data in Fig. D1 in a manner similar to that for fatigue, the number of applications for various axle loads and tire-pavement thickness combinations have been plotted in Figs. D2 - D6.

Similar to that for fatigue, Fig. 11 has been prepared as a summary of all the combined data for rutting behavior. Use of these data are similar to that for Fig. 10. Any two points can be compared in terms of their relative life to failure in terms of their ratio or equivalency.

Climate (Temperature)

Inasmuch as the preceding approach to development of equivalencies was necessarily limited to an "average" set of input values, adjustments may be needed for other conditions.

For the average case, 68.5°F was assumed to be the temperature for asphalt concrete at all depths. This assumption resulted in an average stiffness of approximately 400,000 psi (see Fig. 5). It is known, however, that a range of temperatures is encountered such as during the summer and winter months. For the State of Washington, two general zones can be described: (1) West of the Cascade Mountains where the temperatures are reasonably mild and constant (hence, the "average" case), and (2) East of the Cascade Mountains where more extremes are found ("winter" and "summer" cases). The profile of temperature within the asphalt concrete for these pavements are estimated as shown in Appendix E, Fig. E1.

Because of the excessive computations and analysis required, the effect of temperature on pavement behavior is limited to the case for 10-inch tires, 18-kip axle load, and for the usual range in asphalt concrete thickness, appropriately adjusted for stiffness by sublayers. These conditions are illustrated in Fig. E2 of Appendix E. In a manner similar to that for previous calculations, the subgrade and surface deflections, vertical subgrade strain and horizontal tensile strain in the asphalt concrete were determined and are shown in Figs. E3 - E6, respectively.

Using the same fatigue criteria as before (Fig. C1) the number of load applications to failure were determined and plotted in the format shown in Fig. 12. Remembering that these data are for 18-kip axle loads only, they can be extrapolated to include other axle loads by utilizing the linear nature of curves in Fig. 10.

An analysis similar to that above has been made for rutting and the data are shown in Appendix E, Fig. E7.

Vehicle Speed

It is generally known that pavement response varies with rate and duration (speed) of the applied load (truck). The cause of such variation is a result of the viscoelastic nature of the pavement materials, particularly clay subgrade and asphalt concrete. Since the subgrade is at depth and rate of load application is tempered by load re-distribution, the contribution of the subgrade to non-linear pavement response has been ignored for this study.

Effect of speed, then, is limited to the viscoelastic response of asphalt concrete. As before, analysis has been limited to the standard 18-kip axle load with 10-inch wide tires. Using the 10-inch diameter contact area between tire and pavement as the contributing loaded area, the wheel was assumed to be rolling at a range of speeds and these were converted to load duration as shown in Appendix F, Fig. F1. These loading times were then used to determine stiffness of the asphalt concrete based on the principles of Van der Poel and calculated for a particular mix by Monismith, et al. (23). These are shown in Fig. F2. A direct experimental approach was used by way of comparison using data developed at the University of Washington (3) as shown in Fig. F3. Although the materials are not exactly the same in Figs. F2 and F3, they compare favorably in Fig. F4, especially in the region of normal highway speeds (short load durations).

Further analysis of the effect of speed is very similar to previous variables. Again, analysis is limited to a single case as shown in

Fig. F5, illustrating the principle if not all possible examples. The variation in horizontal tensile strain, vertical compressive strain, surface, and subgrade deflection have been compared to a range of speeds as shown in Figs. F6 - F9. Finally, using fatigue data, the relative effect of speed on the number of applications of load to failure is shown in Fig. 13. A similar plot for rutting damage is in Appendix F, Fig. F10. These data can be used to estimate additional equivalency corrections based on changes in speed. Although the basic equivalency relationships shown earlier in Figs. 10 and 11 did not indicate a speed, most of the stiffness data were developed for testing load duration of about 0.5 sec., i.e., about 10 mph. The user of these data should be cautioned, however, that relative values only should be compared and not actual load applications to failure, for example.

CHAPTER V

SUGGESTED USE AND APPLICATIONS

Appropriate utilization and recognition of the limiting factors in this study are very important. The user must realize that comparisons among the variables considered are only relative and should not be used for actual pavement life predictions, for example. This approach is predicated on the fact that computed data are based on hypothetical pavements, although they are reasonable approximations of typical pavements constructed in Washington.

Using the key relationships developed herein, Figs. 10, 11, 12 and 13 can be used to determine a wide range of equivalencies. This is illustrated in the form of examples or typical situations.

Example 1

Problem

Compare the relative pavement fatigue life expectancy of a 3-inch asphalt pavement when subjected to an 18-kip axle load with 10-inch dual tires and 18.5-inch single flotation tires.

Solution

From Fig. 10, the relative life for the single and dual cases are 250×10^{-3} and 1000×10^{-3}, respectively. Therefore, the equivalency of these two are about four to one ($\frac{1000 \times 10^{-3}}{250 \times 10^{3}} = 4.0$), i.e., the single tire would be four times more damaging in terms of fatigue, or, conversely, the pavement will last four times longer under the dual tires.

One should note that these equivalencies are compared for conditions that are all constant except for those being compared.

Example 2

Problem

Determine the equivalency for the same loads as in Example 1, but in terms of rutting distress.

Solution

From Fig. 11, for 3-inch asphalt concrete, the dual tire $N = 32 \times 10^{-3}$ and the single $N = 14 \times 10^{-3}$. The equivalency would then be $\frac{32 \times 10^{-3}}{14 \times 10^{-3}} = 2.3$ for rutting.

Comparing the values from Examples 1 and 2, the fatigue mode of distress would control since the relative difference (equivalency) is greater between the two cases.

Example 3

Problem

Using the results from Example 1, what difference will it make for summer and winter conditions?

Solution

From Example 1, the equivalency was equal to 4, and this can be considered the "average" condition in Fig. 12. The actual equivalency between 10-inch dual and 18.5-inch single would remain about the same, but actual life to failure (for a particular case) would need to be adjusted. From Fig. 12, summer, average, and winter applications for 3-inch asphalt concrete would be 7.4×10^3, 3.3×10^4 and 2.7×10^5, respectively. Therefore, pavement life could be expected to be increased by:

$$\frac{2.7 \times 10^5}{3.3 \times 10^4} = 8.2 \text{ times in winter, and decreased by}$$

$$\frac{3.3 \times 10^4}{7.4 \times 10^3} = 4.5 \text{ times in summer.}$$

One must realize, however, that the actual range of winter to summer temperatures are distributed throughout the year, month by month, and a weighted average would be more realistic. The data in Fig. 12 are primarily for illustrative purposes only and show that due to higher stiffness of asphalt concrete in winter, it is more resistant to fatigue cracking.

Example 4

Problem

Again using Example 1 results, what is the effect of reducing average truck speed from 70 mph to 55 mph?

Solution

The curve in Fig. 13, although developed for the "standard" load, can be used for general speed comparisons. At 70 mph, load applications to fatigue cracking is 1.25×10^6. At 55 mph, this value is 1.15×10^6. Therefore, pavement life is reduced by a factor of

$$\frac{1.15 \times 10^6}{1.25 \times 10^6} = 0.92 \text{ or } 8\%.$$

Example 5

Problem

A special highway user requested permission to use a 3-mile segment of highway for trucks having average single axle loads of 24-kips and 18.5-inch single flotation tires. The existing pavement is 3 inches of asphalt concrete with other conditions similar

Example 5

Problem (cont.)

similar to those developed in this report. What changes in pavement would be required to provide equivalent pavement life compared to the standard 10-inch dual, 18-kip axle load?

Solution

Provide asphalt concrete overlay. Locate the given conditions on Fig. 10. (22-kip axle load, 18.5-inch single tire, 3-inch AC pavement). This point is approximately 82 x 10^{-3} on the vertical equivalency scale. Next, locate the "standard" condition (18-kip, 10-inch dual, 3-inch AC) which is approximately 300 x 10^{-3}. Pavement thickness must be increased sufficiently to increase the 82 x 10^{-3} to 300 x 10^{-3}. Interpolation of the asphalt concrete thickness curves (vertically on the 22-kip axle line) shows that 6.2 inches of pavement is required. Therefore, an overlay of 3.2 inches would provide equal life to the highway section in question for this special loading.

An additional solution(s) may be more appropriate depending on the conditions:

(1) Add axles to reduce average axle weight.

(2) Change tires to duals (Fig. 1 does not include large enough duals--11- or 12-inch would be required by extrapolation, but may not be practicable).

(3) A combination of the above.

Also note that, for larger special loading, the speed may be reduced considerably and this should be considered in the equivalency evaluation. Further, the time of year may be a factor--special hauling may be seasonal and compensation for temperature correction may increase or decrease the equivalency.

CHAPTER VI

CONCLUDING DISCUSSION AND SUMMARY

This research project was initiated in an attempt to examine relative destructive effects on the pavements of the wide single-tire and conventional dual tires. Basic variables are wheel load, tire width and different thicknesses of asphalt concrete. Based on available laboratory and field data, asphalt concrete surface, untreated aggregate base and clay subgrade were selected as the materials for this study. The Chevron 5-L program was used to compute deflections and critical strains. Prior to determining the fatigue and rutting equivalencies, maximum computed deflections and critical strains were compared with other sources such as the San Diego Test Track. These experimental data seem to agree reasonably well. By using known fatigue and failure design curves, maximum allowable numbers of various axle load applications were determined. Fatigue and rutting equivalencies for various axle loads are established by dividing the maximum number of various axle load applications by the maximum applications of 18-kip axle loads on an asphalt concrete thickness of 6" and the dual 5" tires. These equivalencies, shown in Figures 10 and 11, can be used to compare the destructive effects of various sizes of single and dual tires and axle loads as illustrated in Chapter V. According to these examples, it can be concluded that higher equivalency tends to cause less destructive effect, i.e., longer pavement life.

The effects of variation in temperature between summer and winter are also examined. It can be said that as the temperature is decreased, as in winter, the rigidity of the pavement structure is increased, thus resulting in a decrease of vertical stress and thereby permitting a greater number of load applications. As can be seen in Fig. 12, the destructive effect of a vehicle on the pavement during the summer period

is much greater than in winter, exclusive of spring frost break-up conditions.

The effect of variation in vehicle speed on the pavements was also considered in this study. In general, slower speed tends to cause longer load duration, thus resulting in an increase in vertical stress and thereby permitting fewer load applications to failure as can be seen in Fig. 13. This figure can be used to compare the destructive effect of various speeds as illustrated in Example 4, Ch. V. According to this example, it can be concluded that slower speed tends to cause more destructive effect.

The general nature of Figs. 10-13 provides a wide range of conditions for comparison on a relative basis. Within reason, interpolation is valid. One must keep firmly in mind, however, the fact that these relationships are for assumed conditions (although reasonable) and do not represent actual pavements.

REFERENCES

1. Harr, M. E. and W. J. Head, "Extension of AASHO Road Test Performance Concepts," National Cooperative Highway Research Program Report Number 30, Highway Research Board, 1966.

2. Brown, S. F. and P. S. Pell, "Developments in Structural Design of Flexible Pavements," Road and Road Construction, May 1970.

3. Terrel, R. L. and I. S. Awad, "Resilient Behavior of Asphalt Treated Base Course Materials," Washington State Highway Department Research Report No. 6.1, August 1972.

4. Full-Depth Asphalt Pavements for Air Carrier Airports, The Asphalt Institute, Manual Series No. 11 (MS-11), January 1973.

5. Heukelom, W. and Foster, C. R., "Dynamic Testing of Pavements," Transactions, American Society of Civil Engineers, Vol. 127, Part 1, 1962, pp. 425-427.

6. Soils Manual for Design of Asphalt Pavement Structures, The Asphalt Institute, Manual Series No. 10 (MS-10), May 1964.

7. Izatt, J. O., Letter, J. A. and C. A. Taylor, The Shell Group Methods for Thickness Design of Asphalt Pavements, Shell Oil Company, January 1-3, 1967.

8. Van Der Poel, C., "A General System Describing the Viscoelastic Properties of Bitumins and Its Relation to Routine Test Data," Journal of Applied Chemistry, May 1954.

9. Monismith, C. L., D. A. Kasianchuk and J. A. Epps, "Asphalt Mixture Behavior in Repeated Flexure: A Study of an In-Service Pavement Near Morro Bay, California," Report TE 67-4, University of California, Berkeley, August 1968.

10. Monismith, Carl L. (University of California, Berkeley), Design Considerations for Asphalt Pavements (Seminar), Department of Civil Engineering, University of Washington, April 7, 1970.

11. "Structural Design of Asphalt Concrete Pavements to Prevent Fatigue Cracking," Special Report 140, Highway Research Board, 1973.

12. Vesic, Aleksandar Sedmak and Leonard Domaschuk (Georgia Institute of Technology, Atlanta, Georgia), "Theoretical Analysis of Structural Behavior of Road Test Flexible Pavements," Material Cooperative Highway Research Program Report 10, Highway Research Board, 1964.

13. Shahin, M. Y. and McCullough, B. F., Prediction of Low-Temperature and Thermal Fatigue Cracking, Texas Highway Department; Texas Trasp; Institute, Texas A and M. University; and Center for Highway Research, University of Texas at Austin, Research Report 123-14, 1973.

14. Terrel, R. L., Asst. Prof. of Civil Engineering, University of Washington Seattle, Washington, Analysis of Ring No. 2, Washington State University Test Track, Pullman, Washington, December 1968.

15. Krukar, M. and J. C. Cook, "Experimental Ring No. 2: A Study of Untreated Emulsion Treated, and Asphaltic-Cement Treated Base," Research Project Y-651, Pavement Research at the Washington State University Test Track, Vol. Two, July 1968.

16. Epps, Jon A., Lyon, James W., Jr., Ladd, Donald M. and Ronald L. Terrel, "Transporting Abnormally Heavy Loads on Pavements," Highway Research Circular No. 156, Highway Research Board, May 1974.

17. Dormon, G. M. and Edwards, J. M., "Developments in Application in Practice of a Fundamental Procedure for the Design of Flexible Pavements," Proceedings, 2nd Int'l. Conf., Structural Design of Asphalt Pavements, University of Michigan, 1968, pp. 99-108.

18. Monismith, C. L., R. L. Terrel and C. K. Chan, "Load Transmission Characteristics of Asphalt-Treated Base Courses," Proceedings - 2nd International Conference on the Structural Design of Asphalt Pavements, University of Michigan, Ann Arbor, August 1967.

19. Lysmer, John and James M. Duncan, "Stress and Deflections in Foundations and Pavement," Geotechnical Engineering, 4th Edition, 1969, University of California, Berkeley.

20. Hicks, R. G. and F. N. Finn, Prediction of Pavement Performance from Calculated Stresses and Strains at the San Diego Test Road.

21. Jung, F. W. and W. A. Phang, Elastic Layer Analysis Related to Performance in the Flexible Pavement Design, Research and Development Division Ontario Ministry of Transportation and Communication, March 1974.

22. Epps, Jon A. and Carl L. Monismith, Influence of Mixture Variables on the Flexural Fatigue Properties of Asphalt Concrete, February 10, 1969.

23. Proceedings of the Association of Asphalt Paving Technologists, Vol. 35, Technical Sessions held at Minneapolis, Minnesota, February 14, 15 and 16, 1966.

24. Seed, H. B., Chan, C. K. and Lee, C. E., "Resilient Characteristics of Subgrade Soil and Thin Pavement Relation to Fatigue Failure in Asphalt Pavements," Proceedings First International Conference on the Structural Design of Asphalt Pavements.

25. Papazian, H. S., "The Response of Linear Viscoelastic Materials in the Frequency Domain with Emphasis on Asphalt Concrete," International Conference on the Structural Design of Asphalt Pavements, Michigan, 1962.

26. Deacon, J. A., "Fatigue of Asphalt Concrete," Ph.D. Dissertation, University of California, Berkeley, 1965.

27. Heukelom W. and Klomp, A. J. G., "Road Design and Dynamic Loading," Proceedings of the AAPT, Dallas, Texas, 1964.

28. Barber, Edward S., "Calculation of Maximum Pavement Temperatures from Weather Reports," Bureau of PUblic Roads.

TABLE 1

CATEGORIES OF PAVEMENT DISTRESS FOR ASPHALT PAVEMENTS (10)

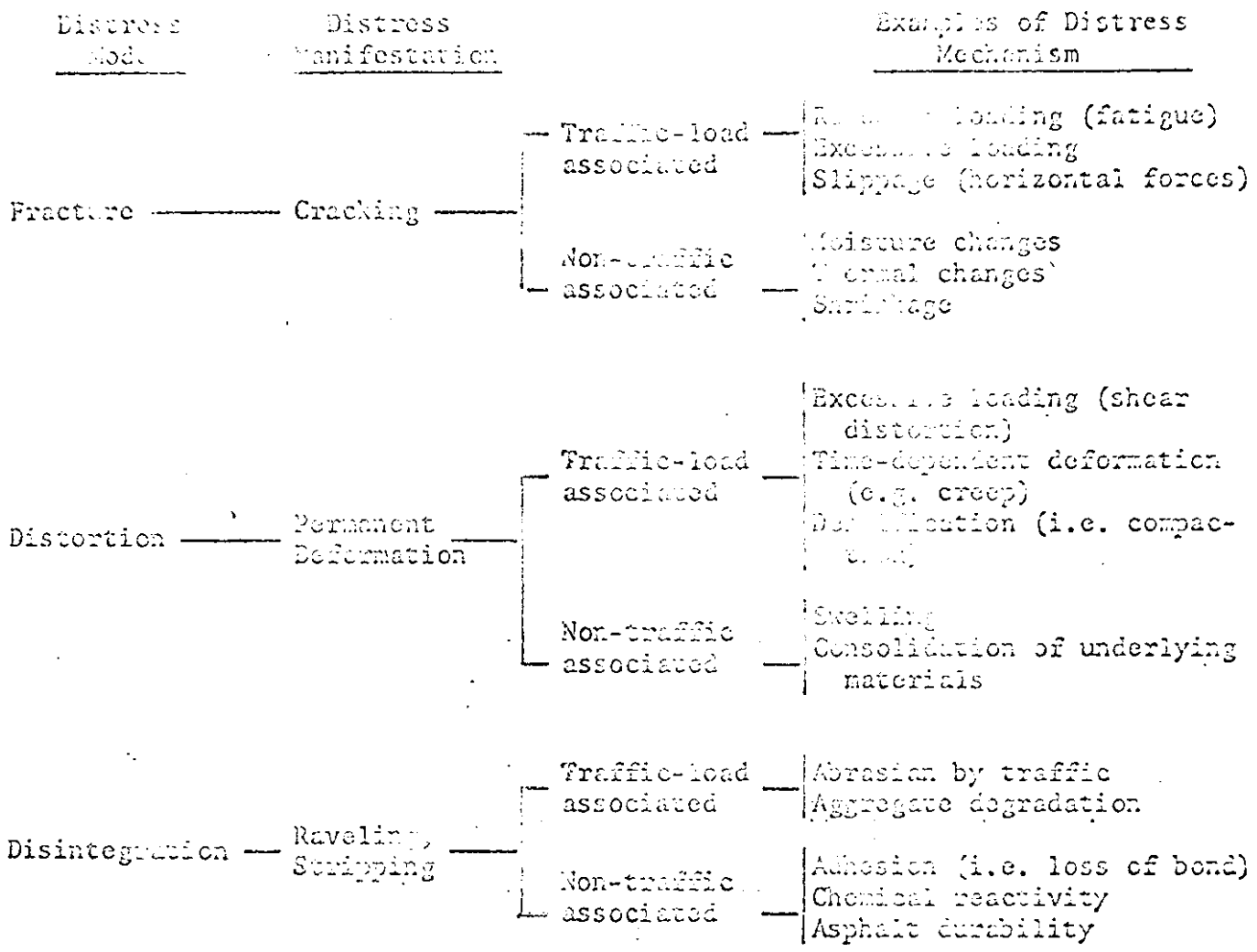

TABLE 2

FACTORS AFFECTING THE STIFFNESS AND FATIGUE BEHAVIOR OF ASPHALT CONCRETE MIXTURES (10)

Factor	Change in Factor	Effect of Change in Factor		
		On Stiffness	On Fatigue Life in Controlled-Stress Mode of Test	On Fatigue Life in Controlled-Strain Mode of Test
Asphalt Penetration	decrease	increase	increase	decrease
Asphalt Content	increase	increase[1]	increase[1]	increase[2]
Aggregate Type	increase roughness and angularity	increase	increase	decrease
Aggregate Gradation	open to dense gradation	increase	increase	decrease[4]
Air Void Content	decrease	increase	increase	increase[4]
Temperature	decrease	increase[3]	increase	decrease

[1] Reaches optimum at level above that required by stability considerations

[2] No significant amount of data; conflicting conditions of increase in stiffness and reduction of strain in asphalt make this speculative.

[3] Approaches upper limit at temperature below freezing.

[4] No significant amount of data.

TABLE 3

SUGGESTED MATRIX FOR WHEEL LOADS AND TIRE WIDTHS BY THE WASHINGTON STATE DEPARTMENT OF HIGHWAYS

	STATIC LOAD				DYNAMIC LOAD			
NOMINAL TIRE WIDTH	8"	10"	15"	18.5"	8"	10"	15"	18.5"
LOAD KIPS								
SINGLE WHEEL								
4	X	X			X	X		
6	X	X	X	X	X	X	X	X
8	X	X	X	X	X	X	X	X
10		X	X	X		X	X	X
12			X	X			X	X
DUAL WHEEL								
4	X	X			X	X		
6	X	X			X	X		
8	X	X			X	X		
10		X				X		
12								

TABLE 4

CALCULATED TIRE CONTACT PRESSURES

Tire Width (in.)	Contact Area ($in.^2$)	Wheel Load (lb.)	Contact Pressure (psi)
8	50.27	4,000	79.58
		6,000	119.37
		8,000	159.15
10	78.54	4,000	50.93
		6,000	76.40
		8,000	101.86
		10,000	127.32
15	176.71	6,000	33.95
		8,000	45.27
		10,000	56.59
		12,000	67.59
18.5	268.80	6,000	22.32
		8,000	29.76
		10,000	37.20
		12,000	44.64

TABLE 5

COMPARISON OF COMPUTED VALUES (UW) AND ACTUAL MEASURED DATA FOR SECTIONS OF SIMILAR DESIGN AT SEVERAL TEST PROJECTS

Test	Max. $\epsilon_{Rad.}$	Max. $\epsilon_{Vert.}$	δ Surface	δ Subgrade
San Diego Test Road	350×10^{-6}	412×10^{-6}	0.0183	
WSU Test Track	296×10^{-6}	550×10^{-6}	0.0176	
UW Computed	300×10^{-6}	500×10^{-6}	0.0178	
UW Computed	230×10^{-6}	502×10^{-6}	0.0189	0.0160
Brampton Ontario Test Road	227×10^{-6}	583×10^{-6}	0.0182	0.0161

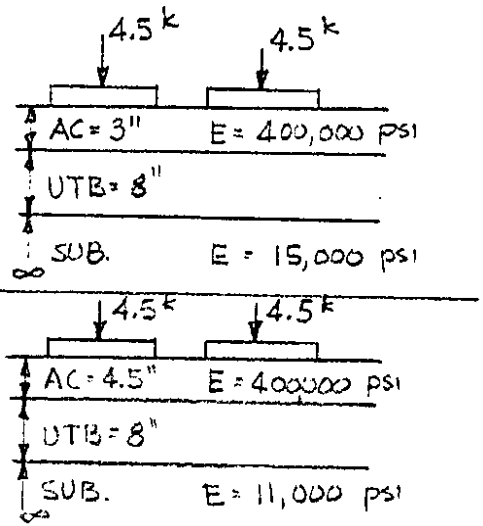

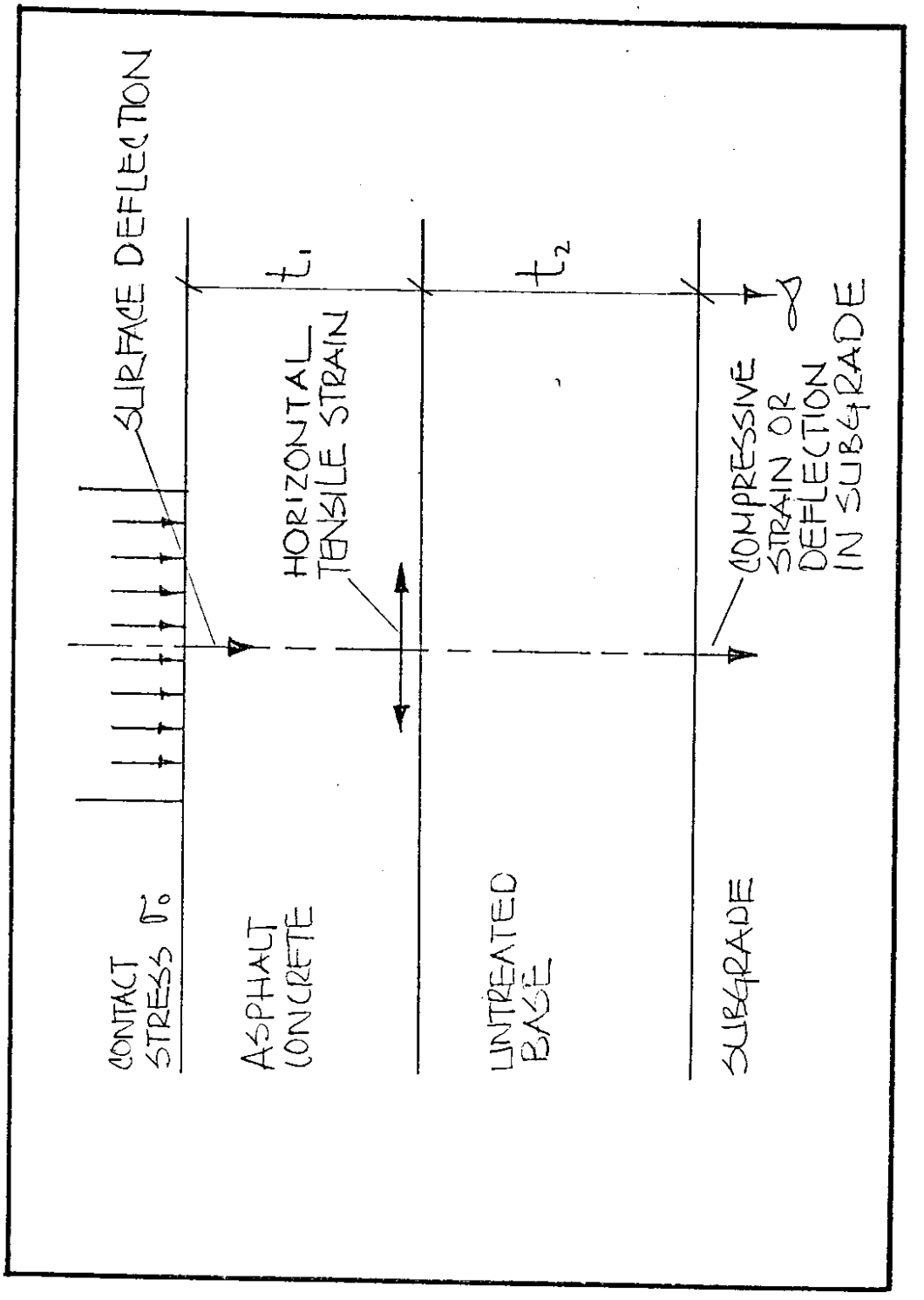

FIGURE 1 - LOCATION OF CRITICAL DEFLECTIONS AND STRAINS IN PAVEMENT STRUCTURE UNDER SINGLE TIRE

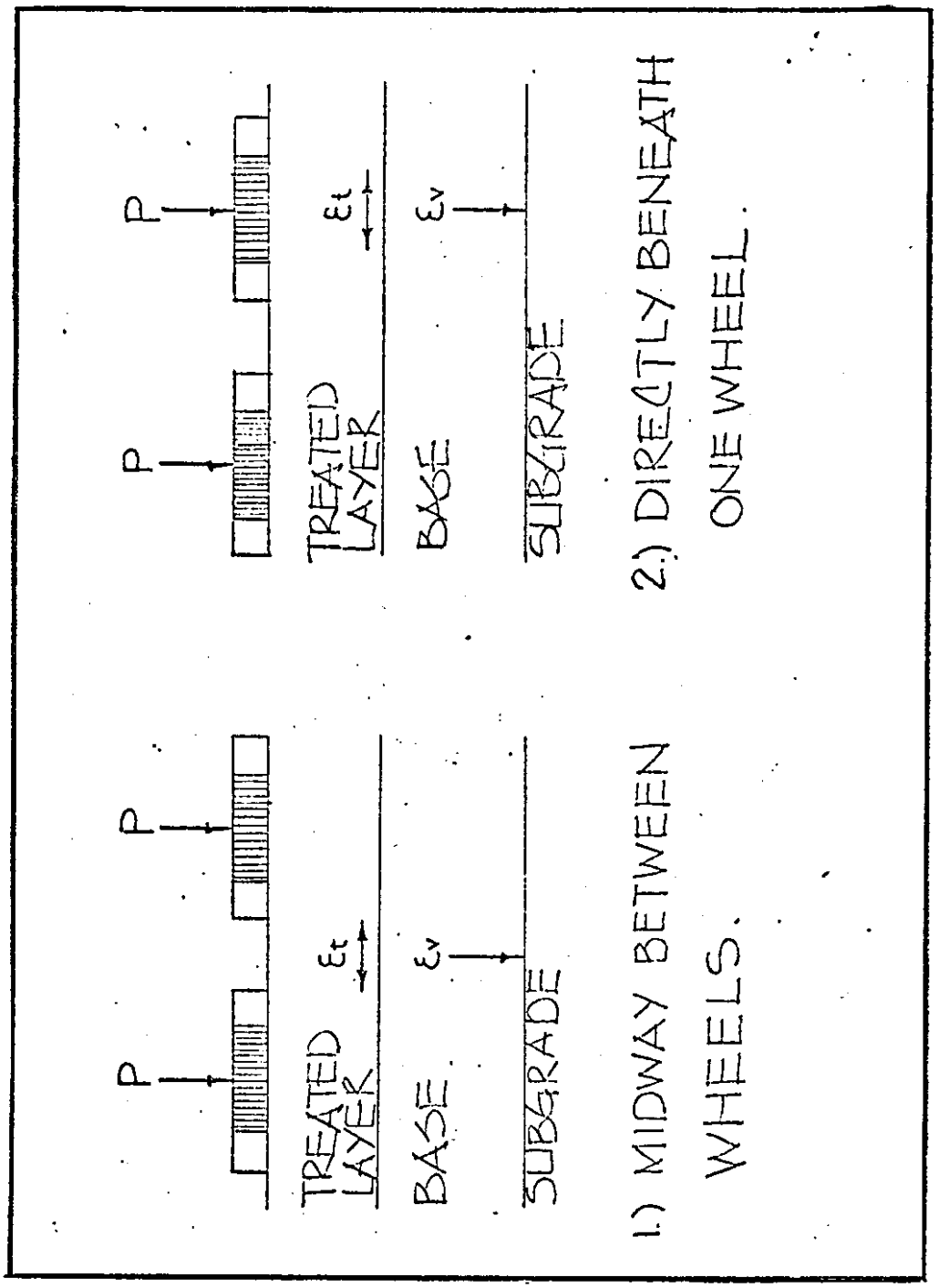

FIGURE 2 - LOCATION OF MAXIMUM HORIZONTAL TENSILE AND VERTICAL COMPRESSIVE SUBGRADE STRAIN IN PAVEMENT STRUCTURE UNDER DUAL WHEELS.

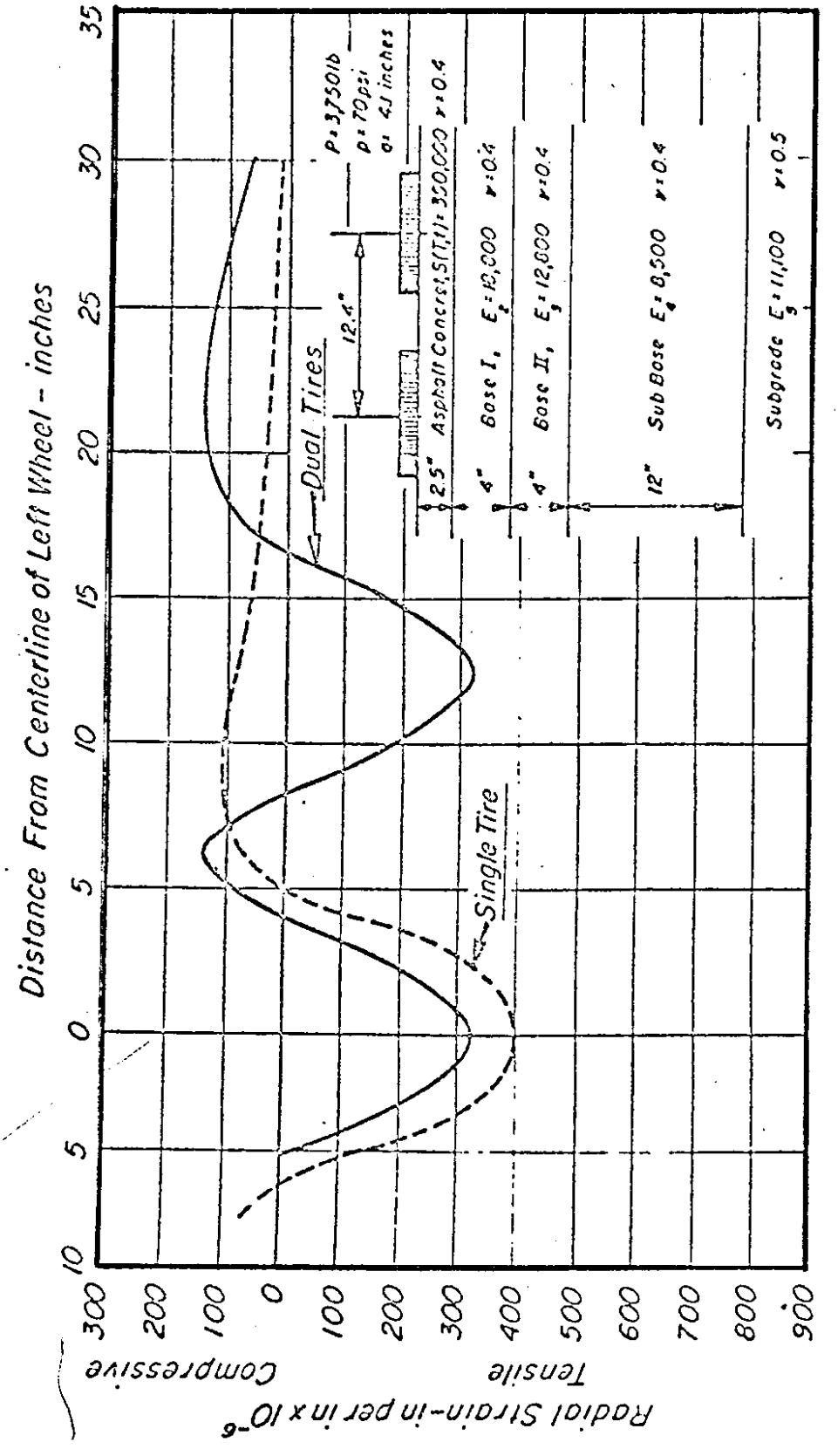

FIGURE 3 - RADIAL STRAINS AT BOTTOM OF ASPHALT CONCRETE LAYER UNDER DUAL TIRES OF 15 KIP AXLE, MORRO BAY PAVEMENT (10)

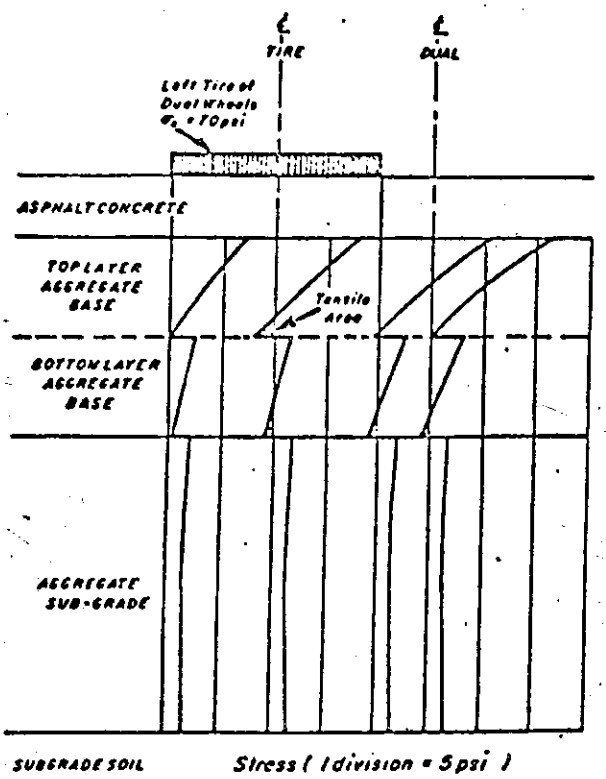

Horizontal radial stresses under one wheel of 15-kip axle load - dual tires (5 layer calculation, S(t, T) = 350.000 psi).

FIGURE 4 - ITERATIVE TYPE OF SOLUTION EXAMPLES (10)

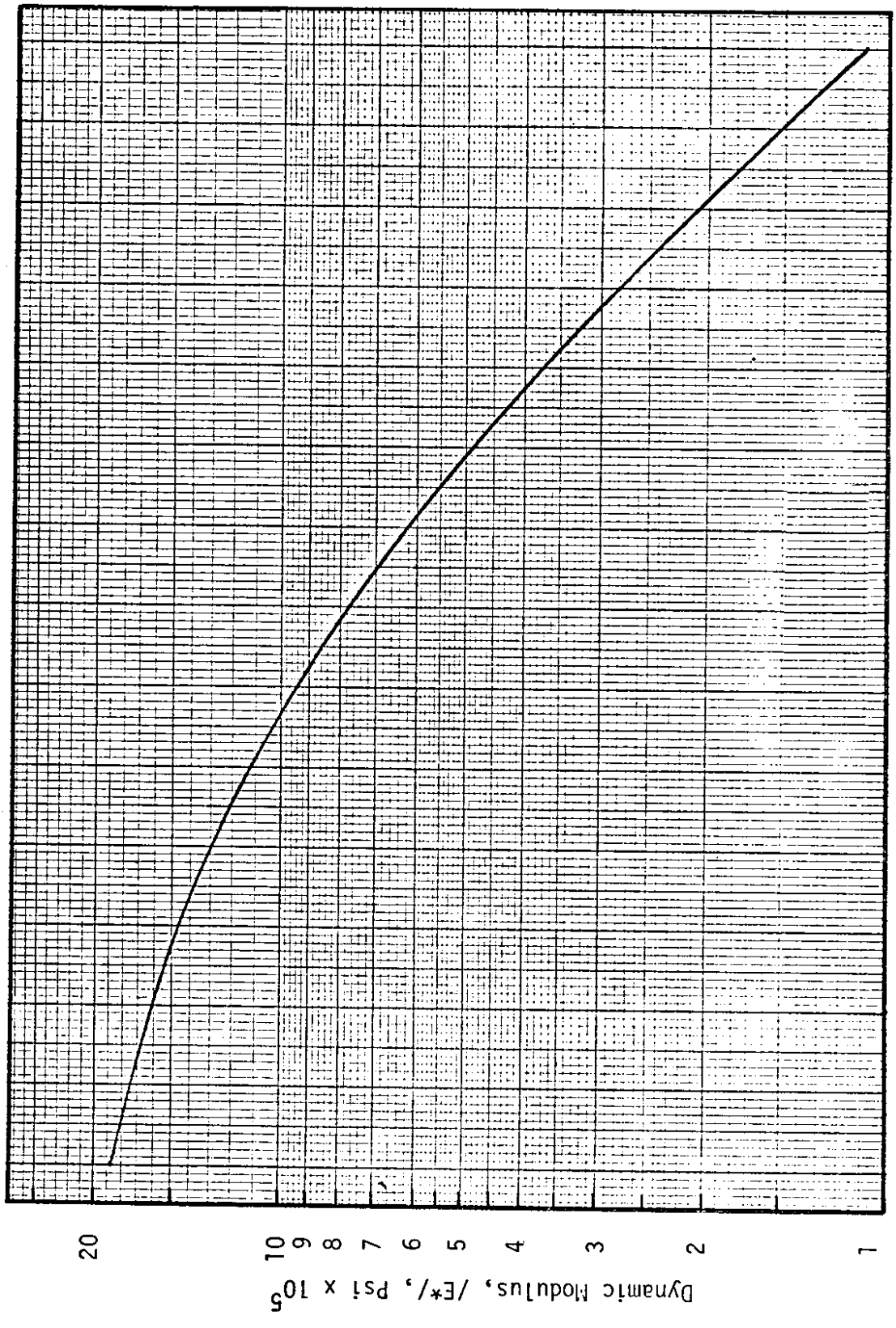

FIGURE 5 - DYNAMIC MODULUS VS. TEMPERATURE RELATIONSHIP FOR ASPHALT CONCRETE SURFACE (14)

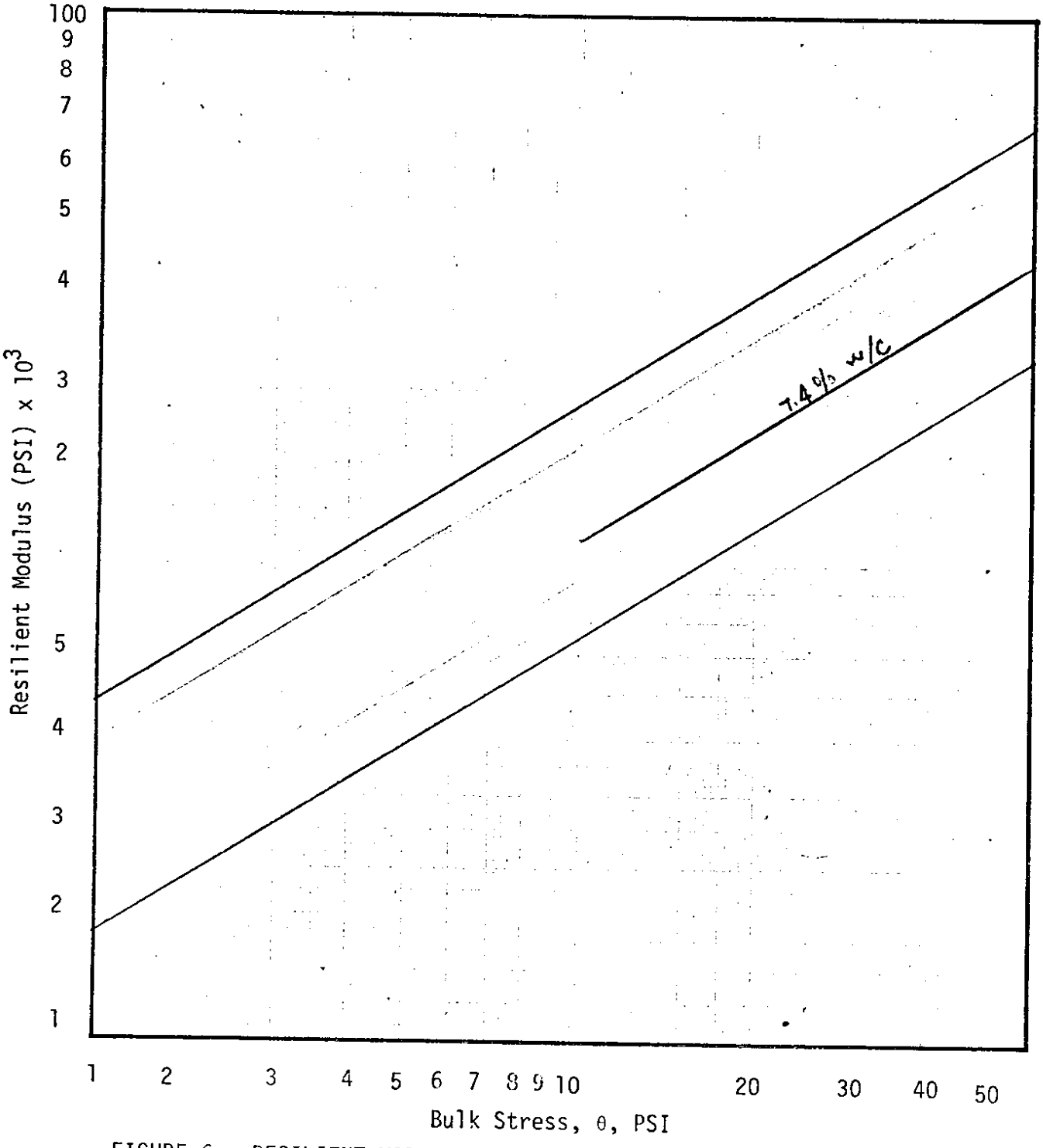

FIGURE 6 - RESILIENT MODULUS VS. BULK STRESS RELATIONSHIPS FOR UNTREATED BASE MATERIAL (14)

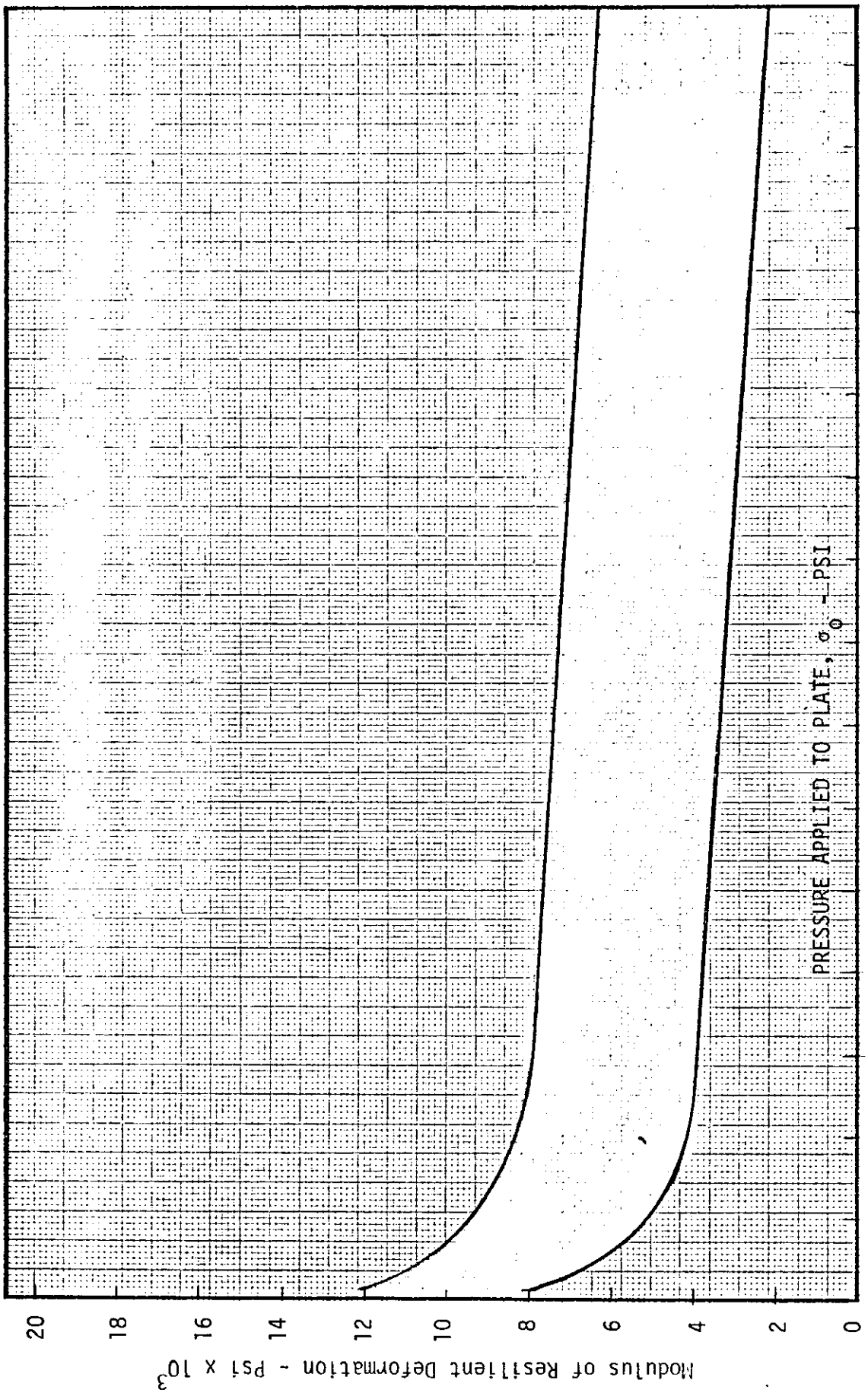

FIGURE 7 - RELATION BETWEEN RESILIENT MODULUS OF THE SUBGRADE, AS DETERMINED BY REPEATED PLATE-LOAD TEST, AND APPLIED PRESSURE (18,p.894)

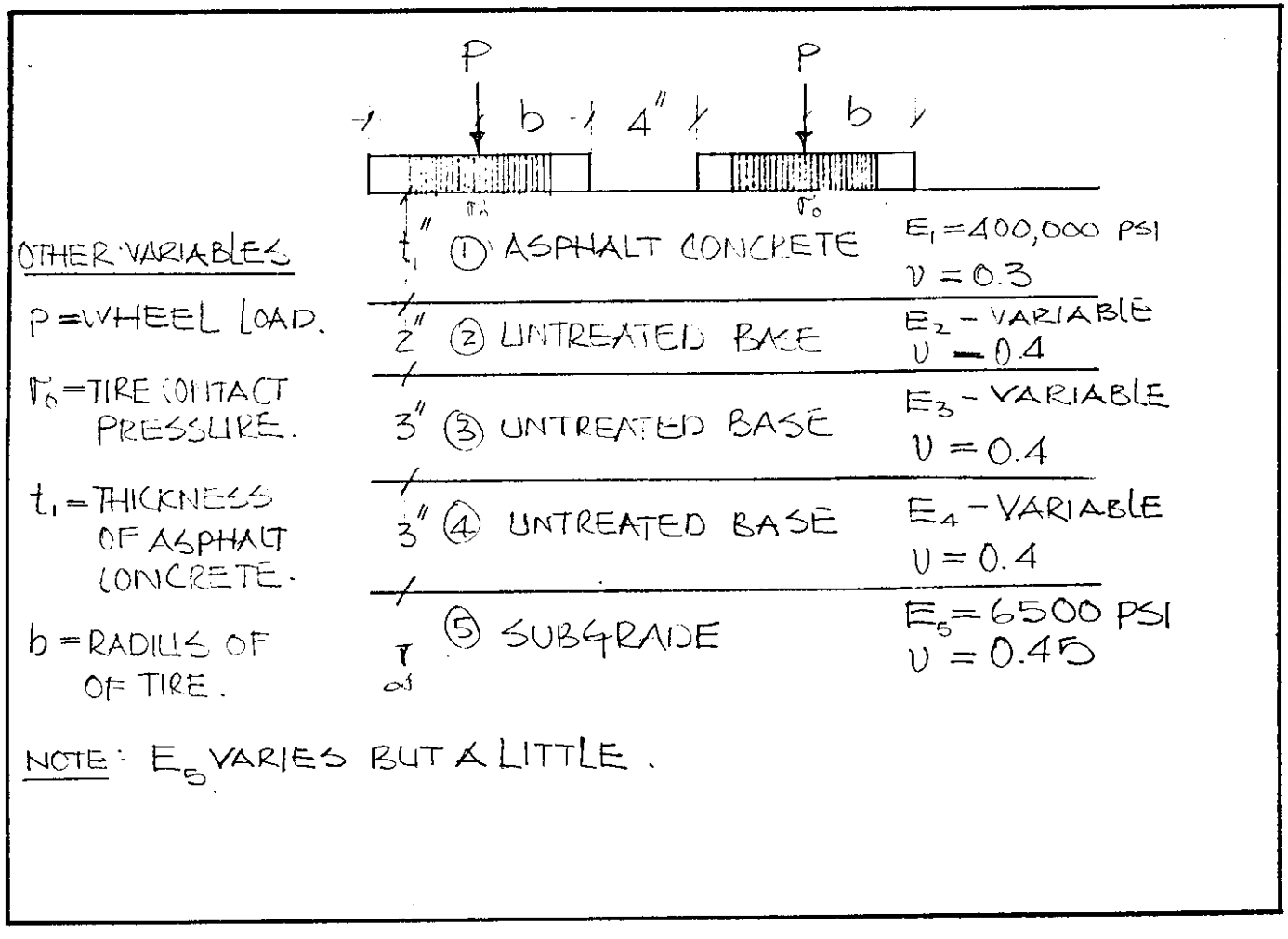

FIGURE 8 - CROSS-SECTION GEOMETRY OF THE PAVEMENT STRUCTURE INCLUDING INPUT VARIABLE AND MATERIAL PARAMETERS AS USED IN THE COMPUTER ANALYSIS

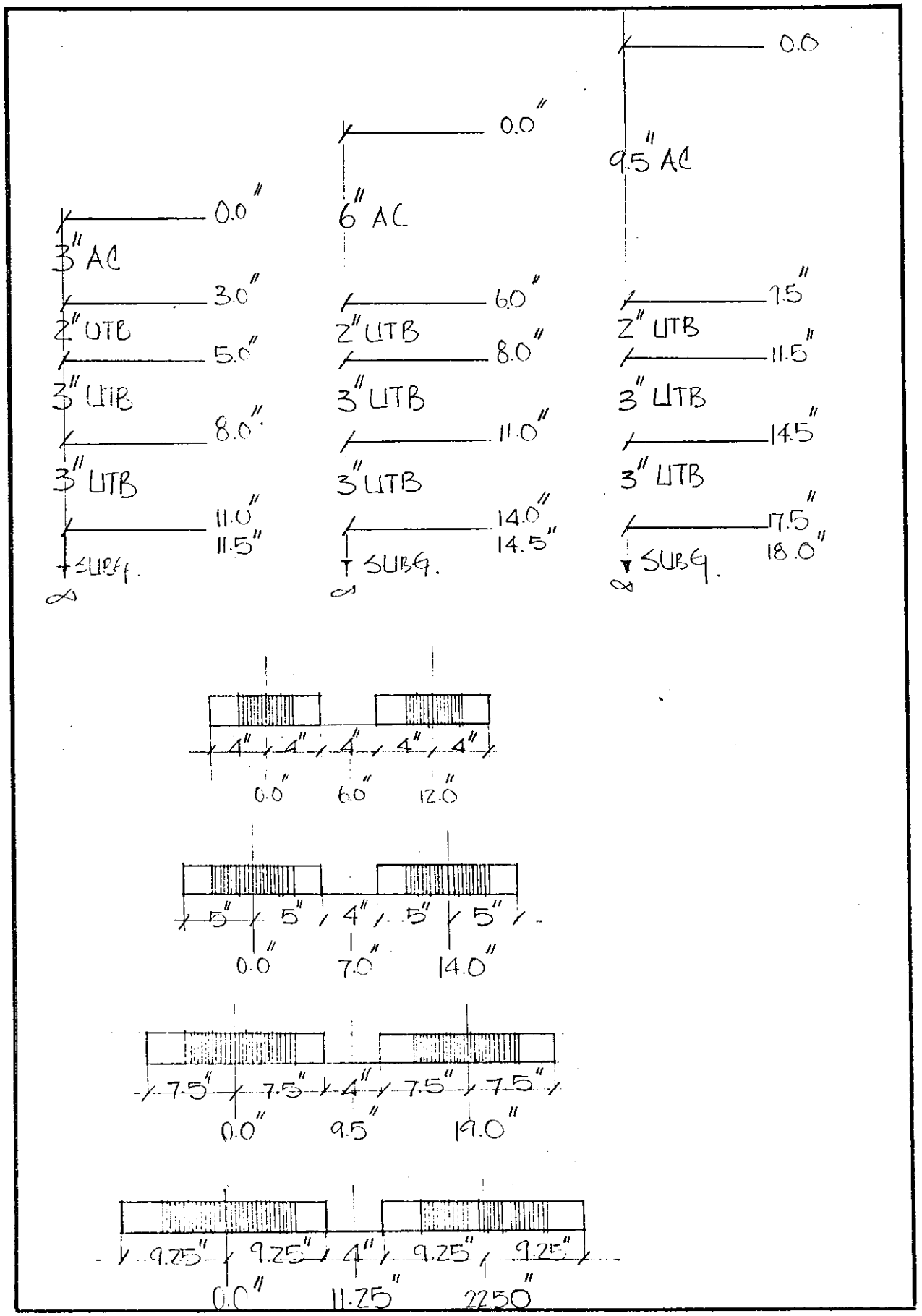

FIGURE 9 - DEPTHS BELOW SURFACE AND RADIAL DISTANCES BEING CONSIDERED

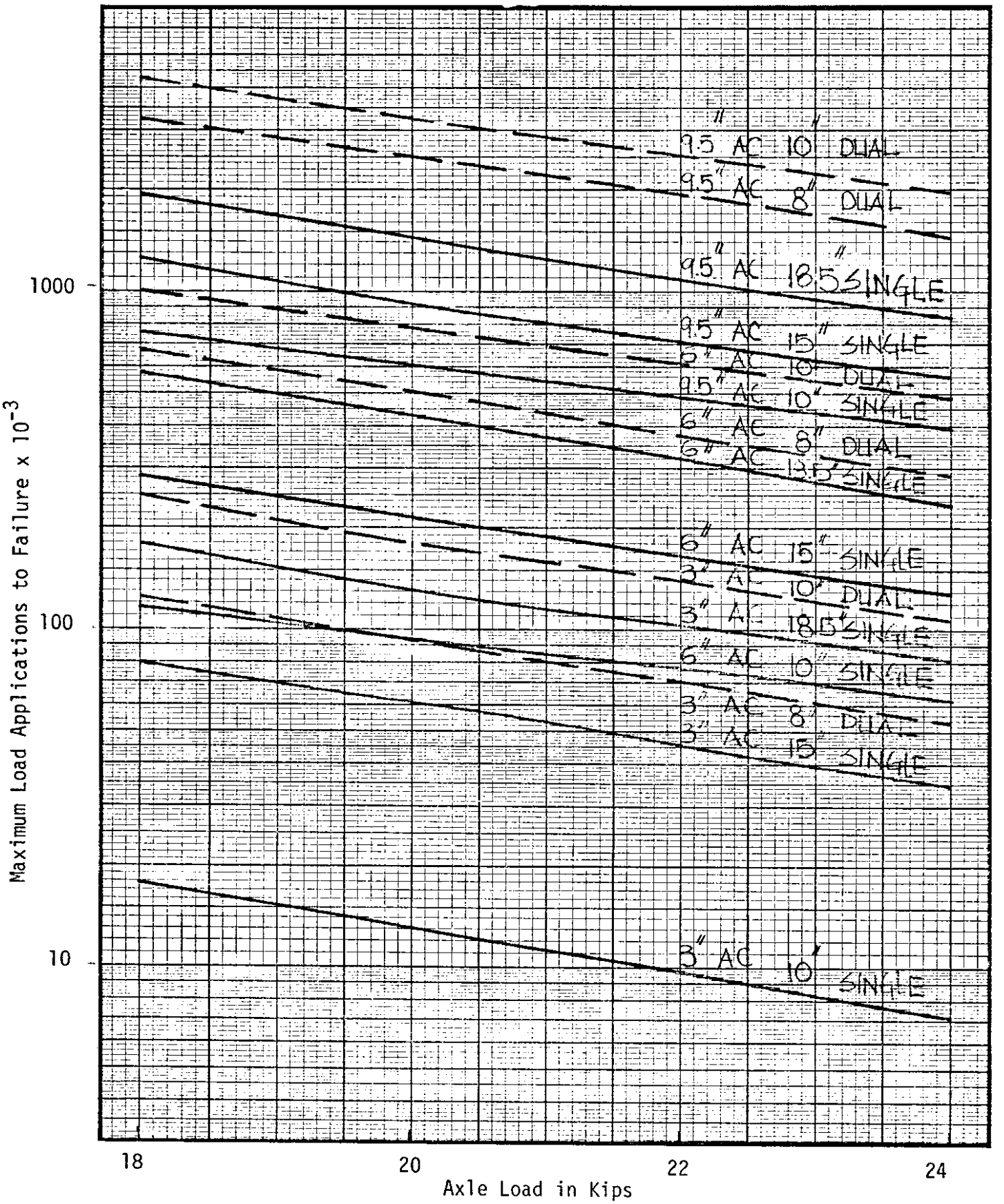

FIGURE 10 - EQUIVALENCIES FOR FATIGUE BEHAVIOR FOR A RANGE OF LOAD AND PAVEMENTS. VALUES HAVE BEEN NORMALIZED TO STANDARD CASE OF 10-INCH DUAL TIRES, 6-INCH ASPHALT CONCRETE AND 18-Kip AXLE LOAD

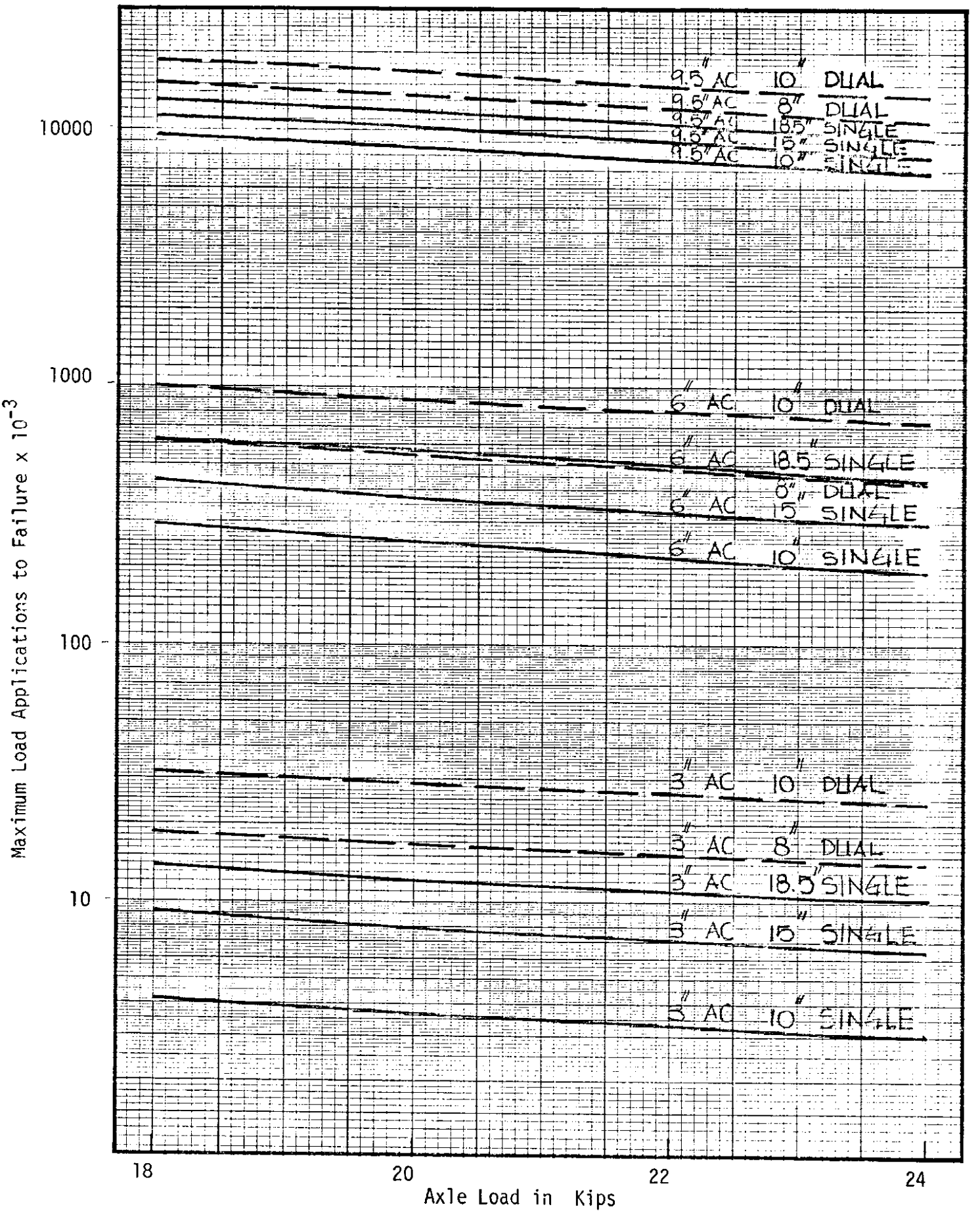

FIGURE 11 - EQUIVALENCIES FOR RUTTING BEHAVIOR FOR A RANGE OF LOAD AND PAVEMENTS. VALUES HAVE BEEN NORMALIZED TO STANDARD CASE OF 10-INCH DUAL TIRES, 6-INCH ASPHALT CONCRETE AND 18-Kip AXLE LOAD

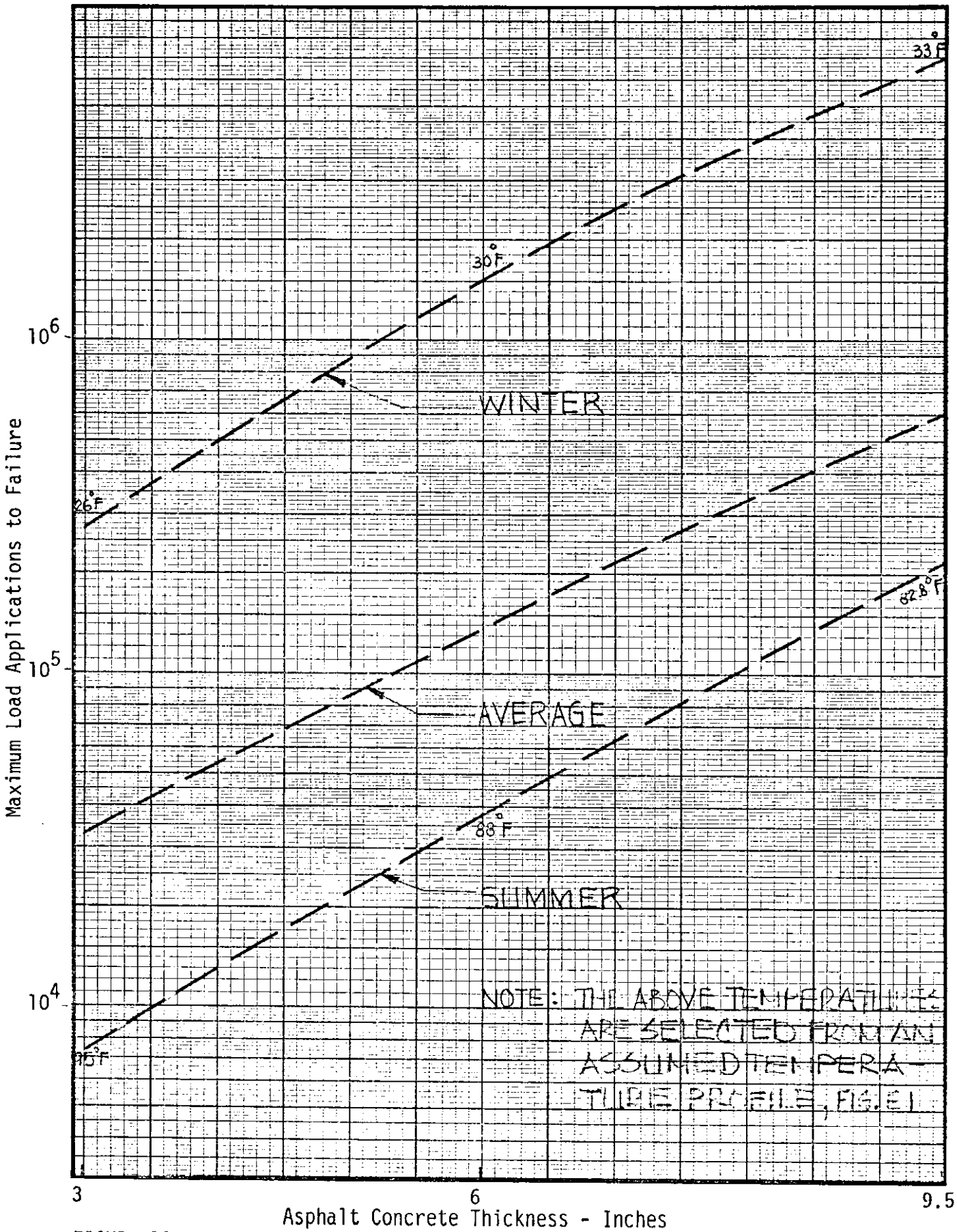

FIGURE 12 - MAXIMUM NUMBER OF 18-Kip AXLE LOAD APPLICATIONS ON ASPHALT CONCRETE VS. ASPHALT CONCRETE THICKNESS RELATIONSHIPS FOR SUMMER, AVERAGE AND WINTER

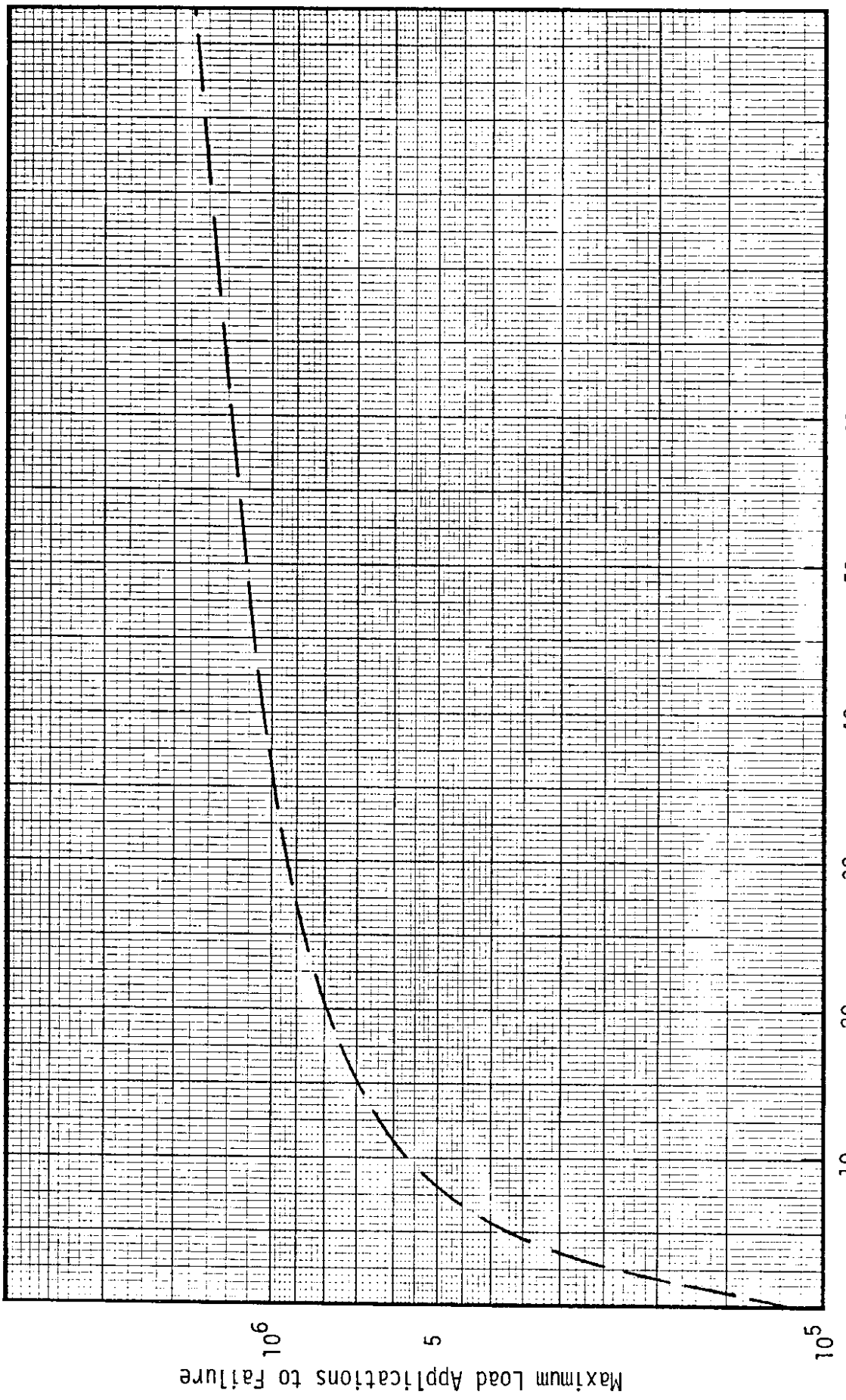

FIGURE 13 - RELATIONSHIP BETWEEN MAXIMUM NUMBER OF 18-Kip AXLE LOAD APPLICATIONS ON ASPHALT CONCRETE AND VEHICLE SPEED

APPENDIX A

SUMMARY OF PAVEMENT RESPONSE FOR RANGE OF:

WHEEL LOAD

TIRE WIDTH

SINGLE AND DUAL TIRES

PAVEMENT THICKNESS

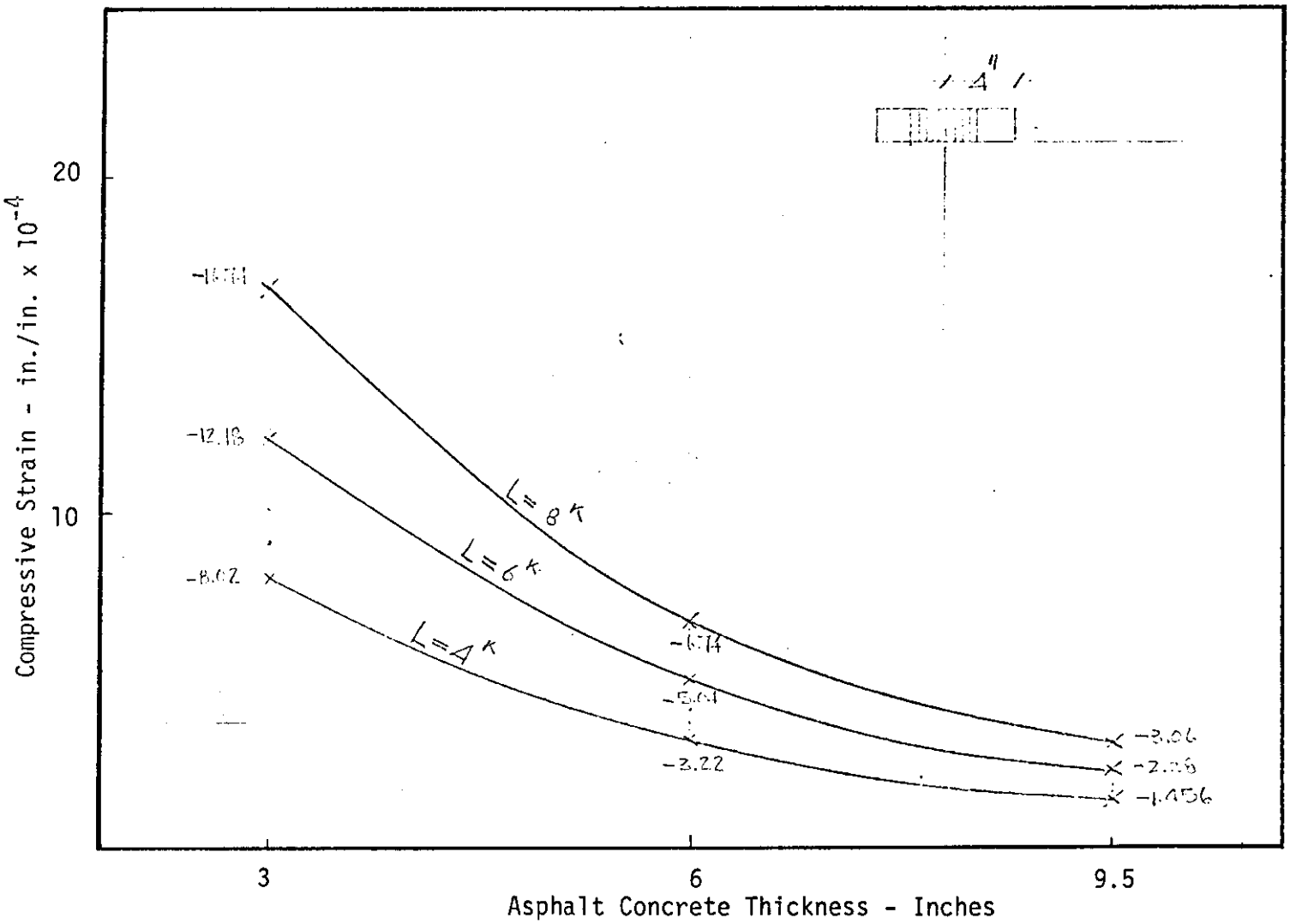

FIGURE A1 - MAXIMUM SUBGRADE COMPRESSIVE STRAIN VS. ASPHALT CONCRETE THICKNESS RELATIONSHIPS FOR VARIOUS WHEEL LOADS

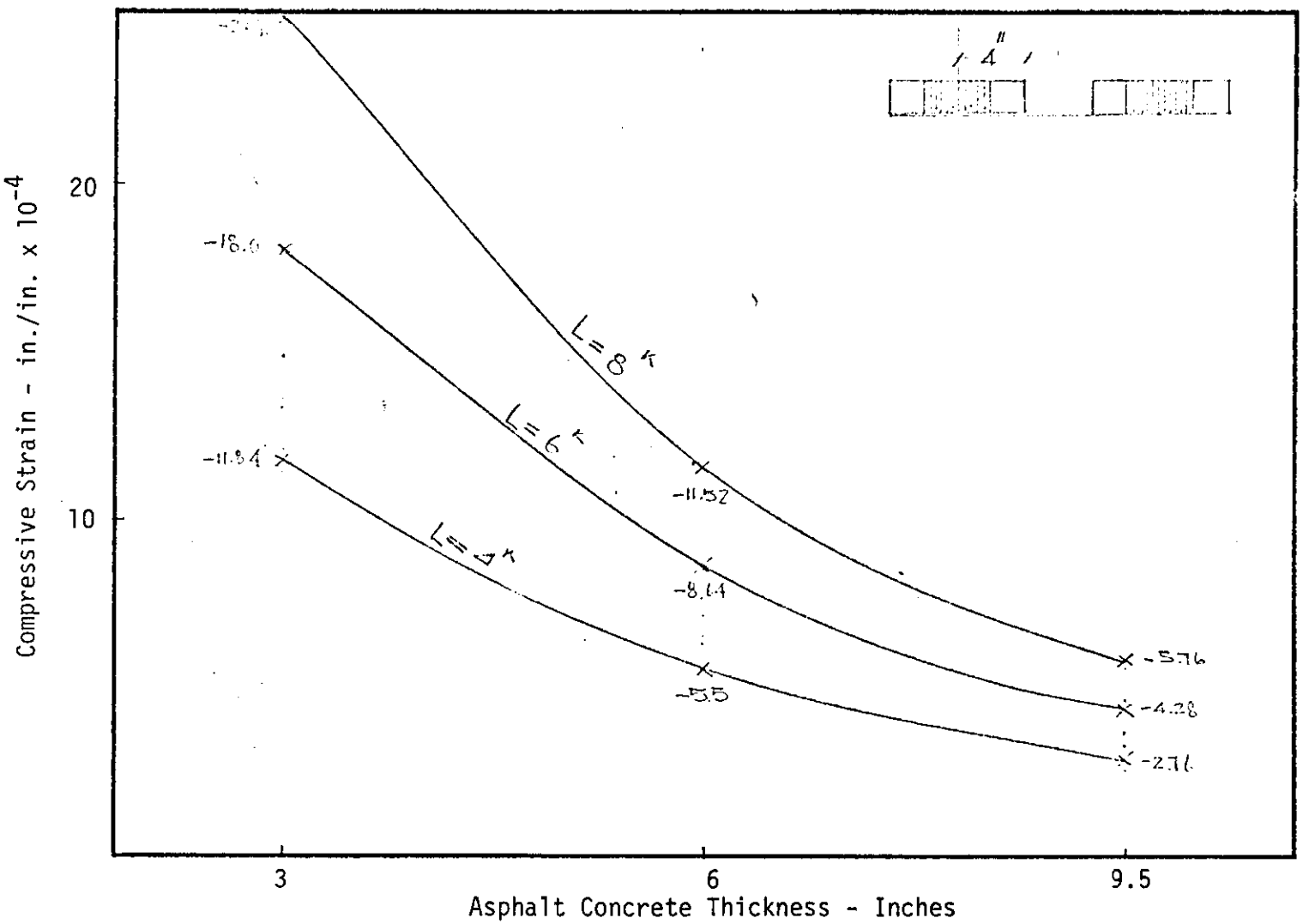

FIGURE A2 - MAXIMUM SUBGRADE COMPRESSIVE STRAIN VS. ASPHALT CONCRETE THICKNESS RELATIONSHIPS FOR VARIOUS WHEEL LOADS

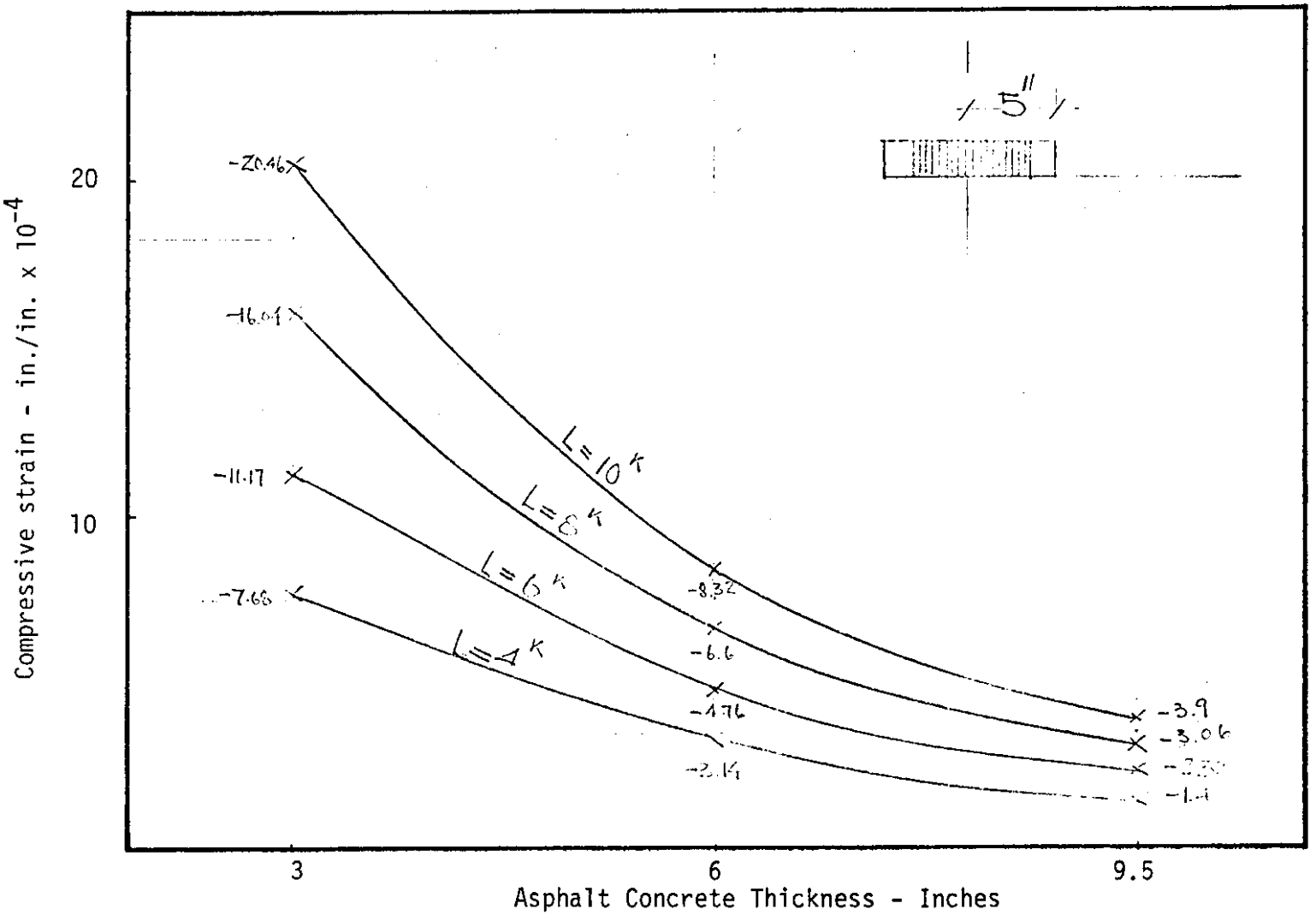

FIGURE A3 - MAXIMUM SUBGRADE COMPRESSIVE STRAIN VS. ASPHALT CONCRETE THICKNESS RELATIONSHIPS FOR VARIOUS WHEEL LOADS

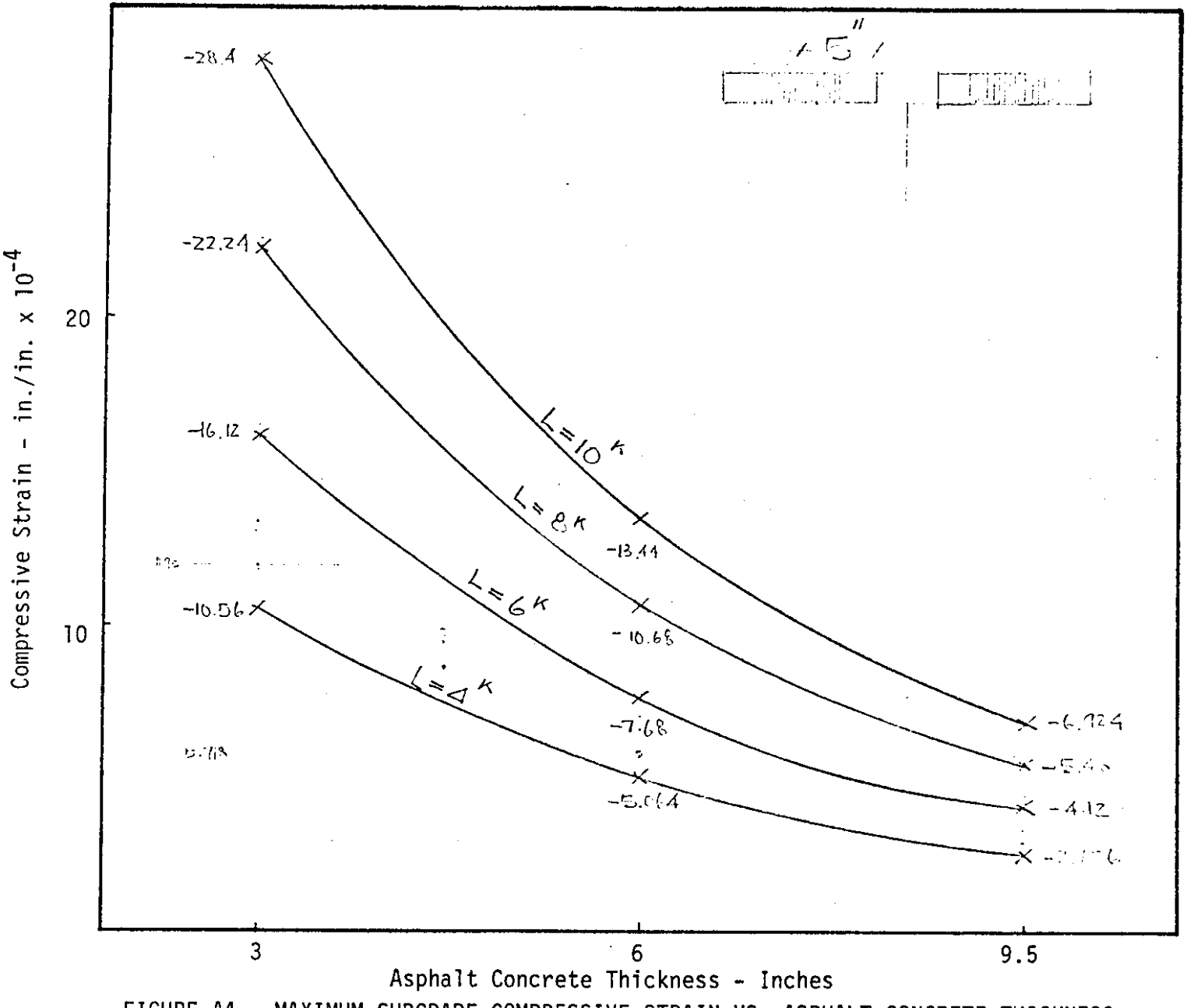

FIGURE A4 - MAXIMUM SUBGRADE COMPRESSIVE STRAIN VS. ASPHALT CONCRETE THICKNESS RELATIONSHIPS FOR VARIOUS WHEEL LOADS

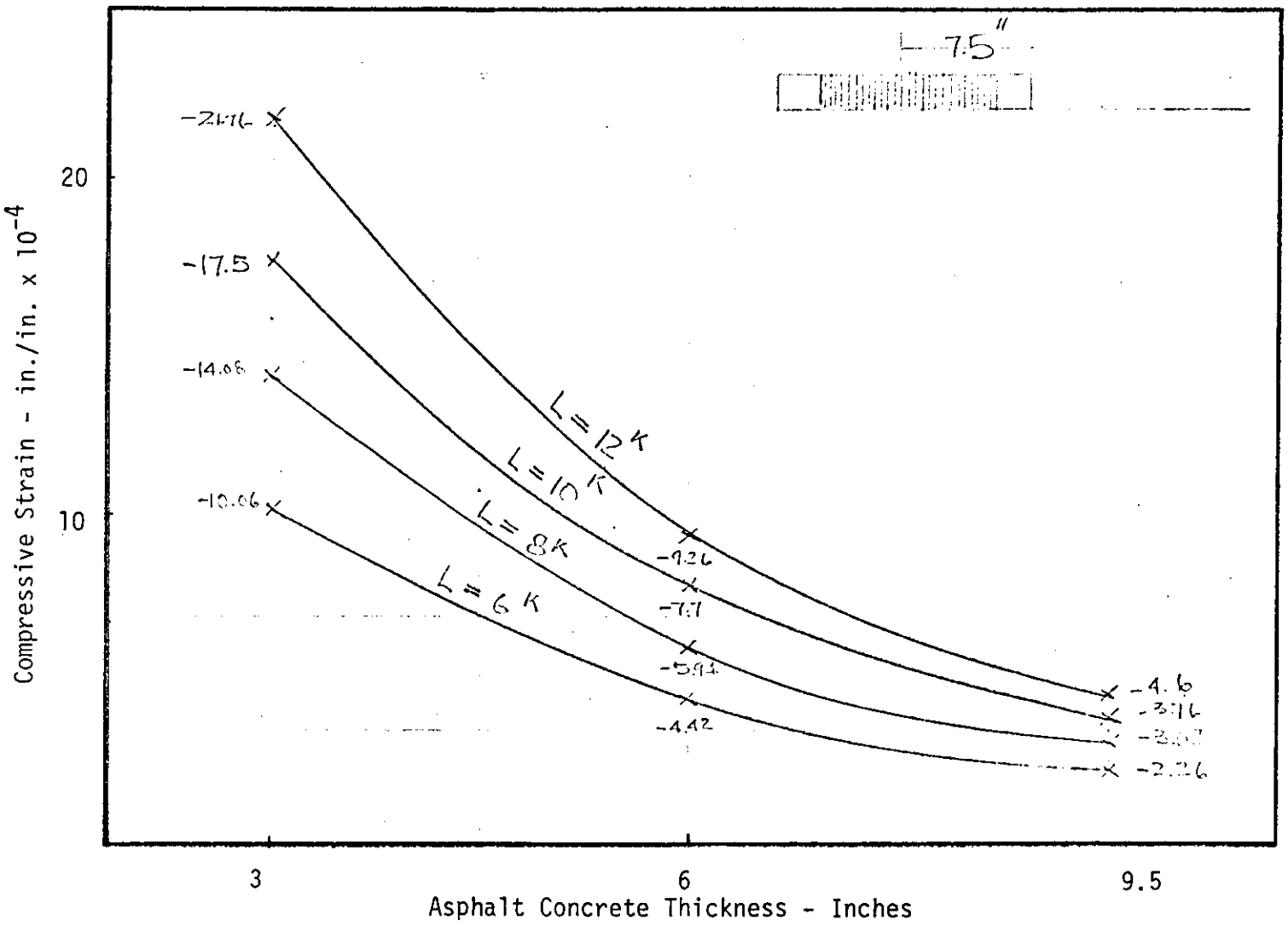

FIGURE A5 - MAXIMUM SUBGRADE COMPRESSIVE STRAIN VS. ASPHALT CONCRETE THICKNESS RELATIONSHIPS FOR VARIOUS WHEEL LOADS

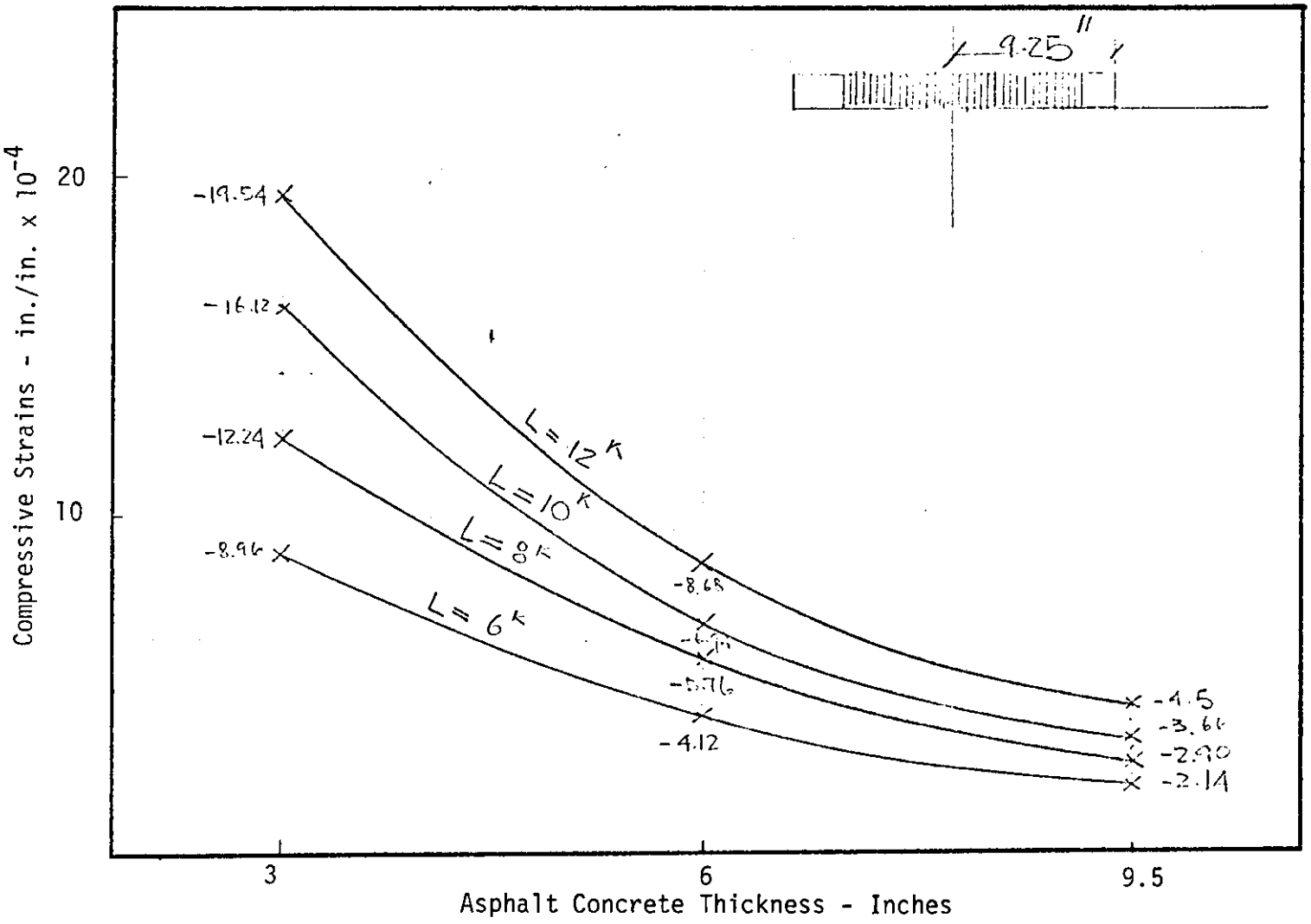

FIGURE A6 - MAXIMUM SUBGRADE COMPRESSIVE STRAIN VS. ASPHALT CONCRETE THICKNESS RELATIONSHIPS FOR VARIOUS WHEEL LOADS

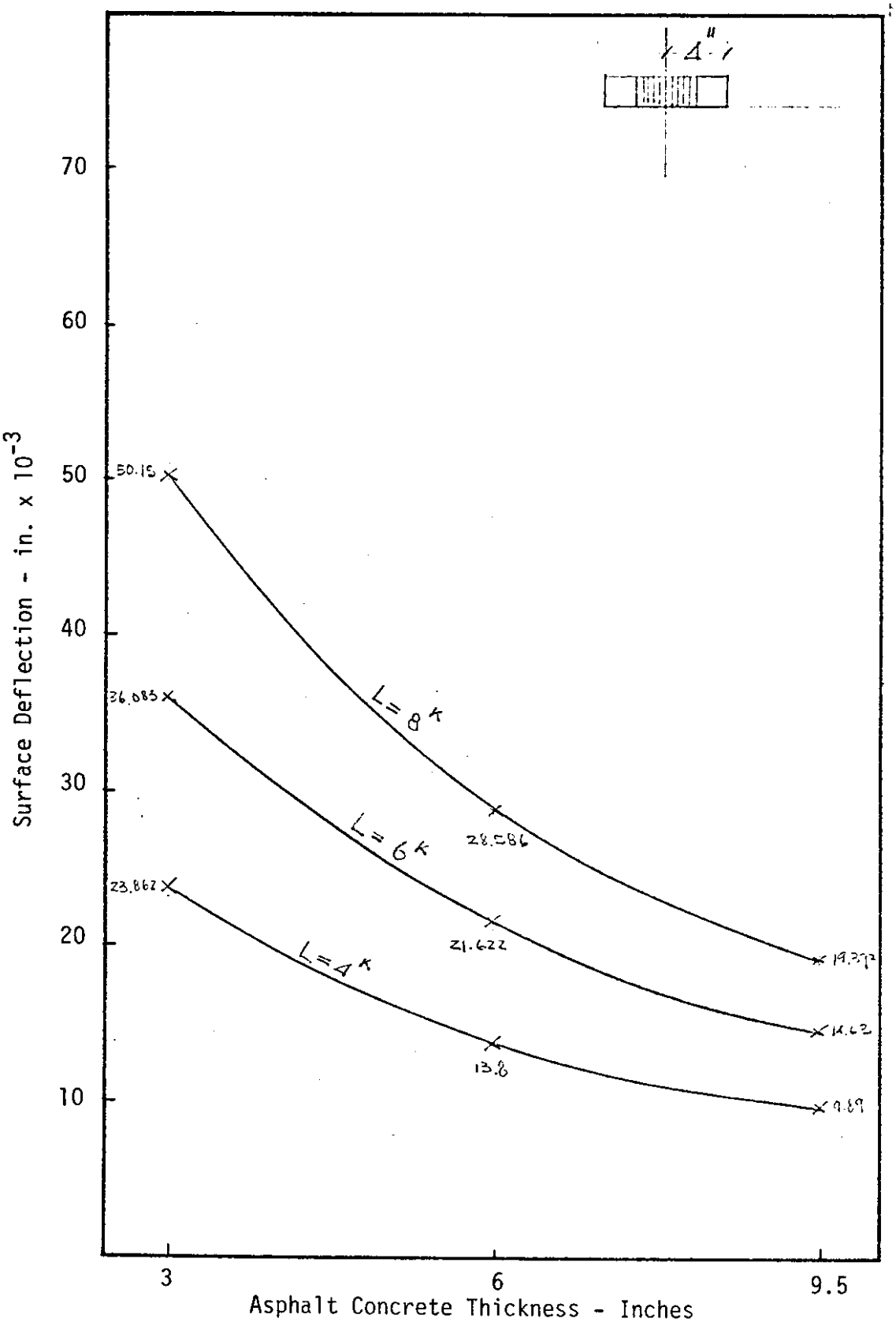

FIGURE A7 - MAXIMUM SURFACE DEFLECTION VS. ASPHALT CONCRETE THICKNESS FOR VARIOUS WHEEL LOADS

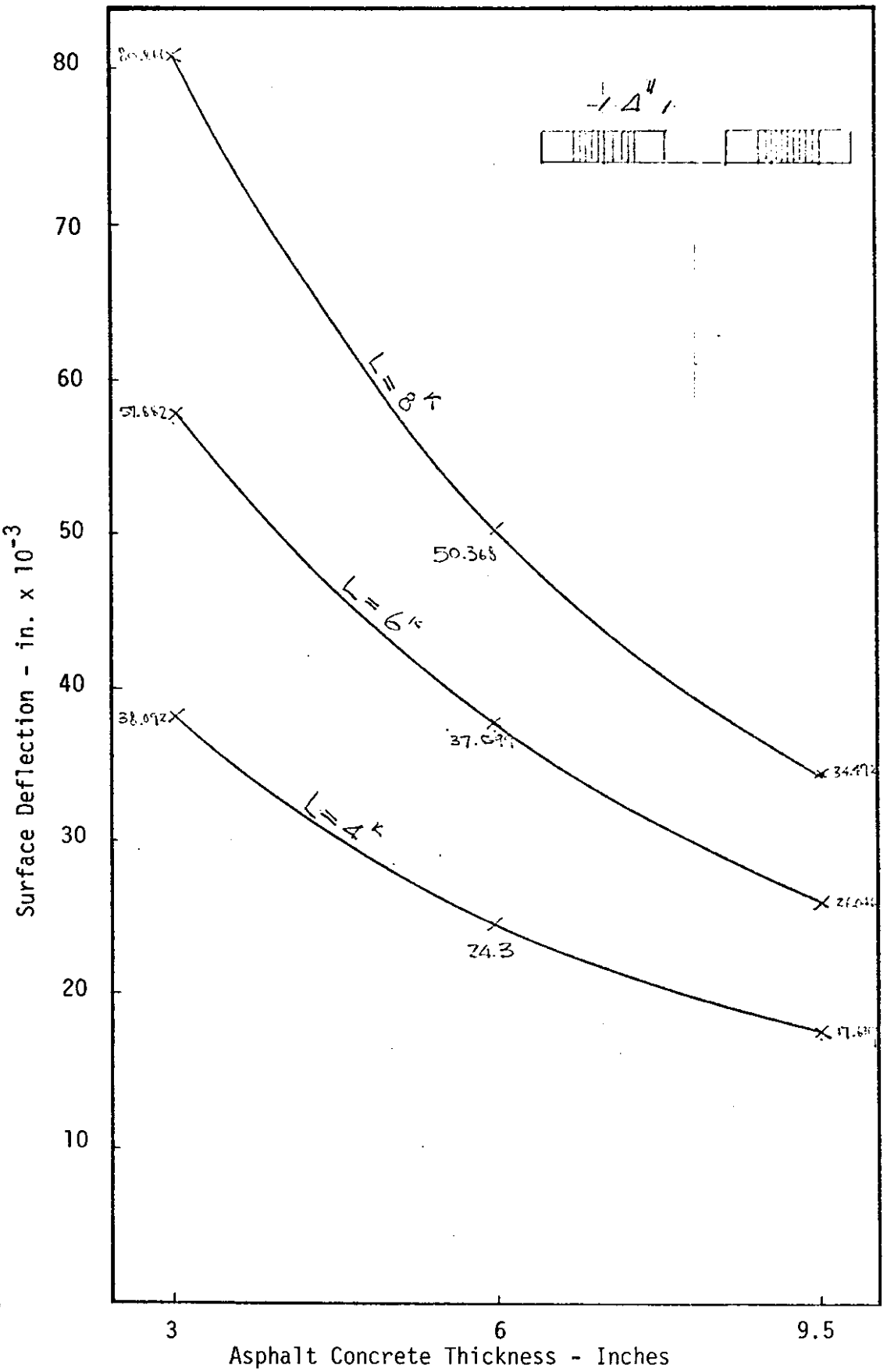

FIGURE A8 - MAXIMUM SURFACE DEFLECTION VS. ASPHALT CONCRETE THICKNESS RELATIONSHIPS FOR VARIOUS WHEEL LOADS

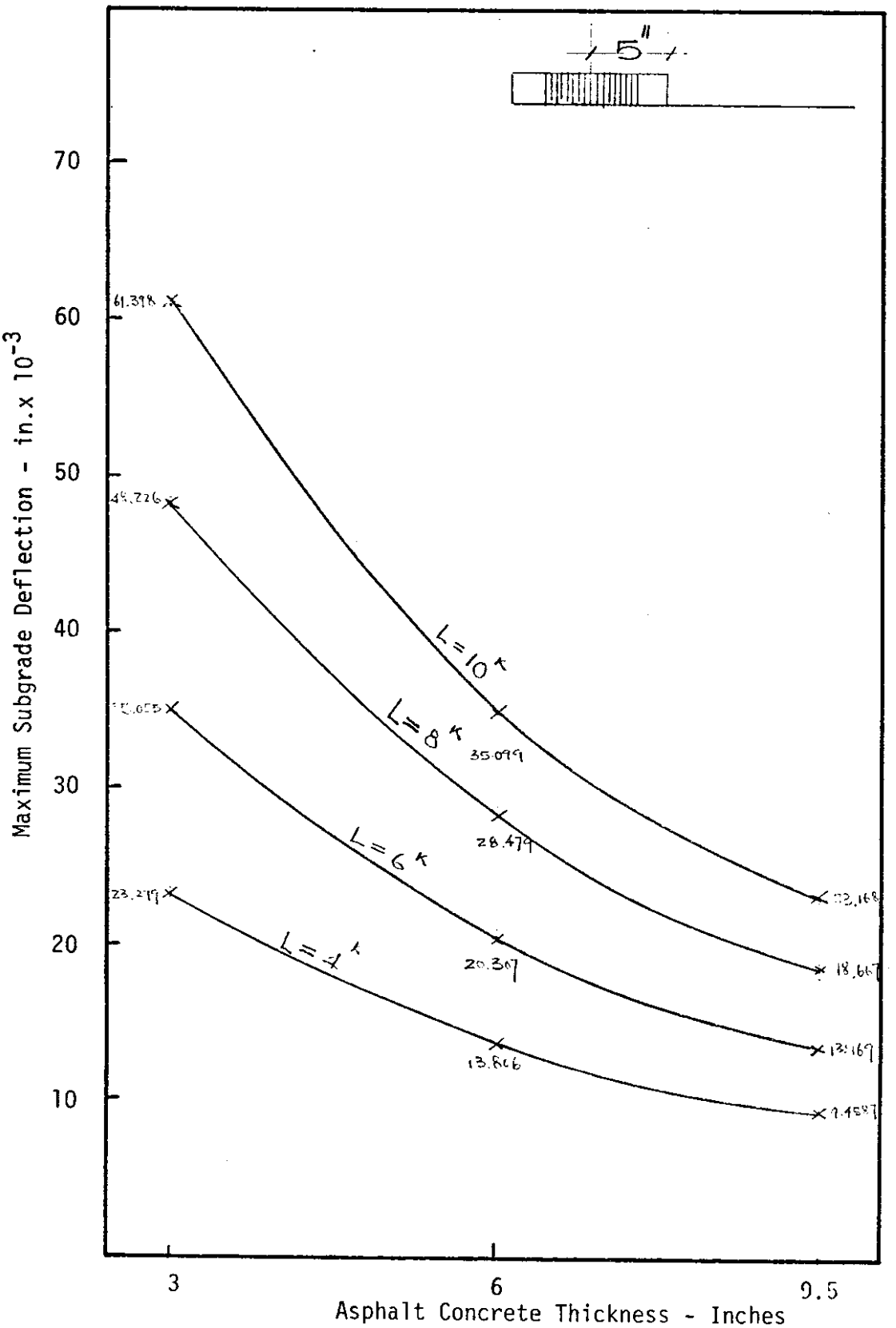

FIGURE A9 - MAXIMUM SURFACE DEFLECTION VS. ASPHALT CONCRETE THICKNESS RELATIONSHIPS FOR VARIOUS WHEEL LOADS

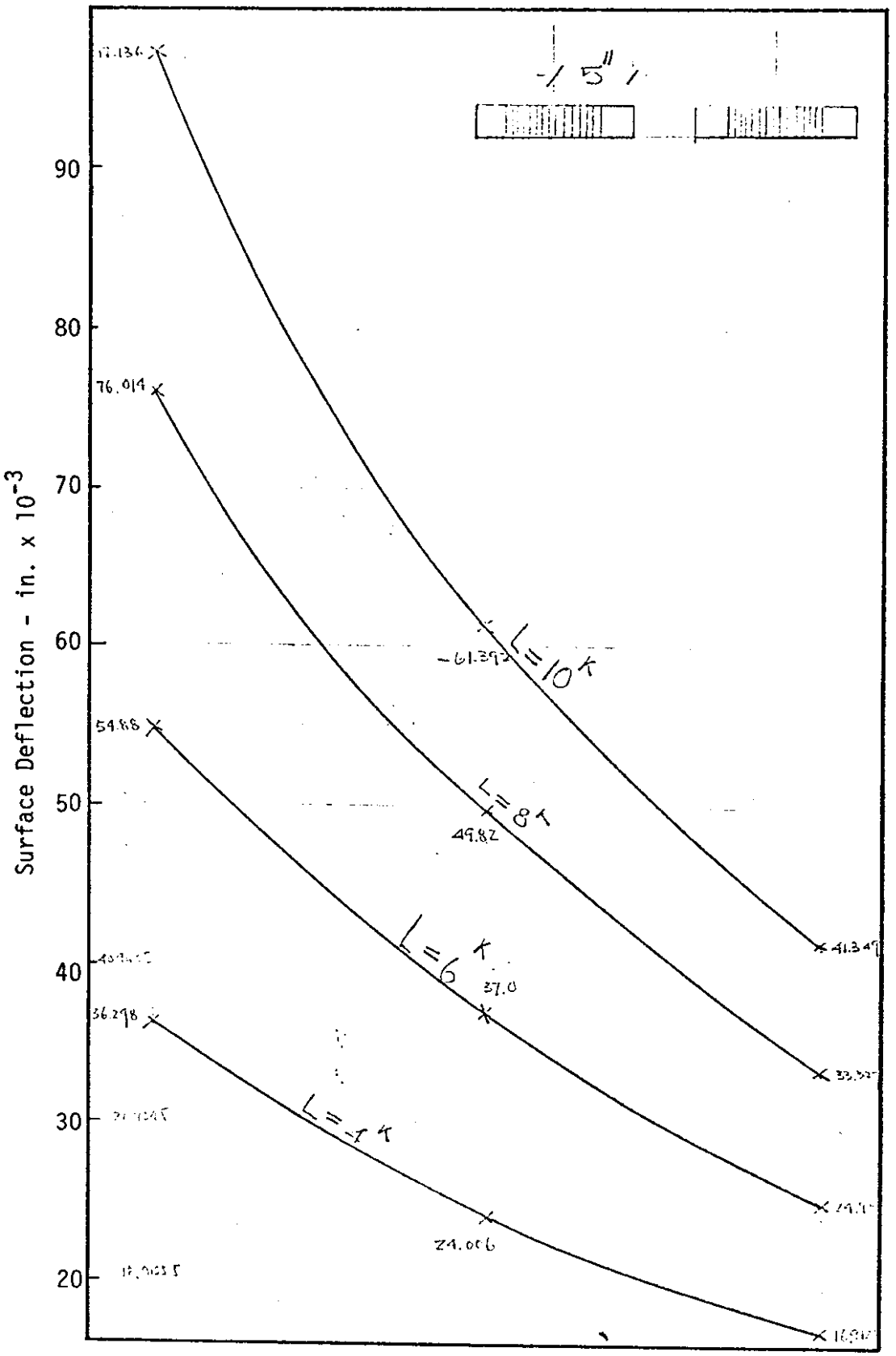

FIGURE A10 - MAXIMUM SURFACE DEFLECTION VS. ASPHALT CONCRETE THICKNESS RELATIONSHIPS FOR VARIOUS WHEEL LOADS

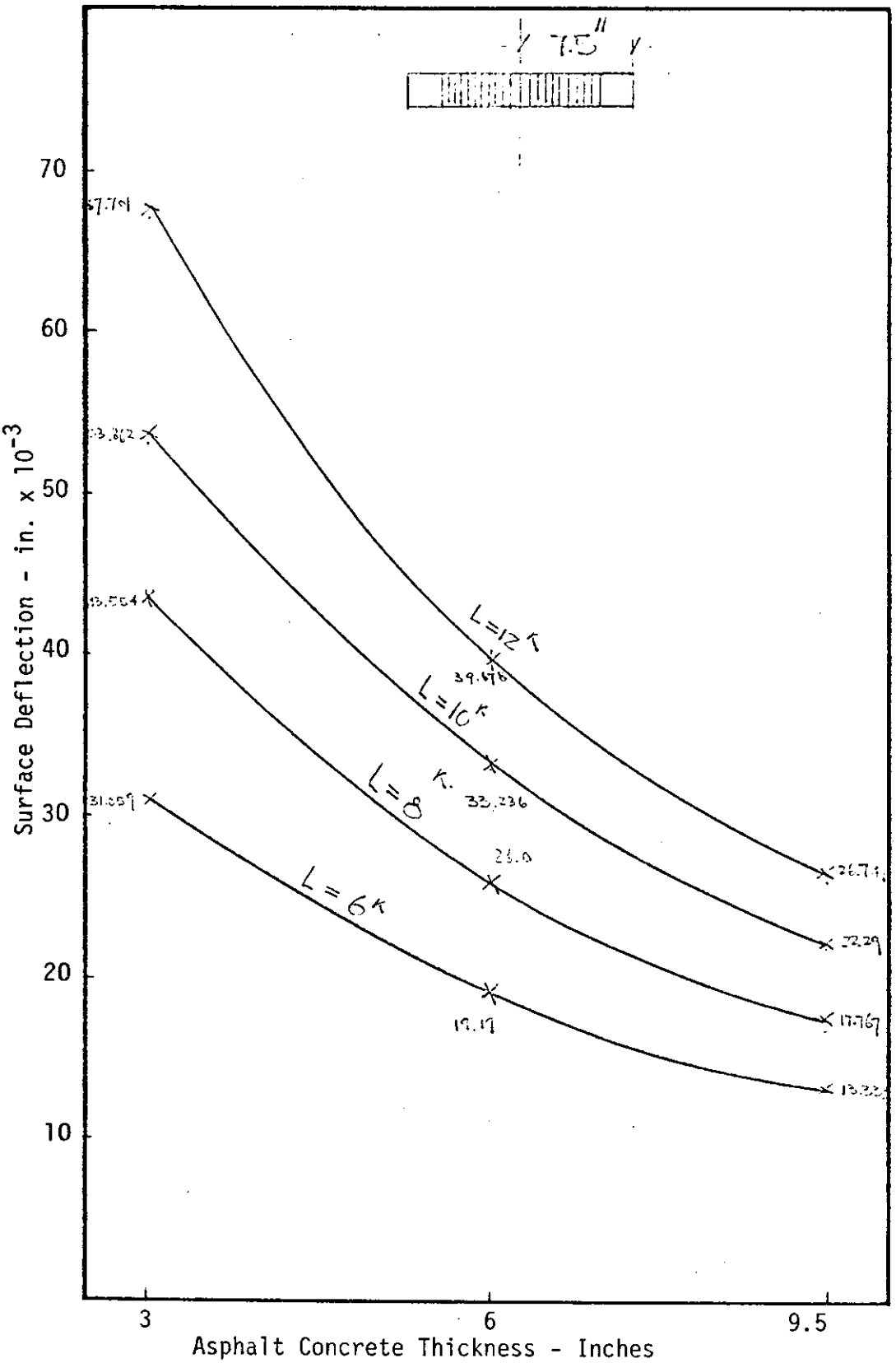

FIGURE A11 - MAXIMUM SURFACE DEFLECTION VS. ASPHALT CONCRETE THICKNESS RELATIONSHIPS FOR VARIOUS WHEEL LOADS

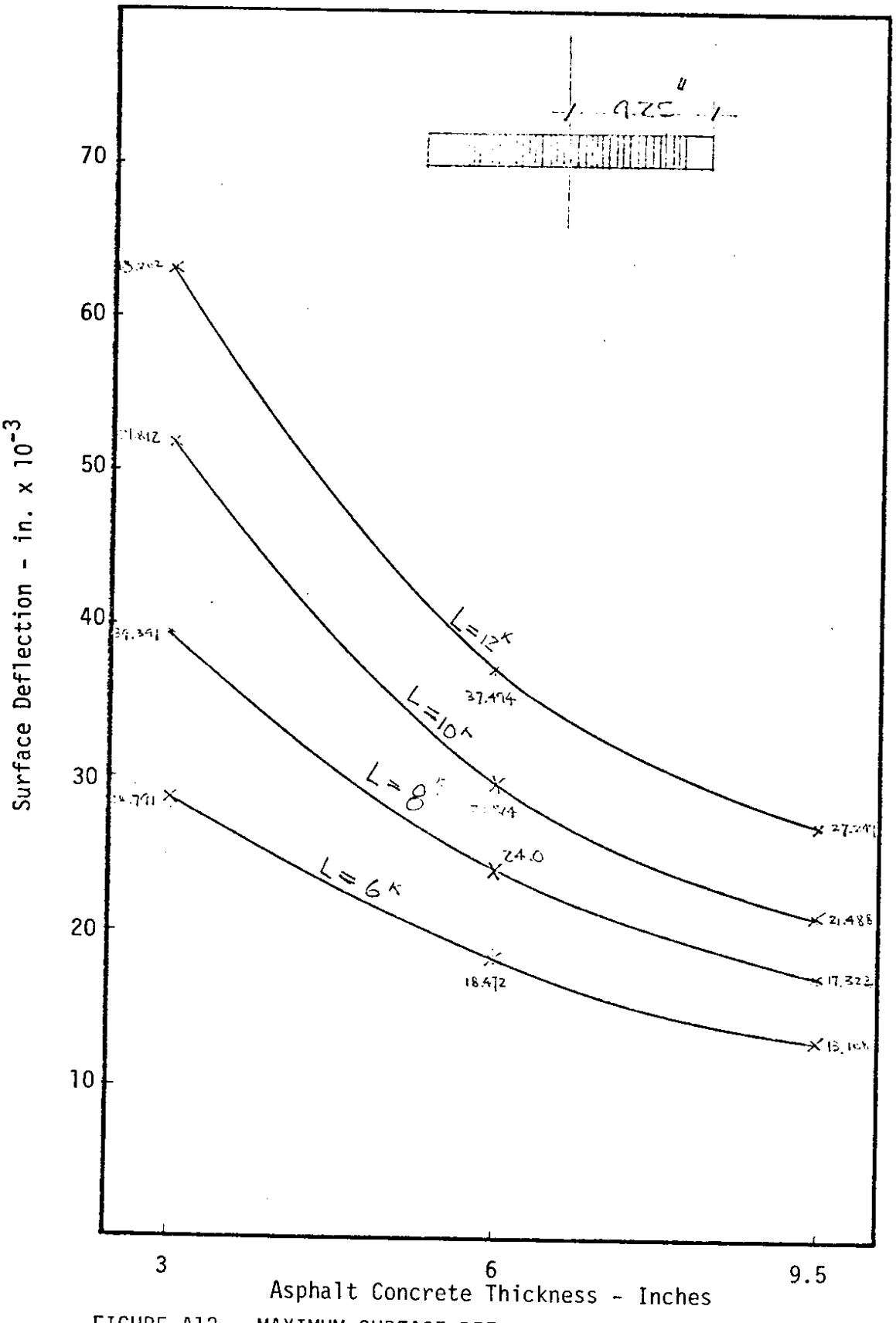

FIGURE A12 - MAXIMUM SURFACE DEFLECTION VS. ASPHALT CONCRETE THICKNESS RELATIONSHIPS FOR VARIOUS WHEEL LOADS

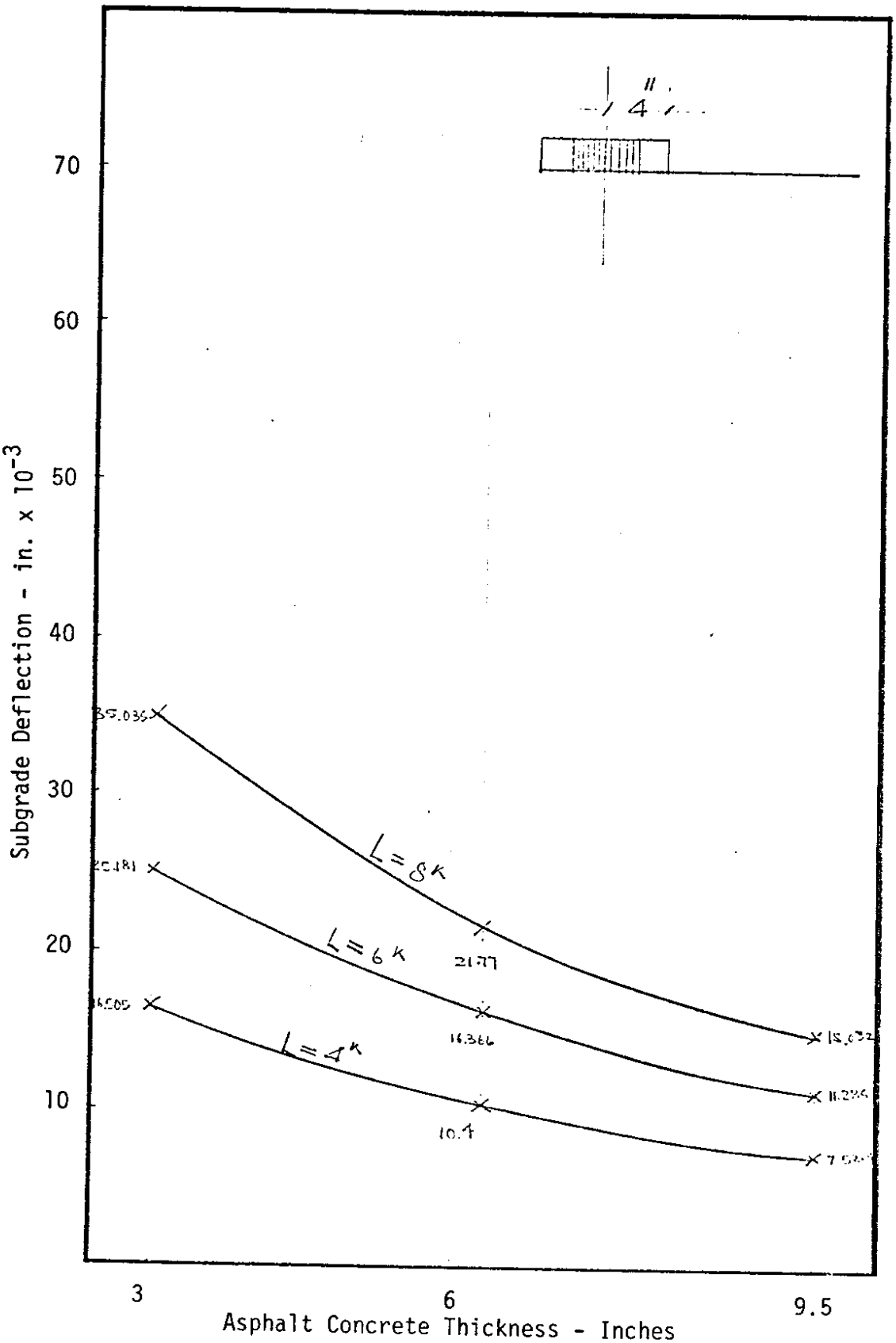

FIGURE A13 - MAXIMUM SUBGRADE DEFLECTION VS. ASPHALT CONCRETE THICKNESS RELATIONSHIPS FOR VARIOUS WHEEL LOADS

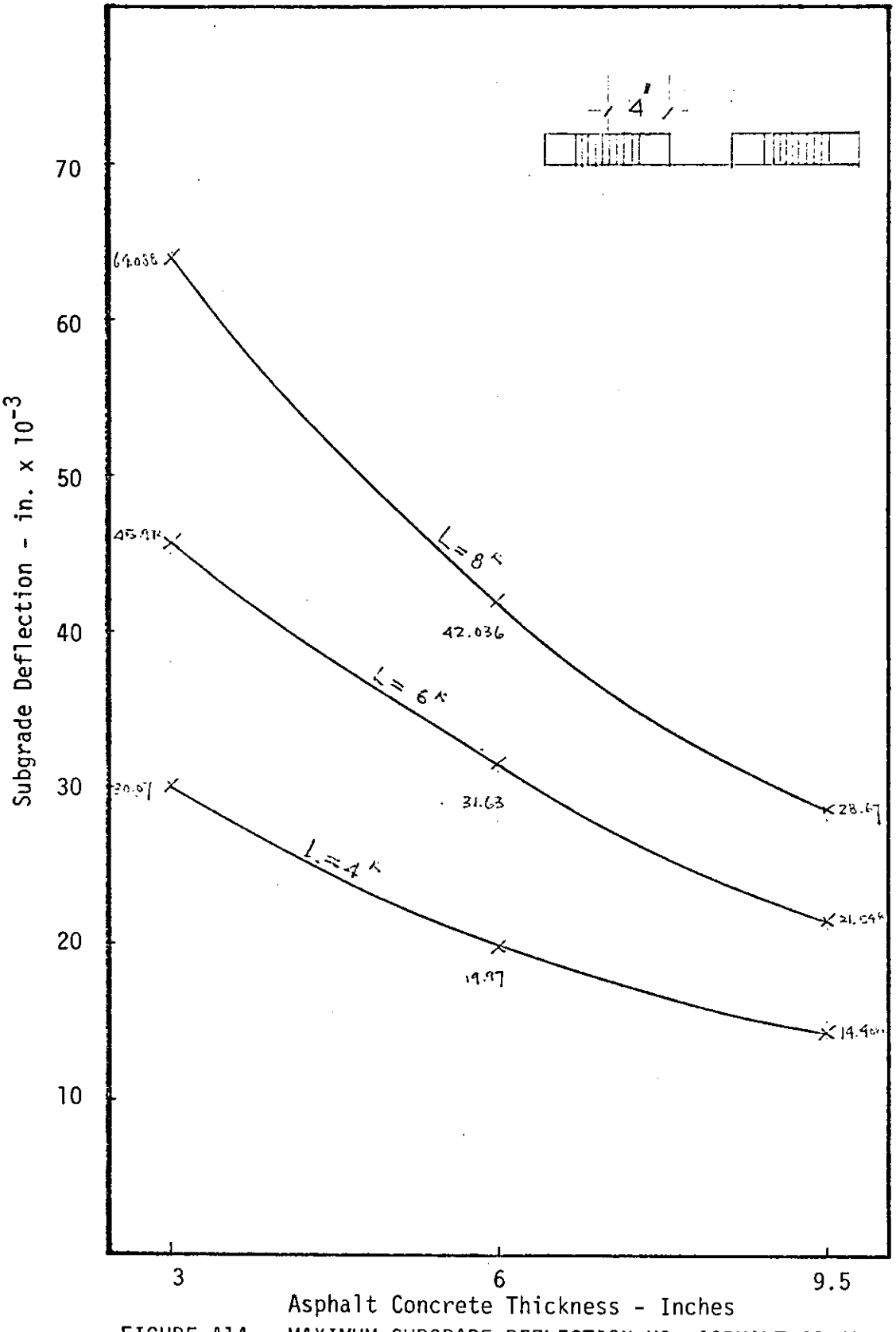

FIGURE A14 - MAXIMUM SUBGRADE DEFLECTION VS. ASPHALT CONCRETE THICKNESS RELATIONSHIPS FOR VARIOUS WHEEL LOADS

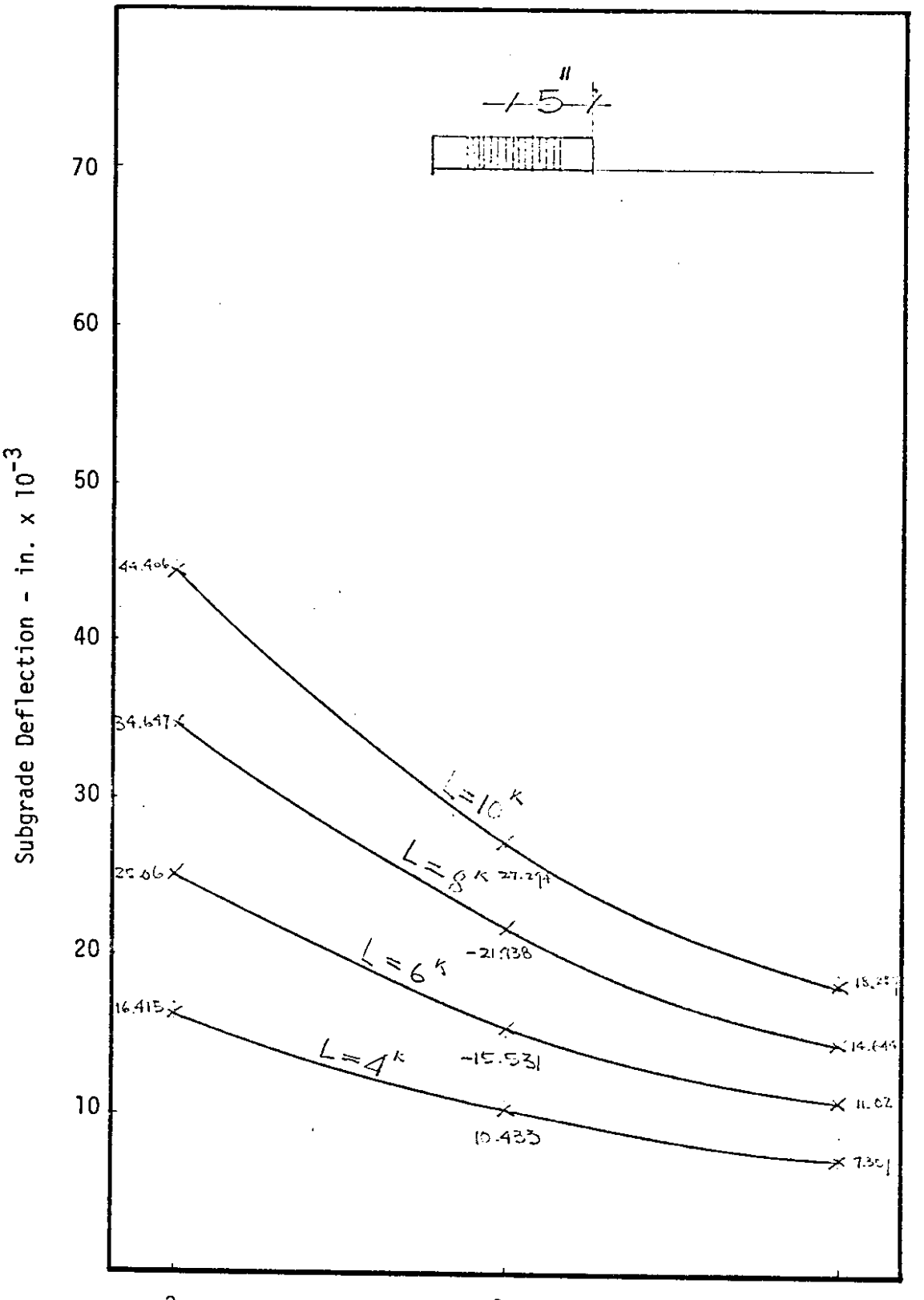

FIGURE A15 - MAXIMUM SUBGRADE DEFLECTION VS. ASPHALT CONCRETE THICKNESS RELATIONSHIPS FOR VARIOUS WHEEL LOADS

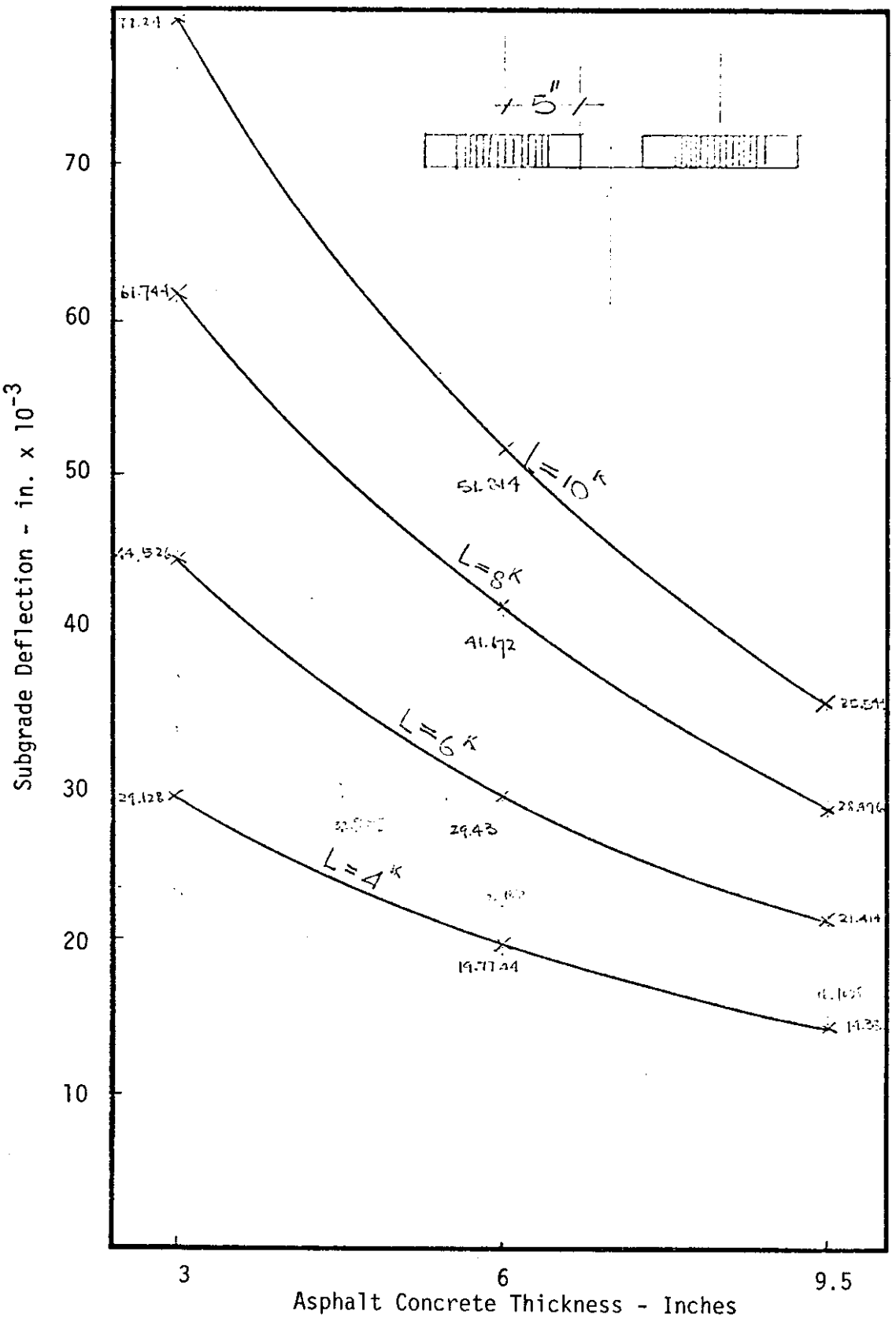

FIGURE A16 - MAXIMUM SUBGRADE DEFLECTION VS. ASPHALT CONCRETE THICKNESS RELATIONSHIPS FOR VARIOUS WHEEL LOADS

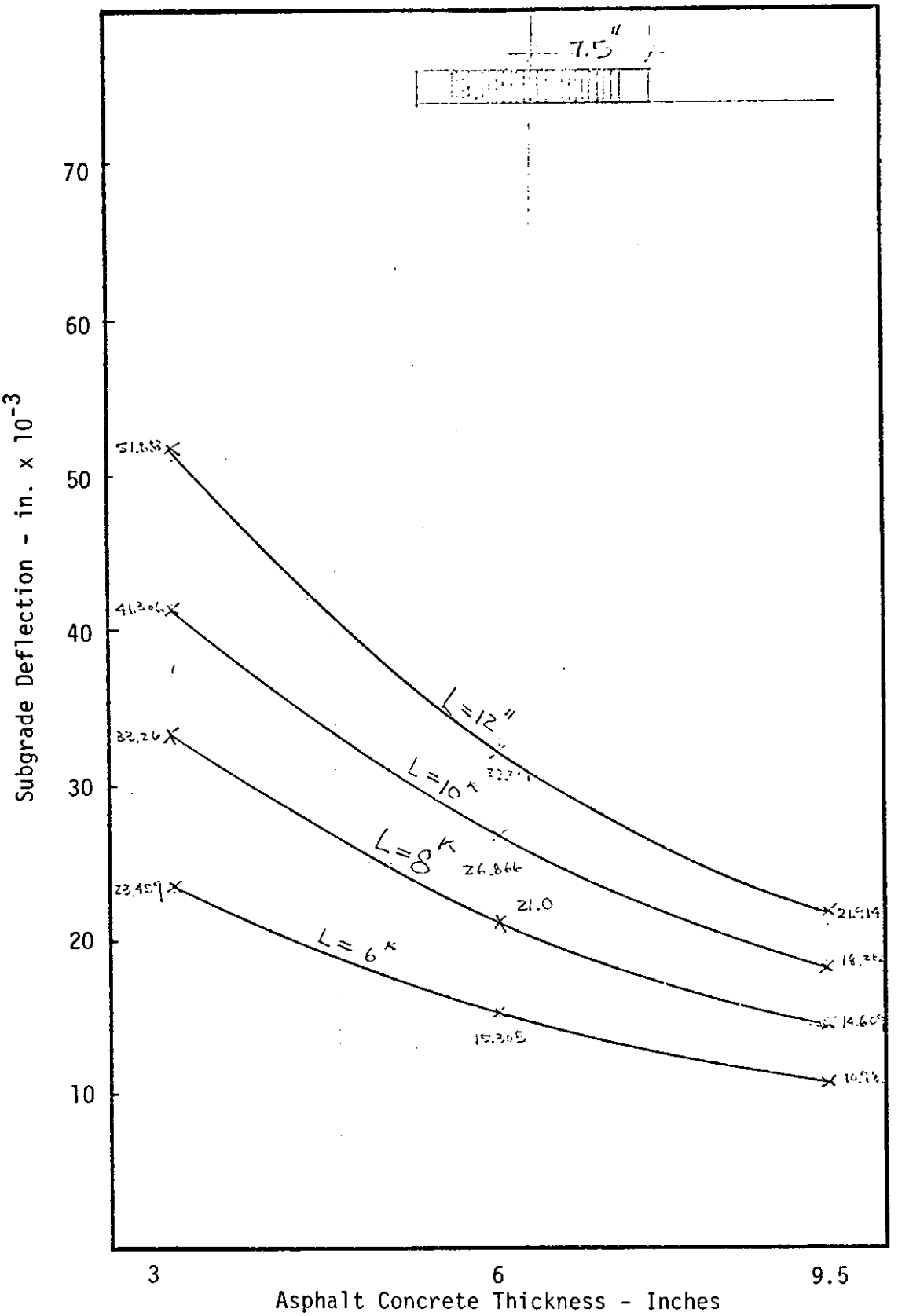

FIGURE A17 - MAXIMUM SUBGRADE DEFLECTION VS. ASPHALT CONCRETE THICKNESS RELATIONSHIPS FOR VARIOUS WHEEL LOADS

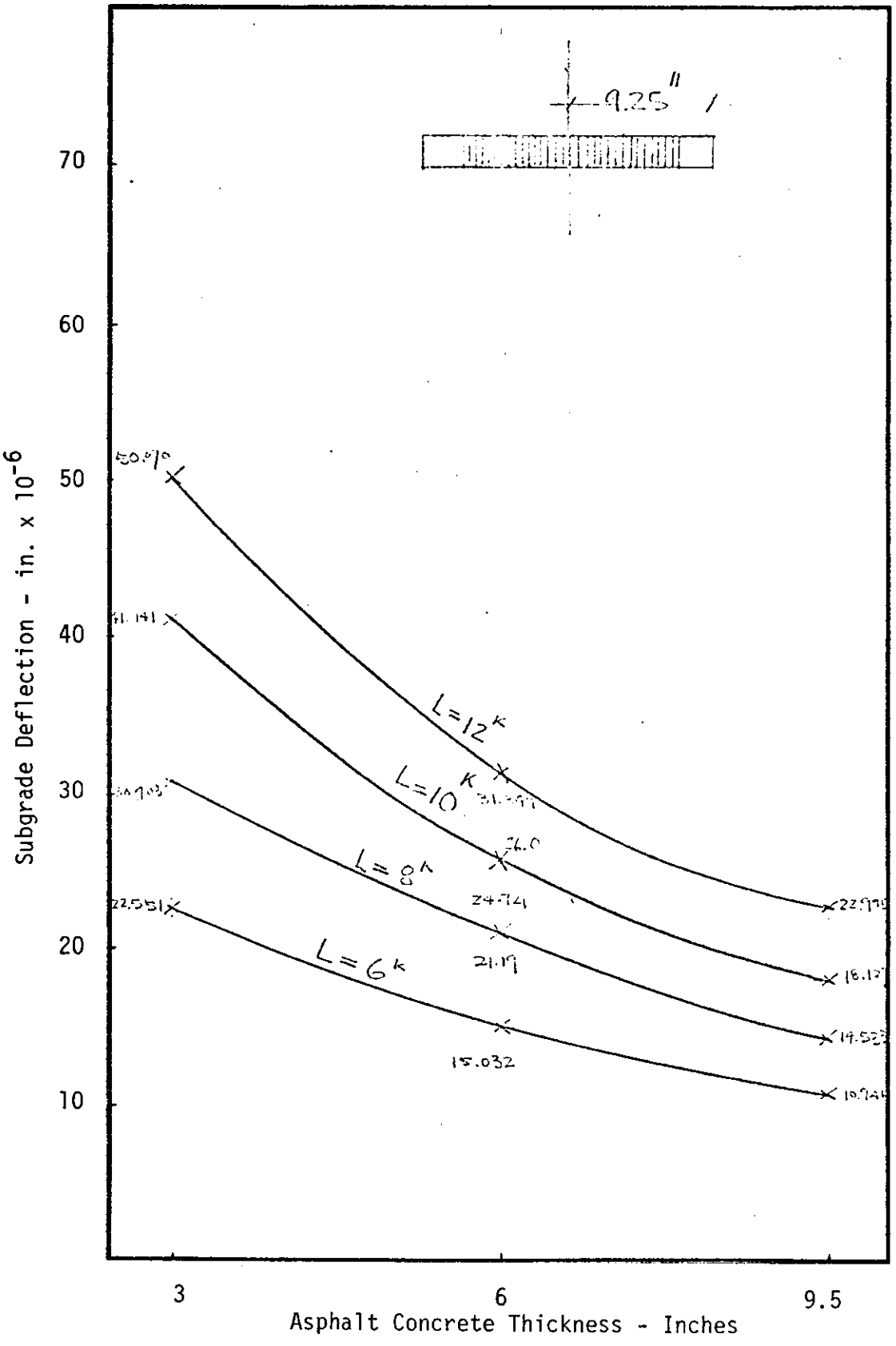

FIGURE A18 - MAXIMUM SUBGRADE DEFLECTION VS. ASPHALT CONCRETE THICKNESS RELATIONSHIPS FOR VARIOUS WHEEL LOADS

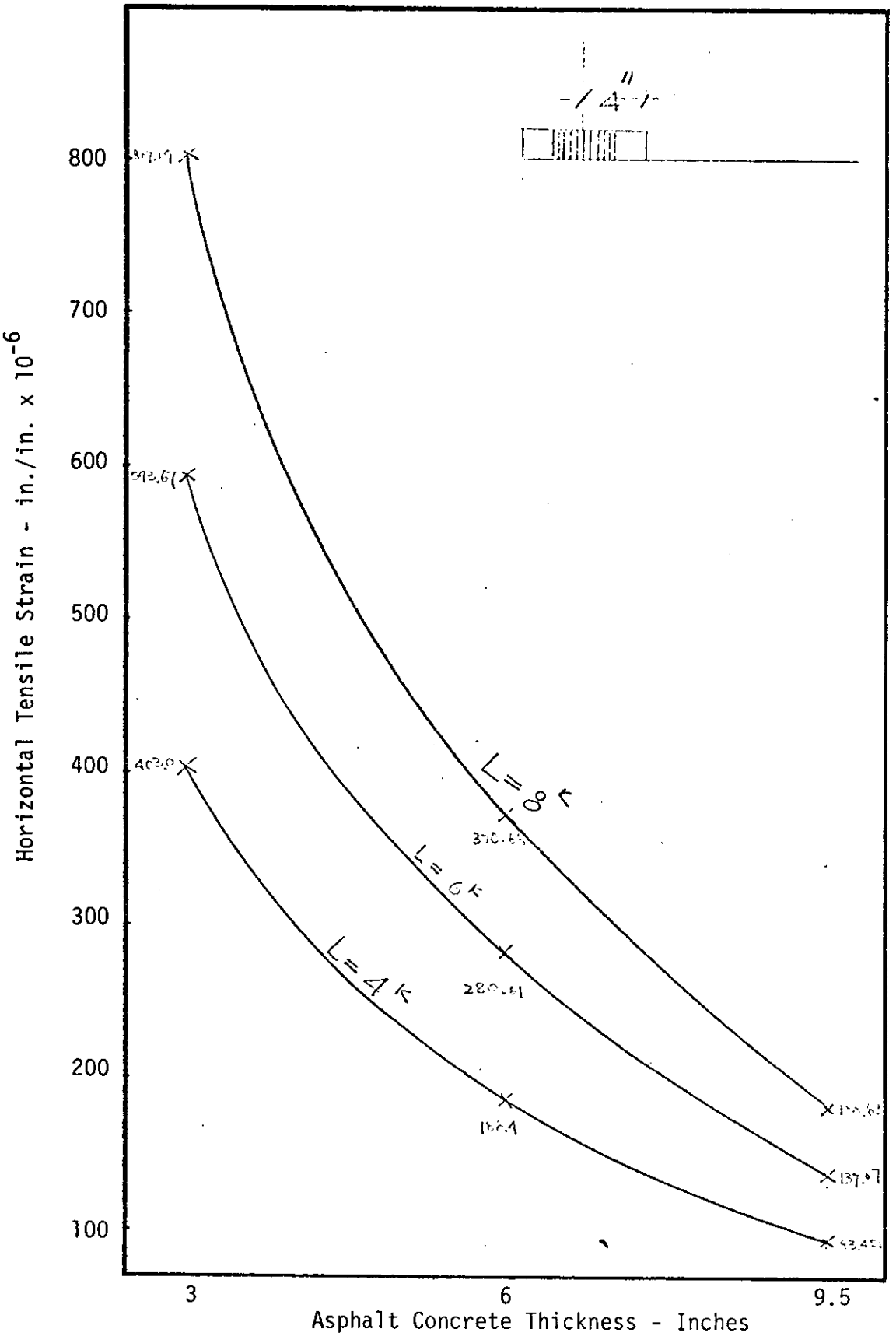

FIGURE A19 - MAXIMUM HORIZONTAL TENSILE STRAIN AT BOTTOM OF ASPHALT CONCRETE LAYER VS. ASPHALT CONCRETE THICKNESS RELATIONSHIPS FOR VARIOUS WHEEL LOADS

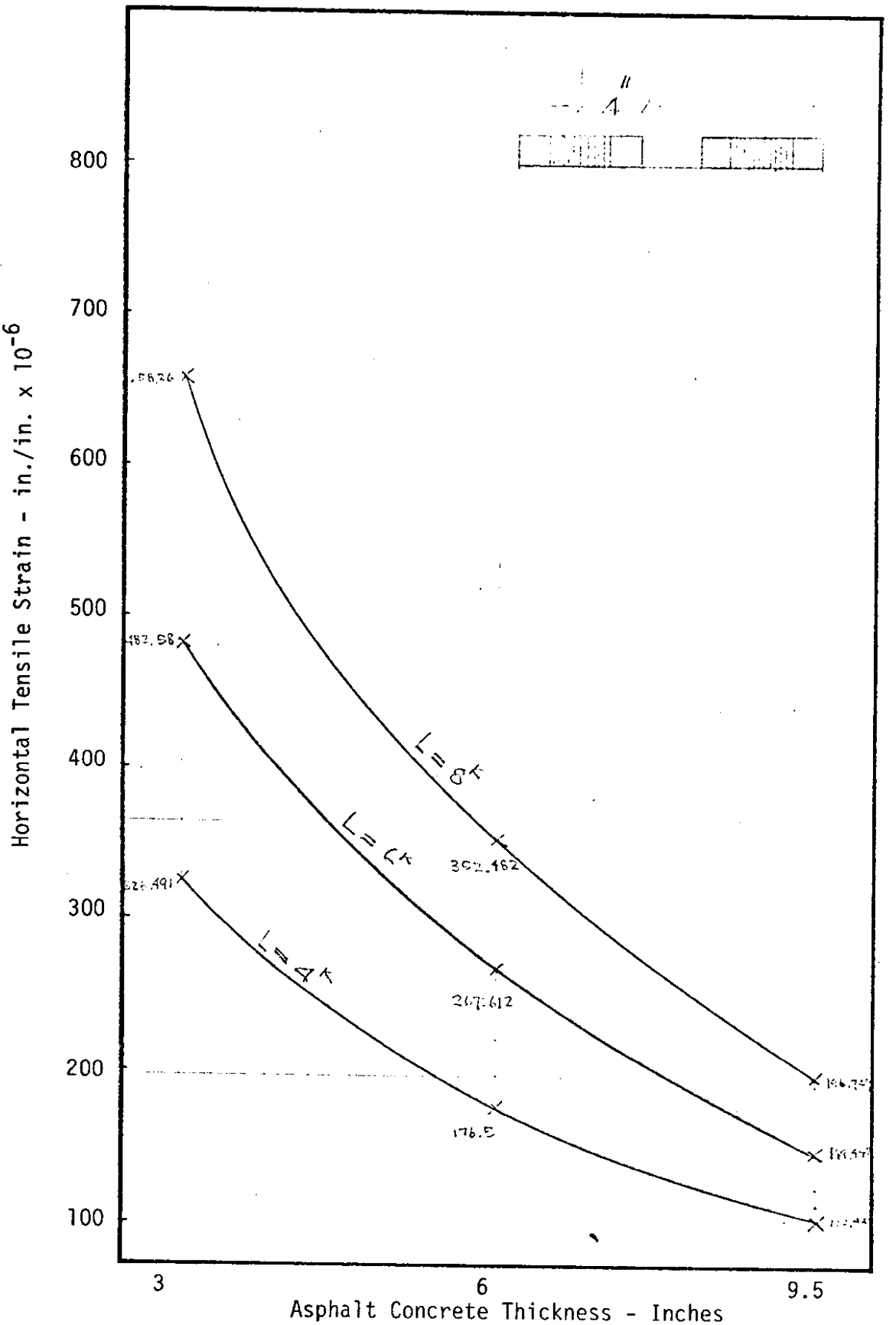

FIGURE A20 - MAXIMUM HORIZONTAL TENSILE STRAIN AT BOTTOM OF ASPHALT CONCRETE LAYER VS. ASPHALT CONCRETE THICKNESS RELATIONSHIPS FOR VARIOUS WHEEL LOADS

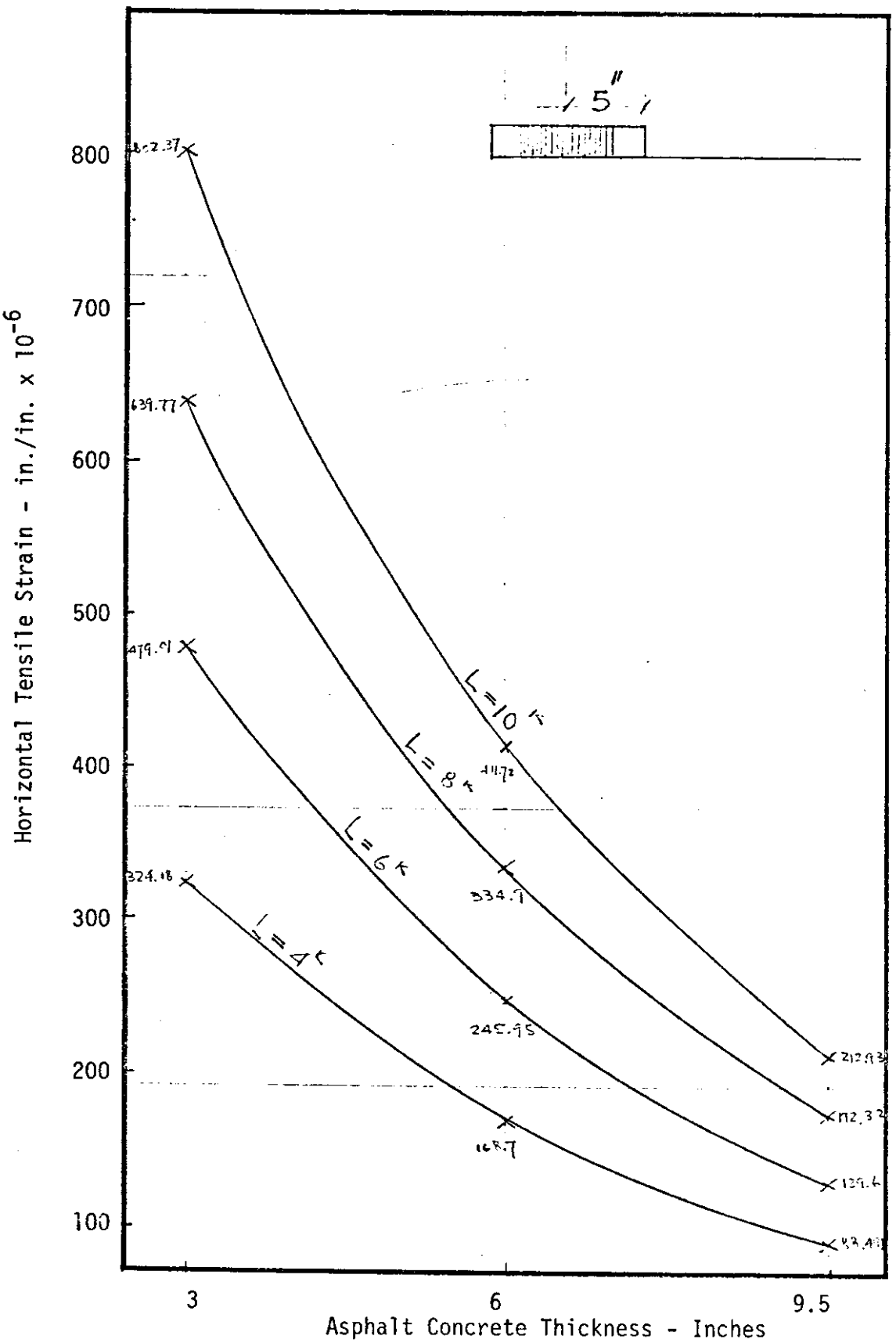

FIGURE A21 - MAXIMUM HORIZONTAL TENSILE STRAIN AT BOTTOM OF ASPHALT CONCRETE LAYER VS. ASPHALT CONCRETE THICKNESS RELATIONSHIPS FOR VARIOUS WHEEL LOADS

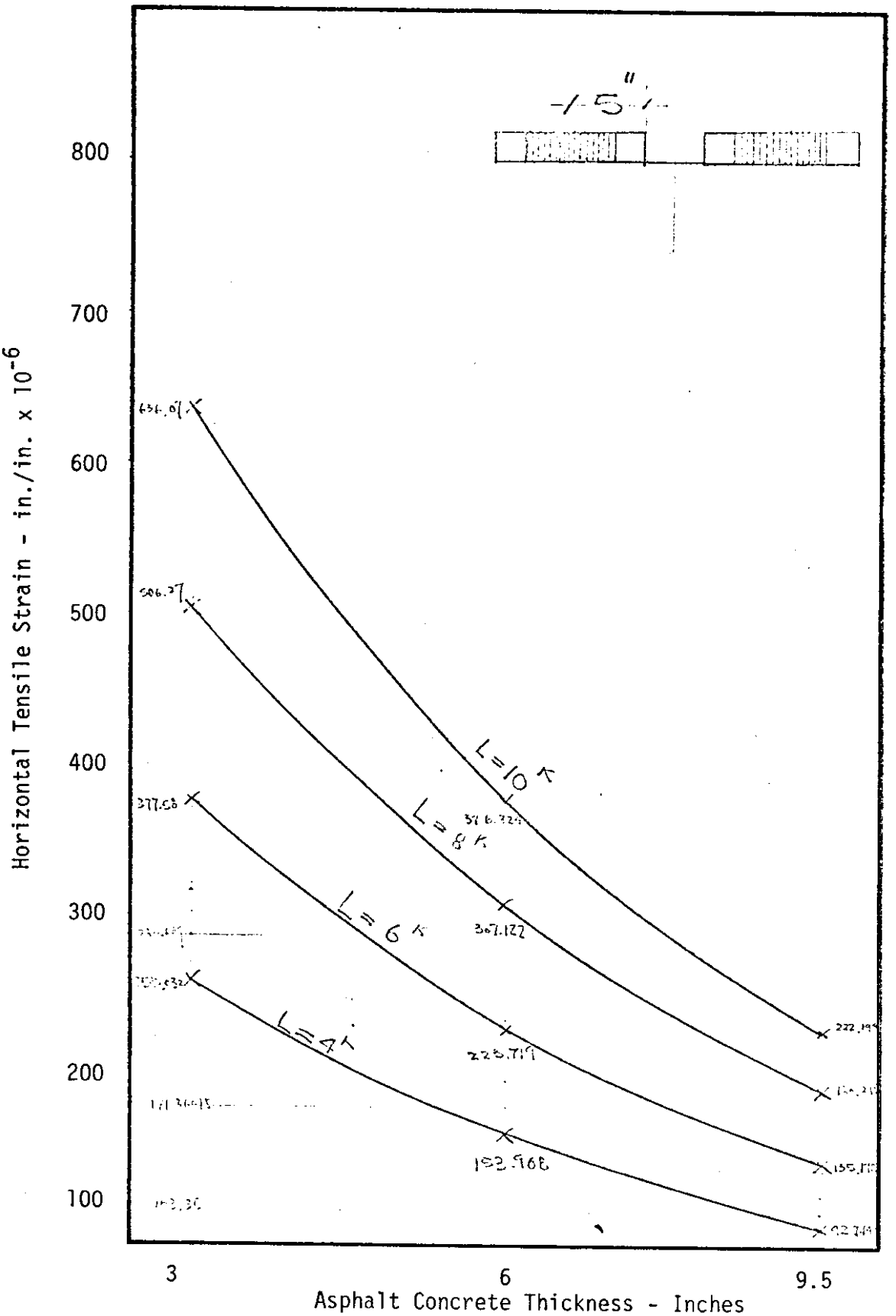

FIGURE A22 - MAXIMUM HORIZONTAL TENSILE STRAIN AT BOTTOM OF ASPHALT CONCRETE LAYER VS. ASPHALT CONCRETE THICKNESS RELATIONSHIPS FOR VARIOUS WHEEL LOADS

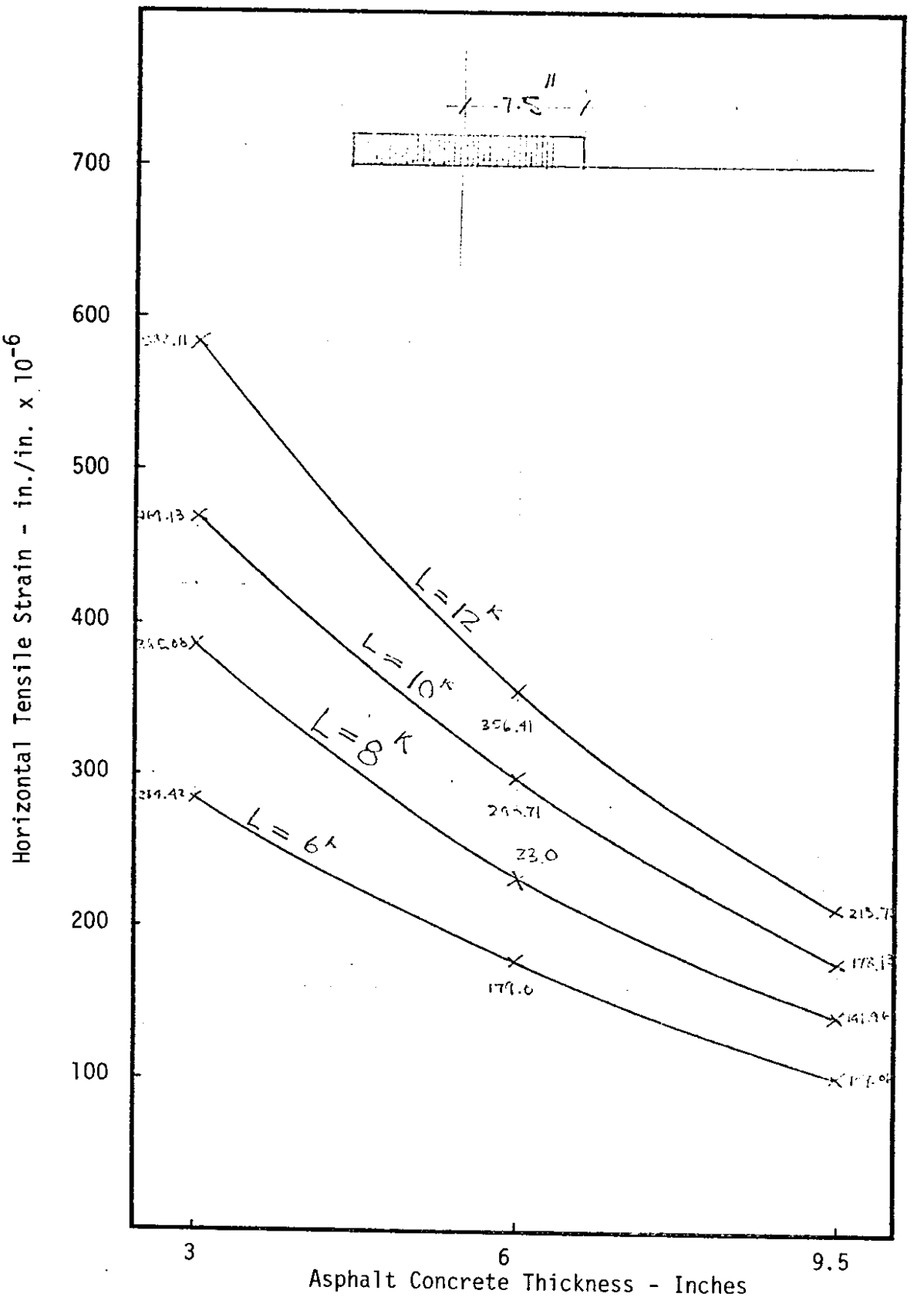

FIGURE A23 - MAXIMUM HORIZONTAL TENSILE STRAIN AT BOTTOM OF ASPHALT CONCRETE LAYER VS. ASPHALT CONCRETE THICKNESS RELATIONSHIPS FOR VARIOUS WHEEL LOADS

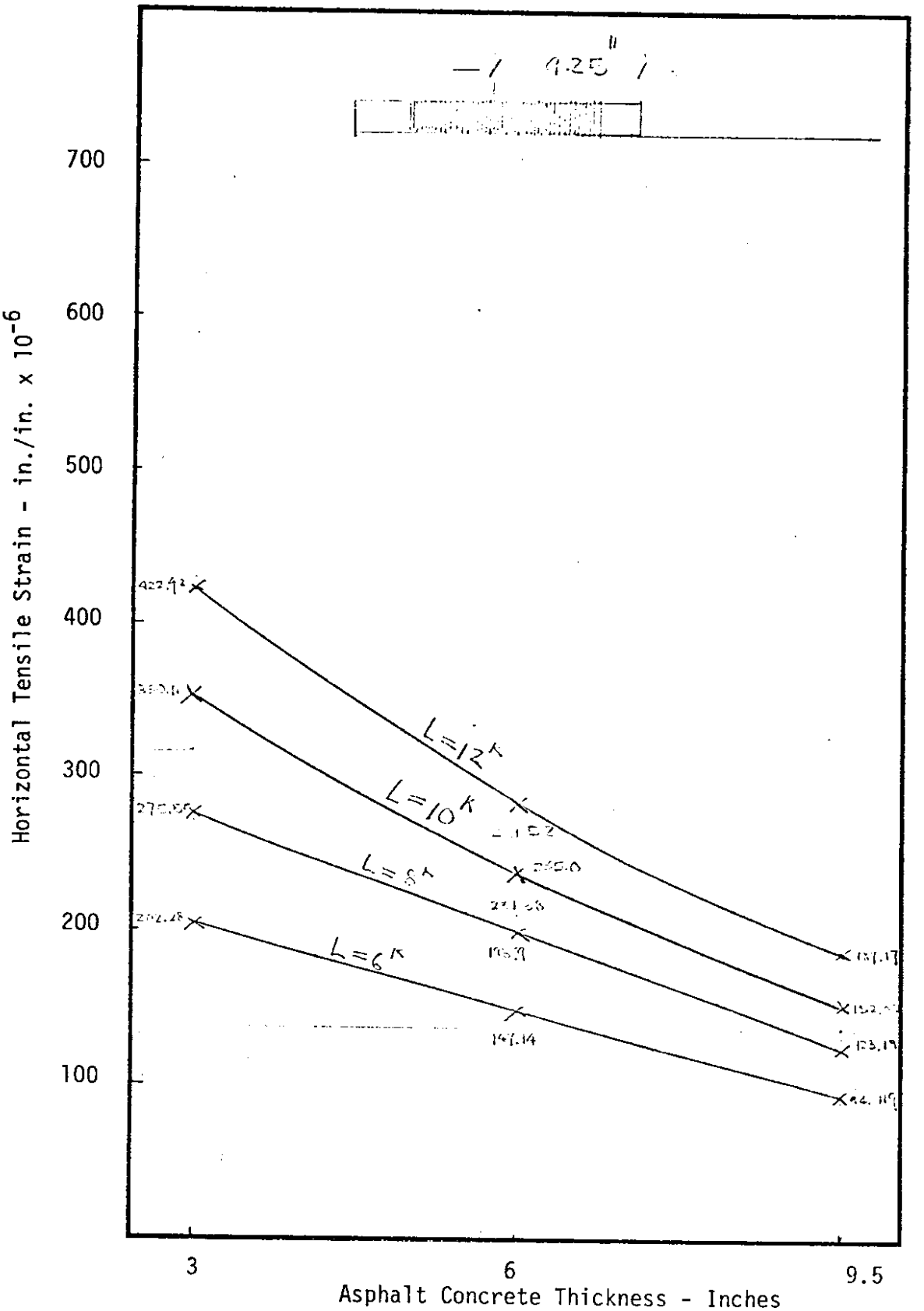

FIGURE A24 - MAXIMUM HORIZONTAL TENSILE STRAIN AT BOTTOM OF ASPHALT CONCRETE LAYER VS. ASPHALT CONCRETE THICKNESS RELATIONSHIPS FOR VARIOUS WHEEL LOADS

APPENDIX B

MAXIMUM HORIZONTAL TENSILE STRAINS AND MAXIMUM VERTICAL COMPRESSIVE STRAINS FOR 18, 20, 22 and 24-Kip AXLE LOADS

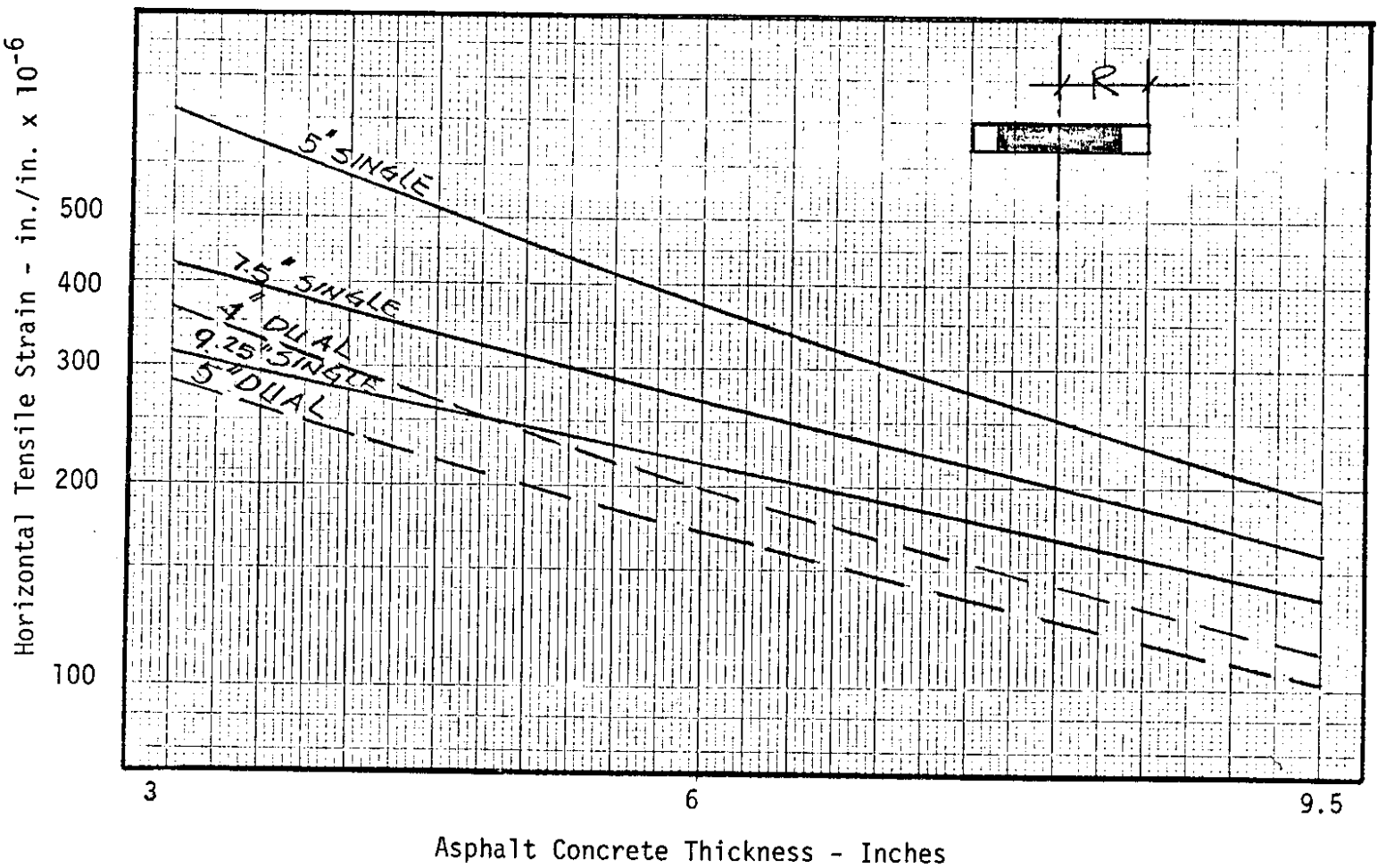

FIGURE B1 - HORIZONTAL TENSILE STRAIN AT BOTTOM OF ASPHALT CONCRETE LAYER VS. ASPHALT CONCRETE THICKNESS RELATIONSHIP FOR VARIOUS TIRE SIZES, SHOWN IN RADIUS, OF SINGLE AND DUAL TIRES UNDER 18 KIP AXLE LOAD

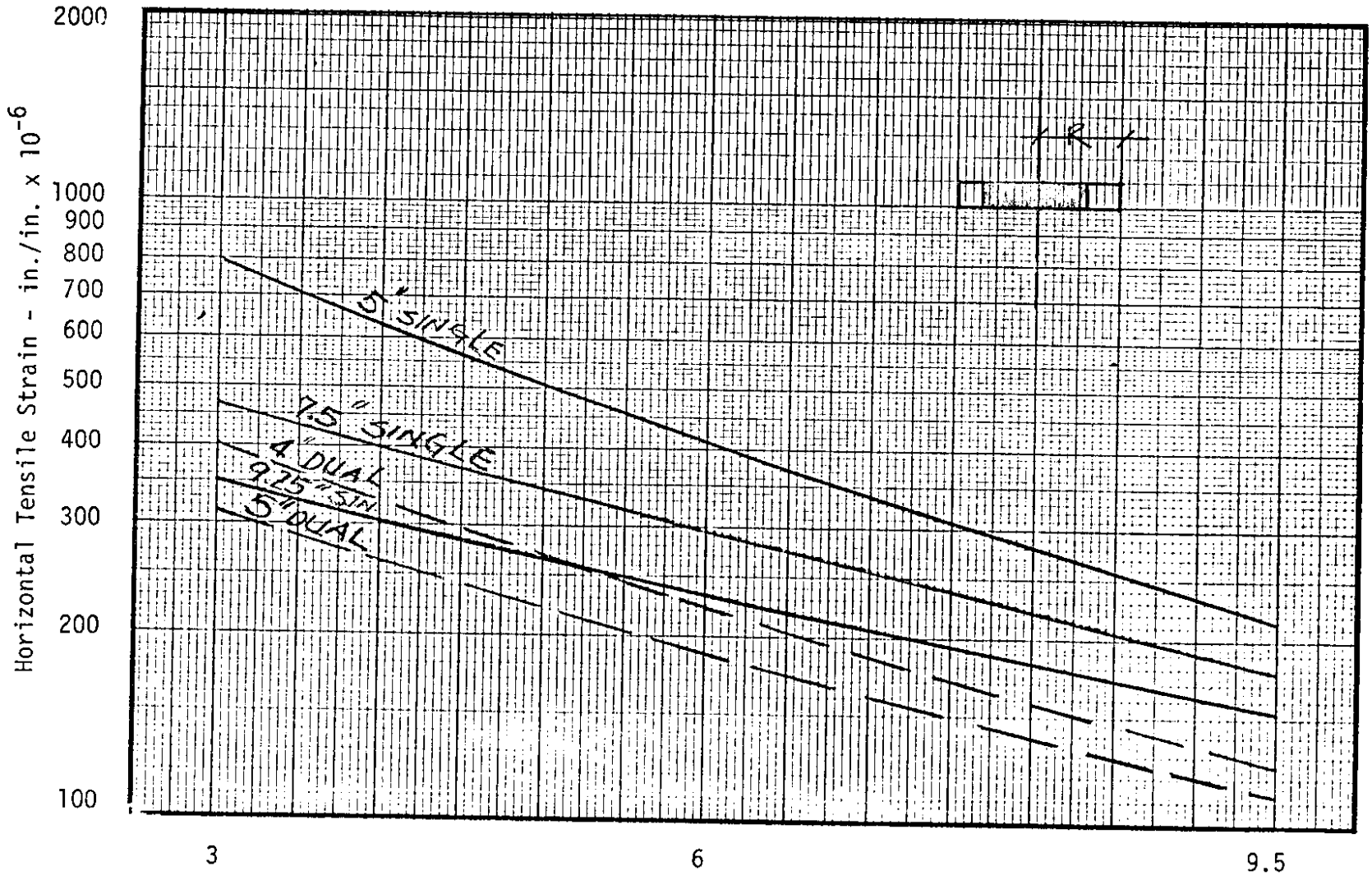

FIGURE B2 - HORIZONTAL TENSILE STRAIN AT BOTTOM OF ASPHALT CONCRETE LAYER VS. ASPHALT CONCRETE RELATIONSHIPS FOR VARIOUS TIRE SIZES, SHOWN IN RADIUS, OF SINGLE AND DUAL TIRES UNDER 20 KIP AXLE LOAD

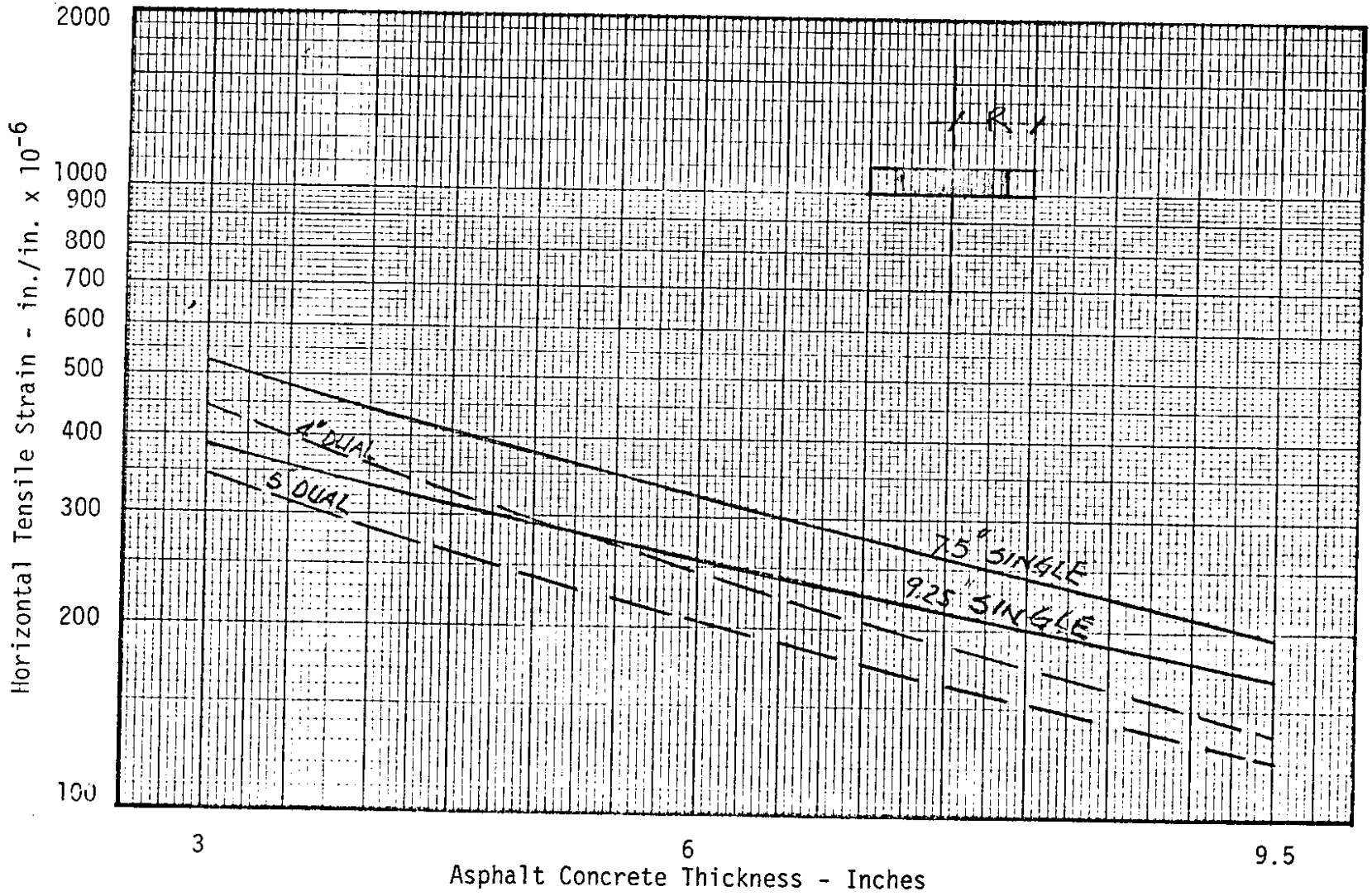

FIGURE B3 - HORIZONTAL TENSILE STRAIN AT BOTTOM OF ASPHALT CONCRETE LAYER VS. ASPHALT CONCRETE THICKNESS RELATIONSHIPS FOR VARIOUS TIRE SIZES, SHOWN IN RADIUS, OF SINGLE AND DUAL TIRES UNDER 22 KIP AXLE LOADS

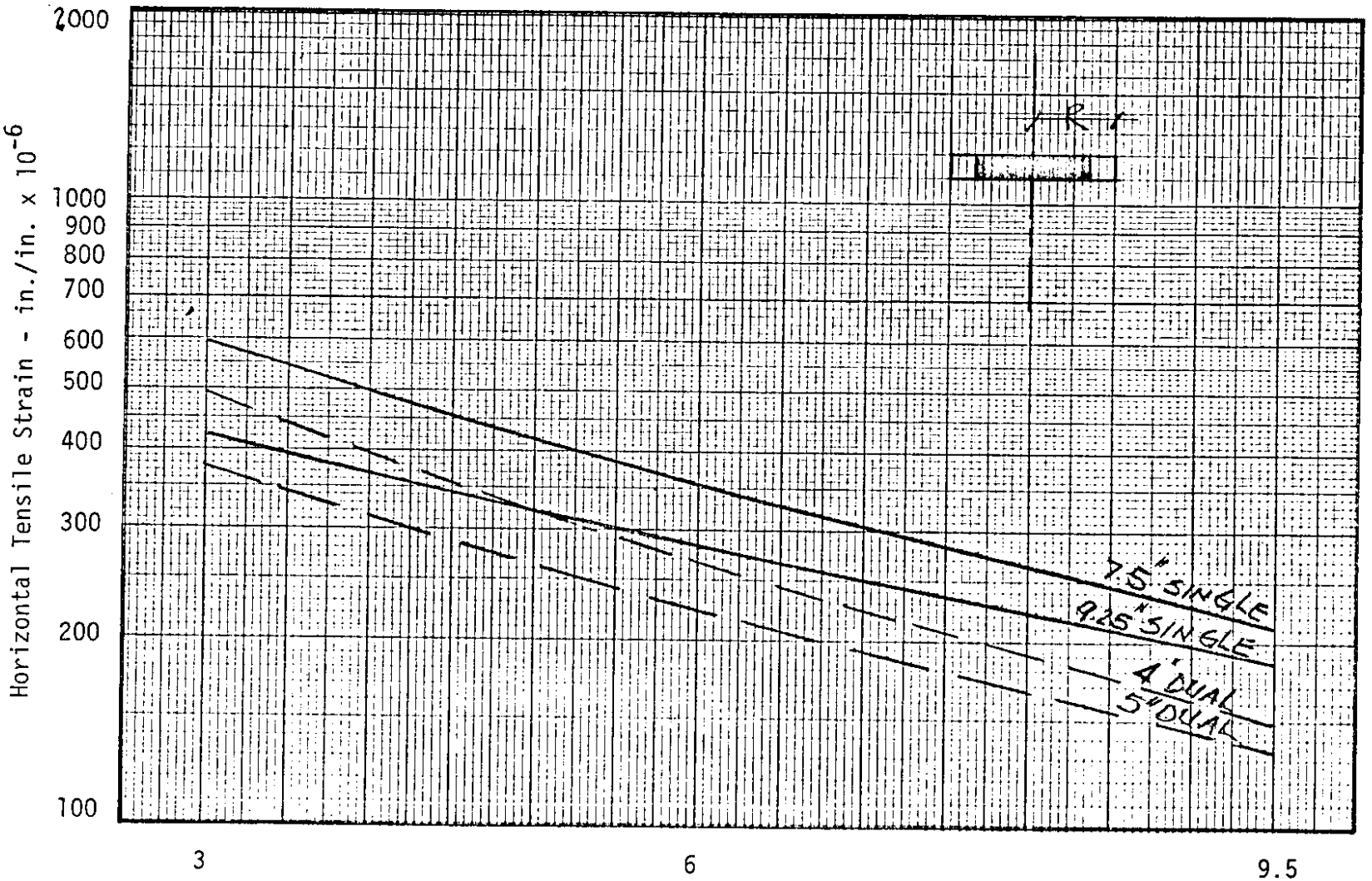

FIGURE B4 - HORIZONTAL TENSILE STRAIN AT BOTTOM OF ASPHALT CONCRETE LAYER VS. ASPHALT CONCRETE THICKNESS RELATIONSHIPS FOR VARIOUS TIRE SIZES, SHOWN IN RADIUS, OF SINGLE AND DUAL TIRES UNDER 24 KIP AXLE LOAD

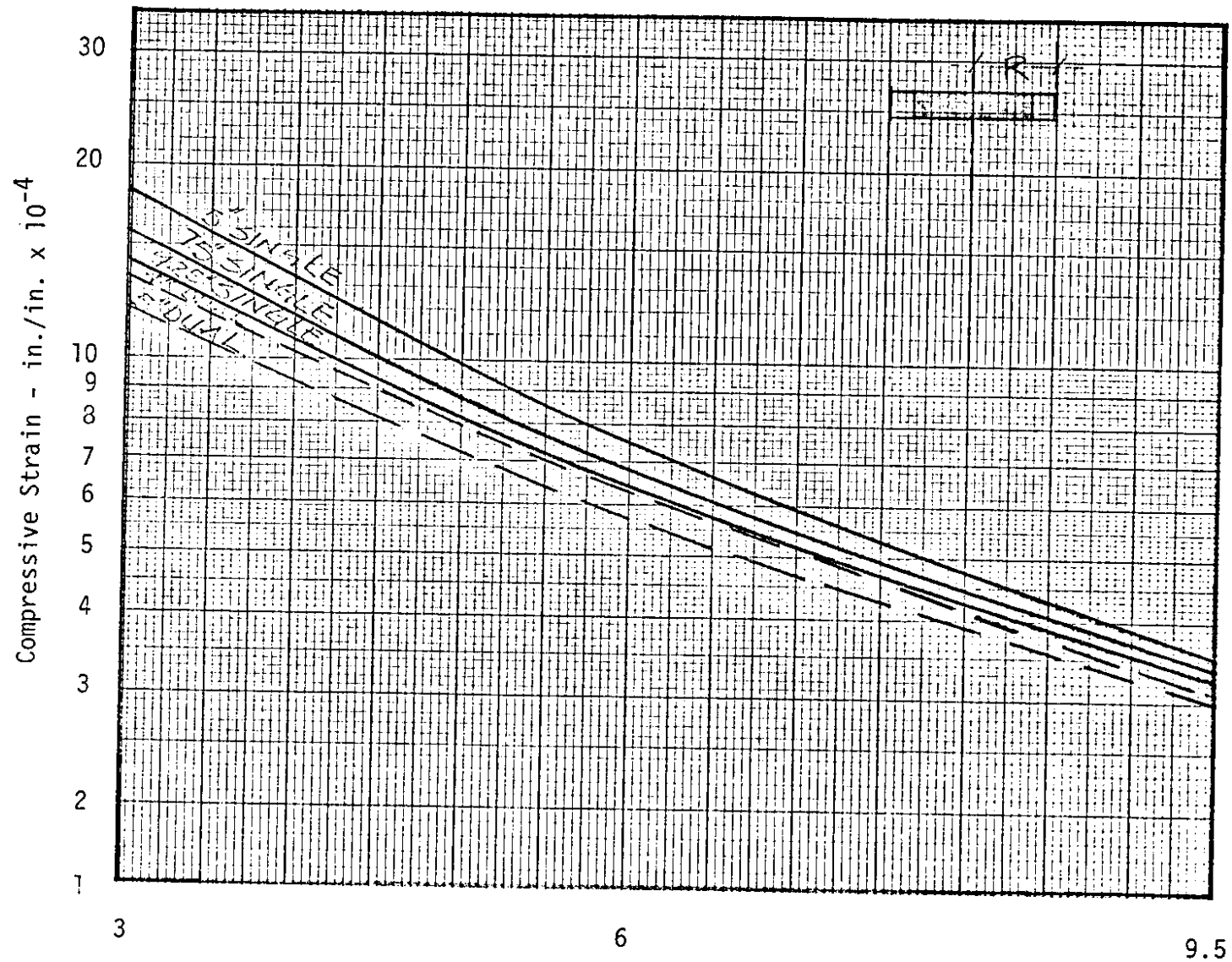

FIGURE B5 - COMPRESSIVE STRAIN AT TOP OF SUBGRADE VS. ASPHALT CONCRETE THICKNESS FOR VARIOUS TIRE SIZES, SHOWN IN RADIUS, OF SINGLE AND DUAL TIRES, UNDER 18 KIP AXLE LOAD

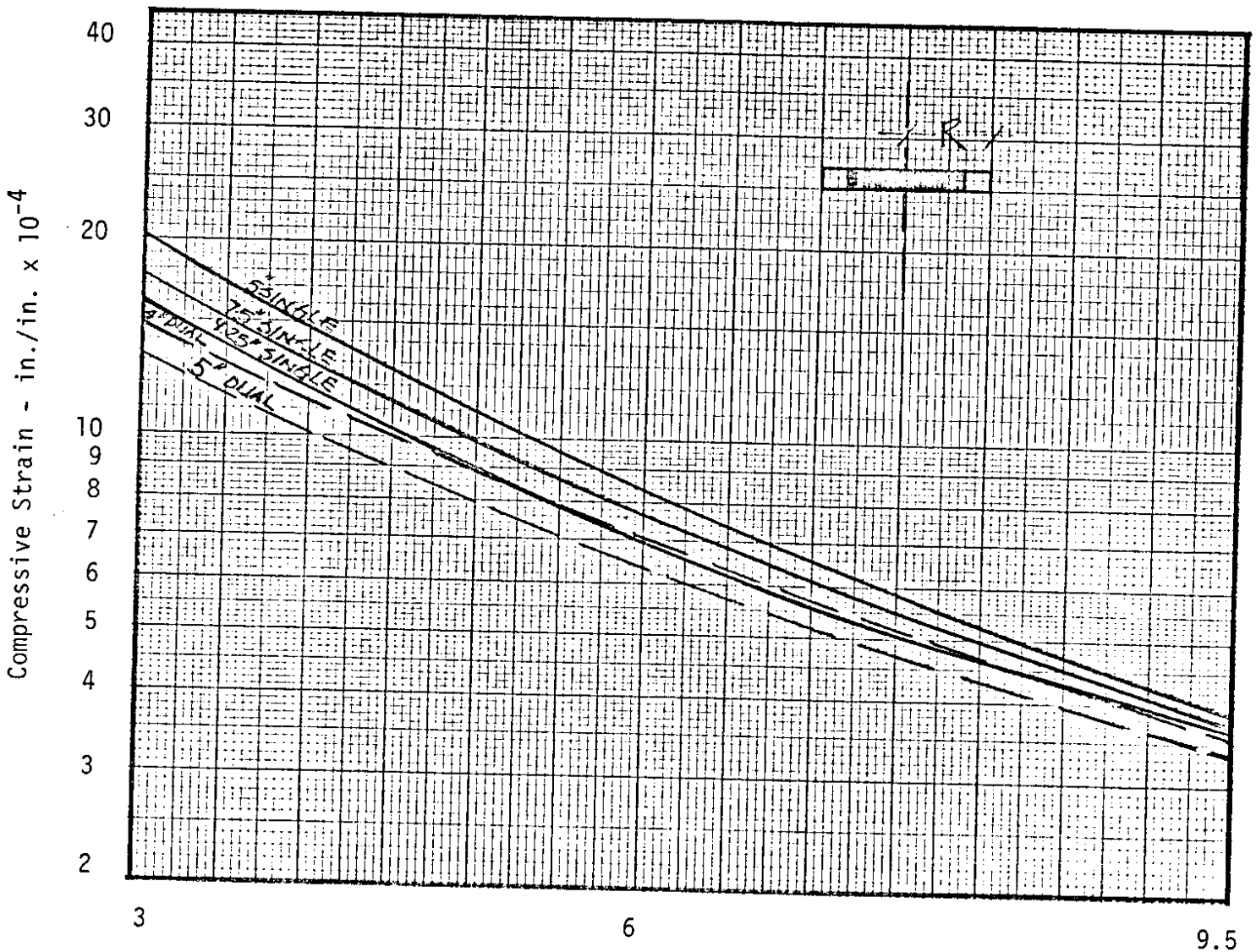

FIGURE B6 - COMPRESSIVE STRAIN AT TOP OF SUBGRADE VS. ASPHALT CONCRETE THICKNESS RELATIONSHIPS FOR VARIOUS TIRE SIZES, SHOWN IN RADIUS, OF SINGLE AND DUAL TIRES UNDER 20 KIP AXLE LOAD

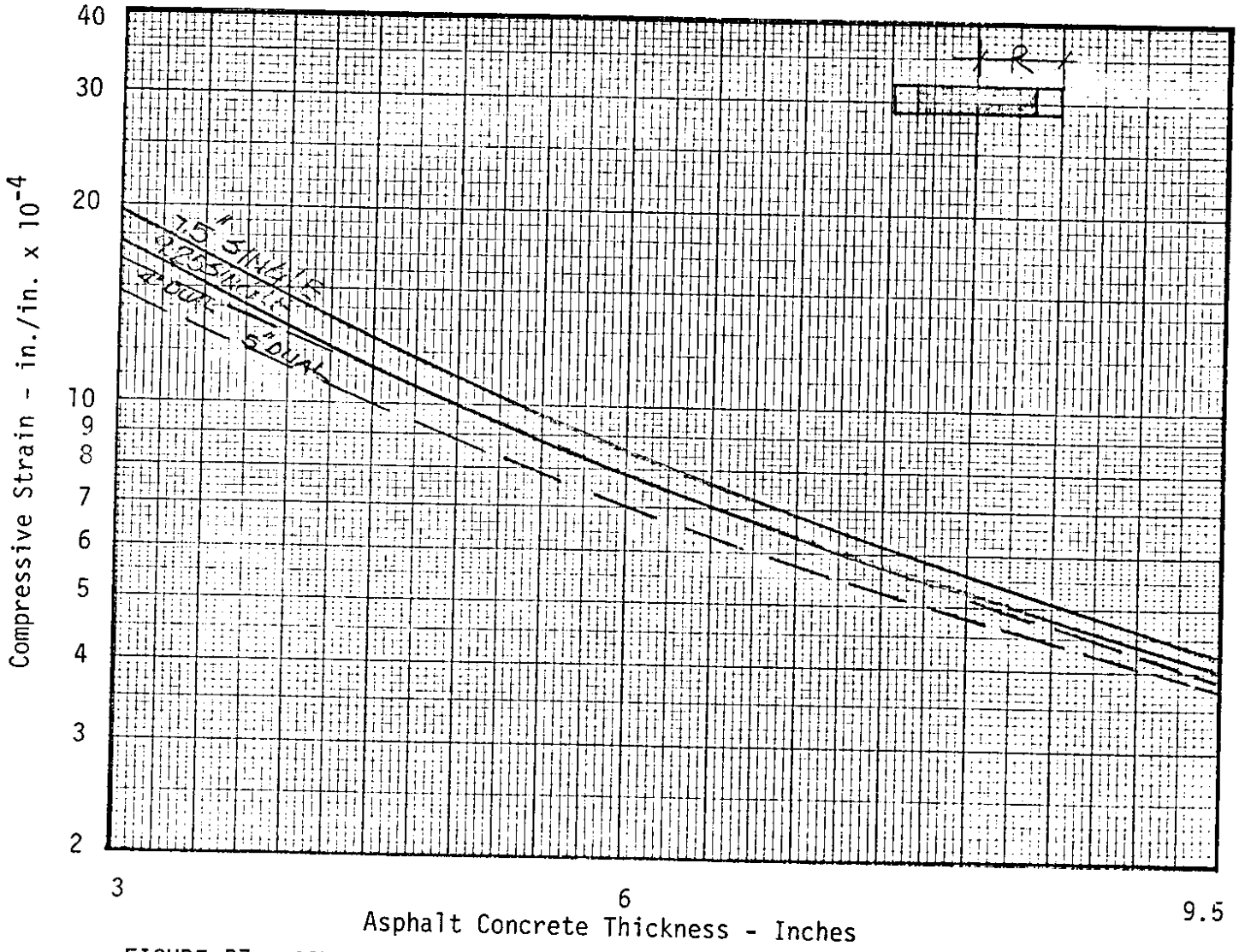

FIGURE B7 - COMPRESSIVE STRAIN AT TOP OF SUBGRADE VS. ASPHALT CONCRETE THICKNESS RELATIONSHIPS FOR VARIOUS TIRE SIZES, SHOWN IN RADIUS, OF SINGLE AND DUAL TIRES UNDER 22 KIP AXLE LOAD

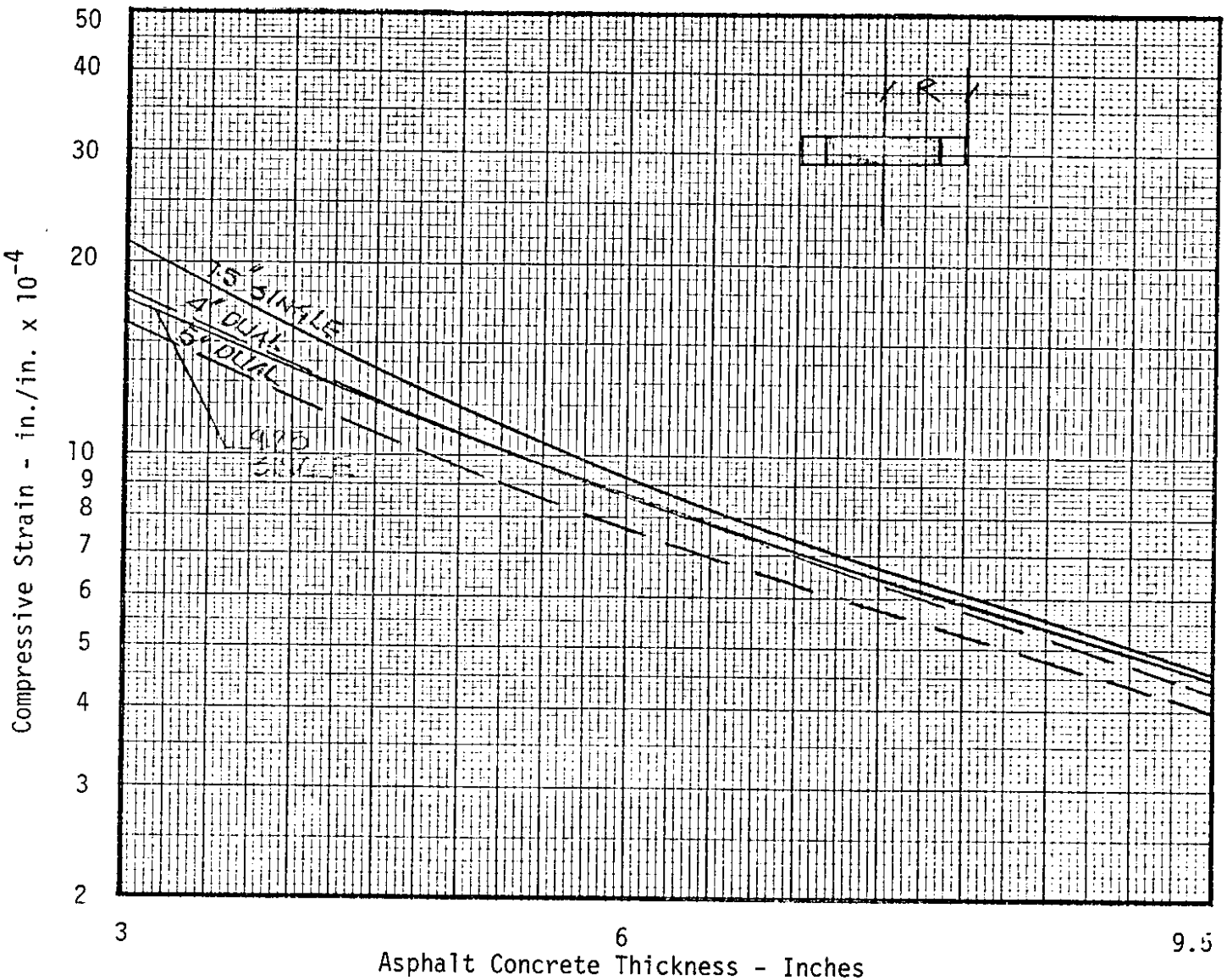

FIGURE B8 - COMPRESSIVE STRAIN AT TOP OF SUBGRADE VS. ASPHALT CONCRETE THICKNESS, RELATIONSHIPS FOR VARIOUS TIRE SIZES, SHOWN IN RADIUS, OF SINGLE AND DUAL TIRES UNDER 24 KIP AXLE LOAD

APPENDIX C

LABORATORY FATIGUE DATA FOR ASPHALT CONCRETE

AND

COMPUTED APPLICATIONS OF LOADS TO FAILURE IN FATIGUE FOR VARIOUS TIRE SIZES, LOADS, AND PAVEMENT THICKNESSES

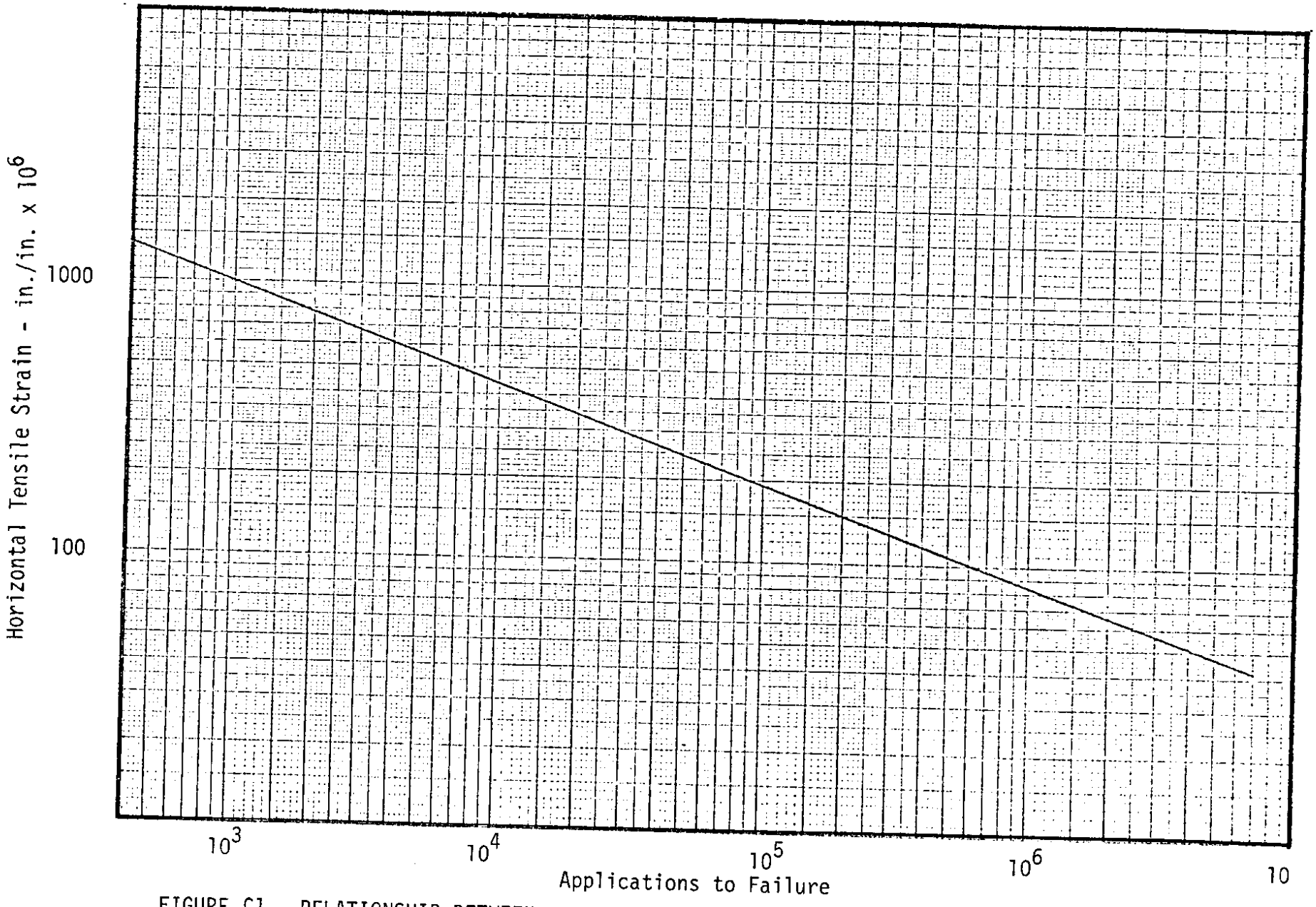

FIGURE C1 - RELATIONSHIP BETWEEN HORIZONTAL TENSILE STRAIN AT BOTTOM OF ASPHALT CONCRETE AND ALLOWABLE NUMBER OF LOAD APPLICATIONS (22).

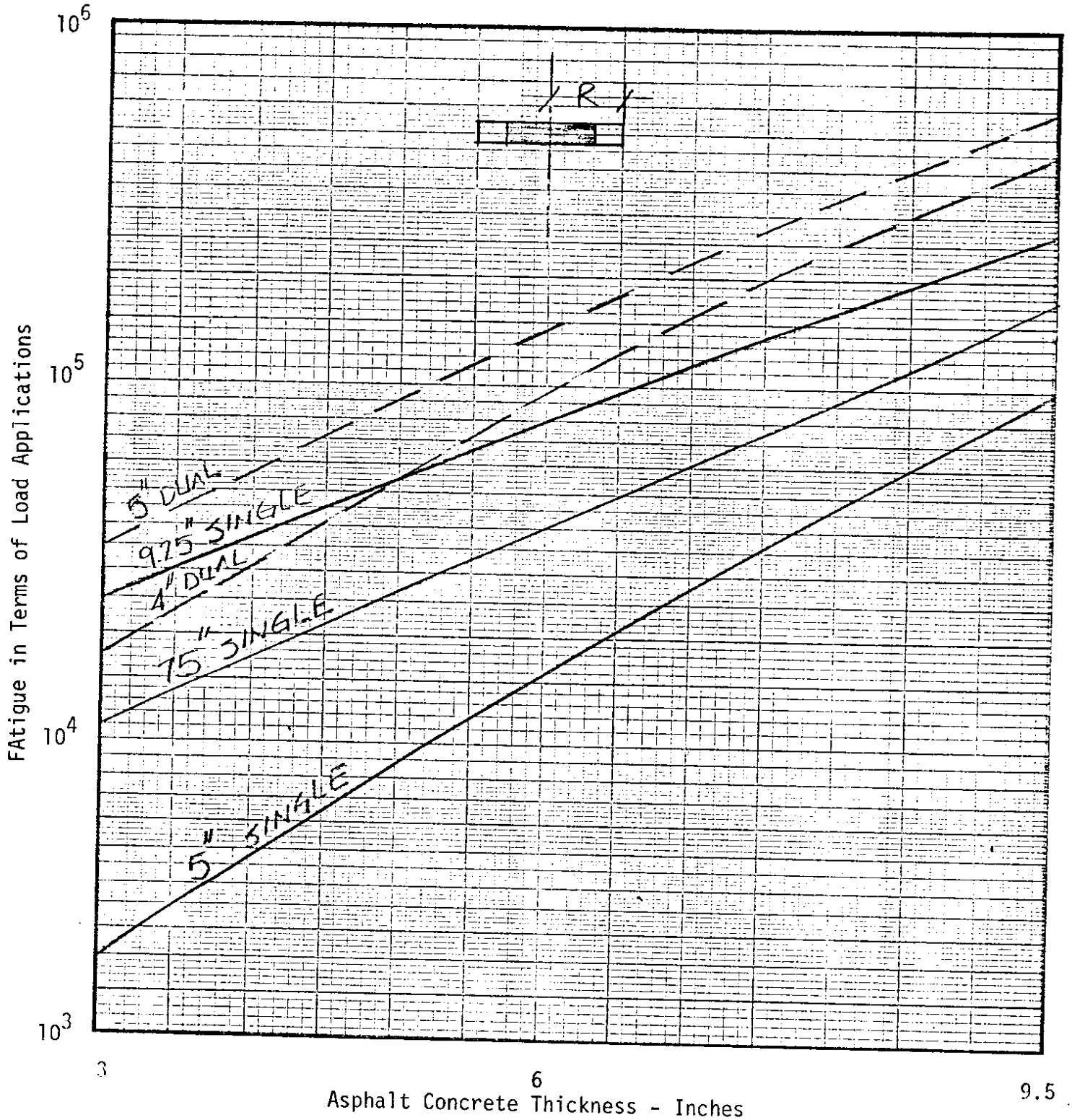

FIGURE C2 - MAXIMUM NUMBER OF 18 KIP AXLE LOAD APPLICATIONS ON ASPHALT CONCRETE VS. ASPHALT CONCRETE THICKNESS RELATIONSHIPS FOR VARIOUS TIRE SIZES, SHOWN IN RADIUS, OF SINGLE AND DUAL TIRES

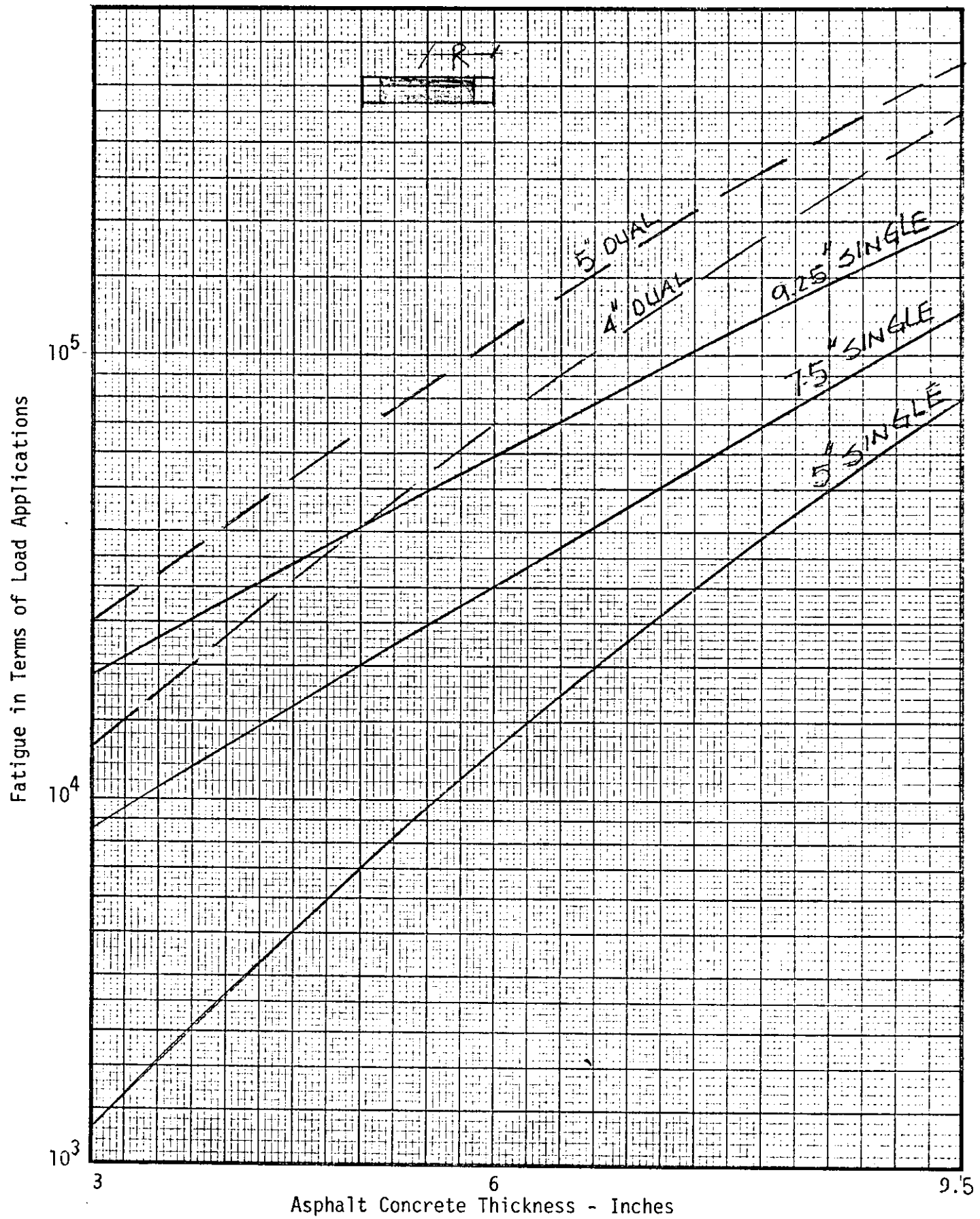

FIGURE C3 - MAXIMUM NUMBER OF 20 KIP AXLE LOAD APPLICATIONS ON ASPHALT CONCRETE VS. ASPHALT CONCRETE THICKNESS RELATIONSHIPS FOR VARIOUS TIRE SIZES, SHOWN IN RADIUS, OF SINGLE AND DUAL TIRES

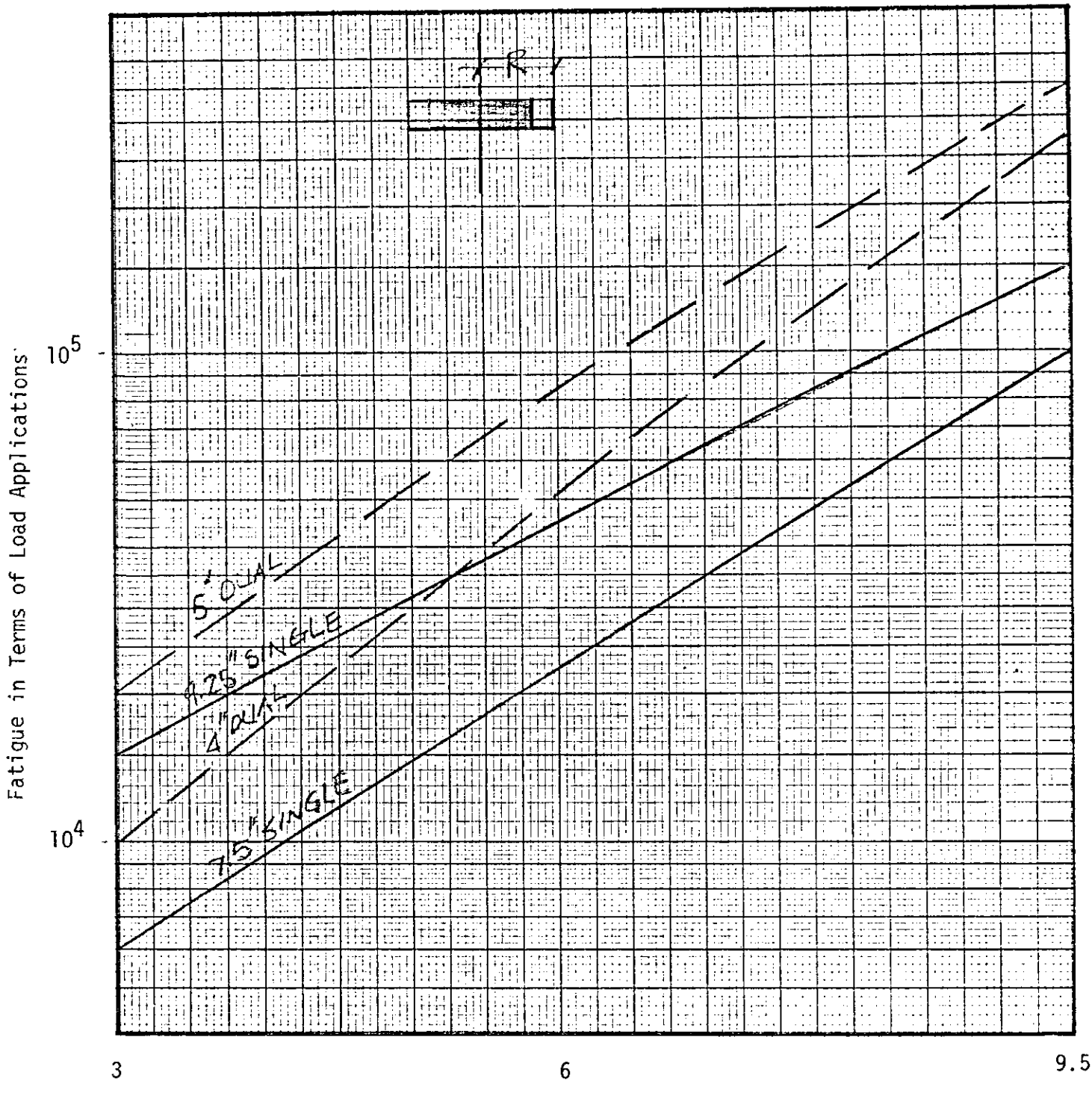

FIGURE C4 - MAXIMUM NUMBER OF 22 KIP AXLE LOAD APPLICATIONS ON ASPHALT CONCRETE VS. ASPHALT CONCRETE THICKNESS RELATIONSHIPS FOR VARIOUS TIRE SIZES, SHOWN IN RADIUS, OF SINGLE AND DUAL TIRES

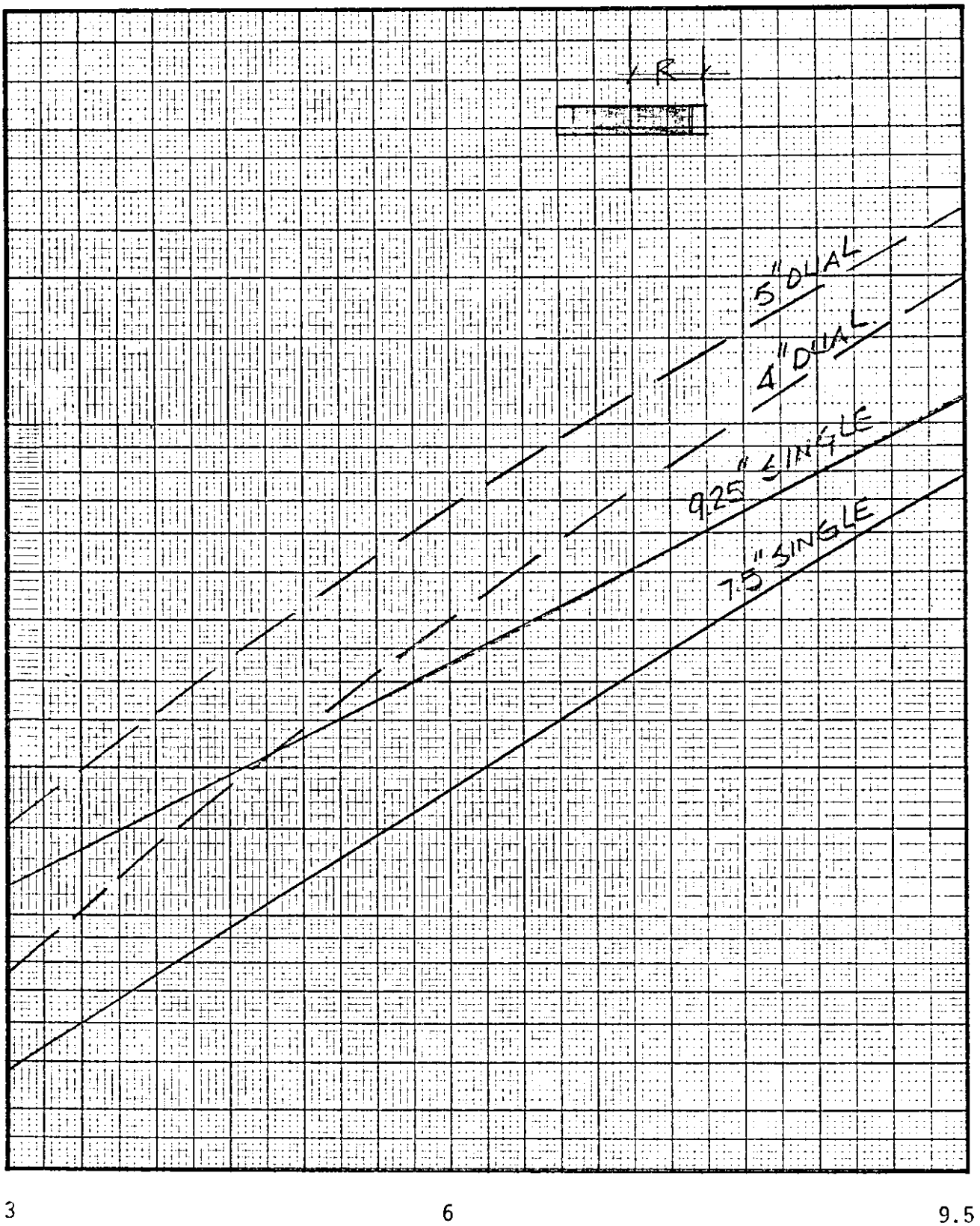

FIGURE C5 - MAXIMUM NUMBER OF 24 AXLE LOAD APPLICATIONS ON ASPHALT CONCRETE VS. ASPHALT CONCRETE THICKNESS RELATIONSHIPS FOR VARIOUS TIRE SIZES, SHOWN IN RADIUS, OF SINGLE AND DUAL TIRES

APPENDIX D

STRAIN-LOAD APPLICATION RELATIONSHIP FOR ASPHALT PAVEMENTS

AND

COMPUTED APPLICATIONS OF LOADS TO FAILURE IN PERMANENT DEFORMATION FOR VARIOUS TIRE SIZES, LOADS, AND PAVEMENT THICKNESSES

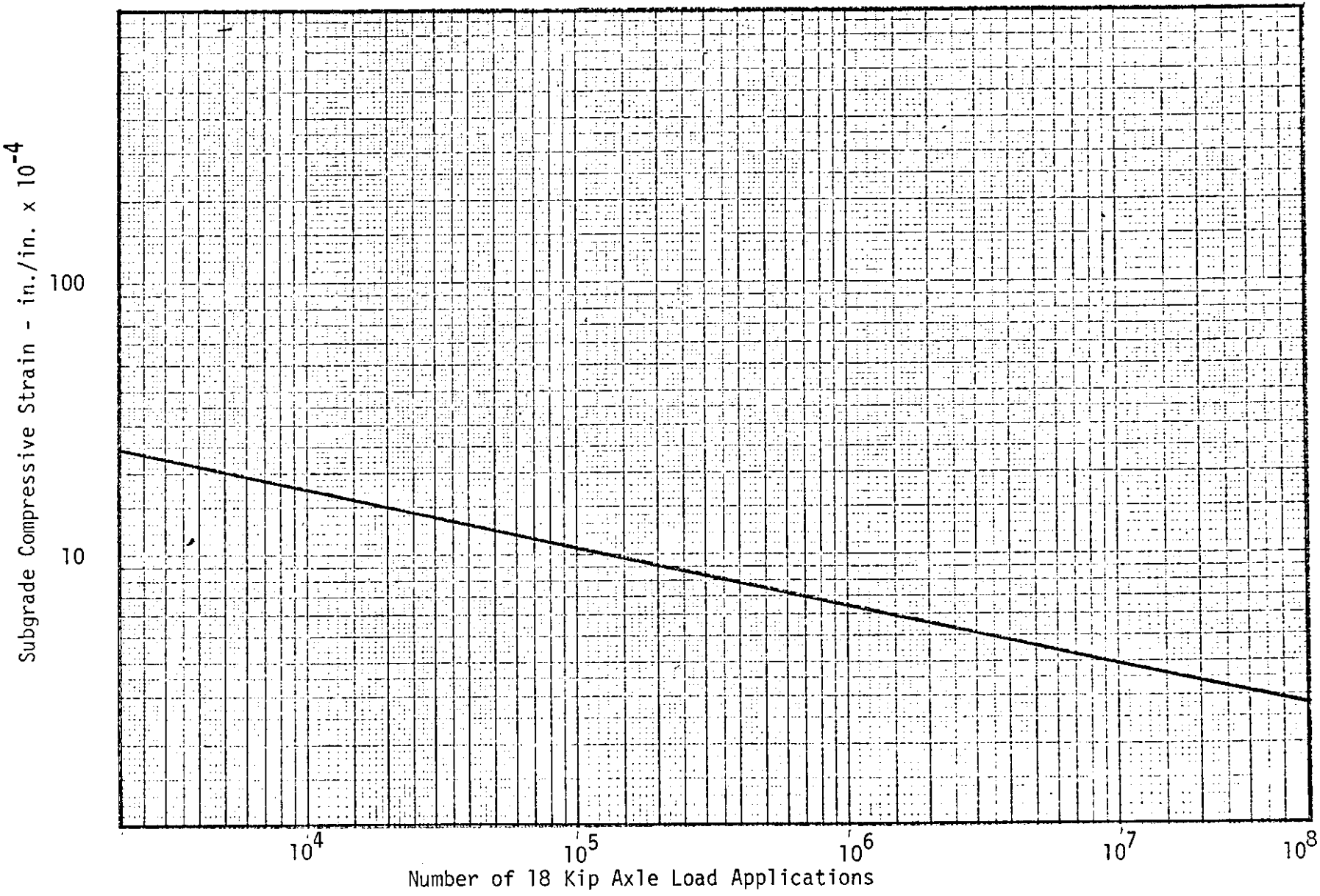

FIGURE D1 - RELATIONSHIP BETWEEN ALLOWABLE SUBGRADE COMPRESSIVE STRAIN AND MAXIMUM NUMBER of 18 KIP AXLE LOAD APPLICATIONS (7)

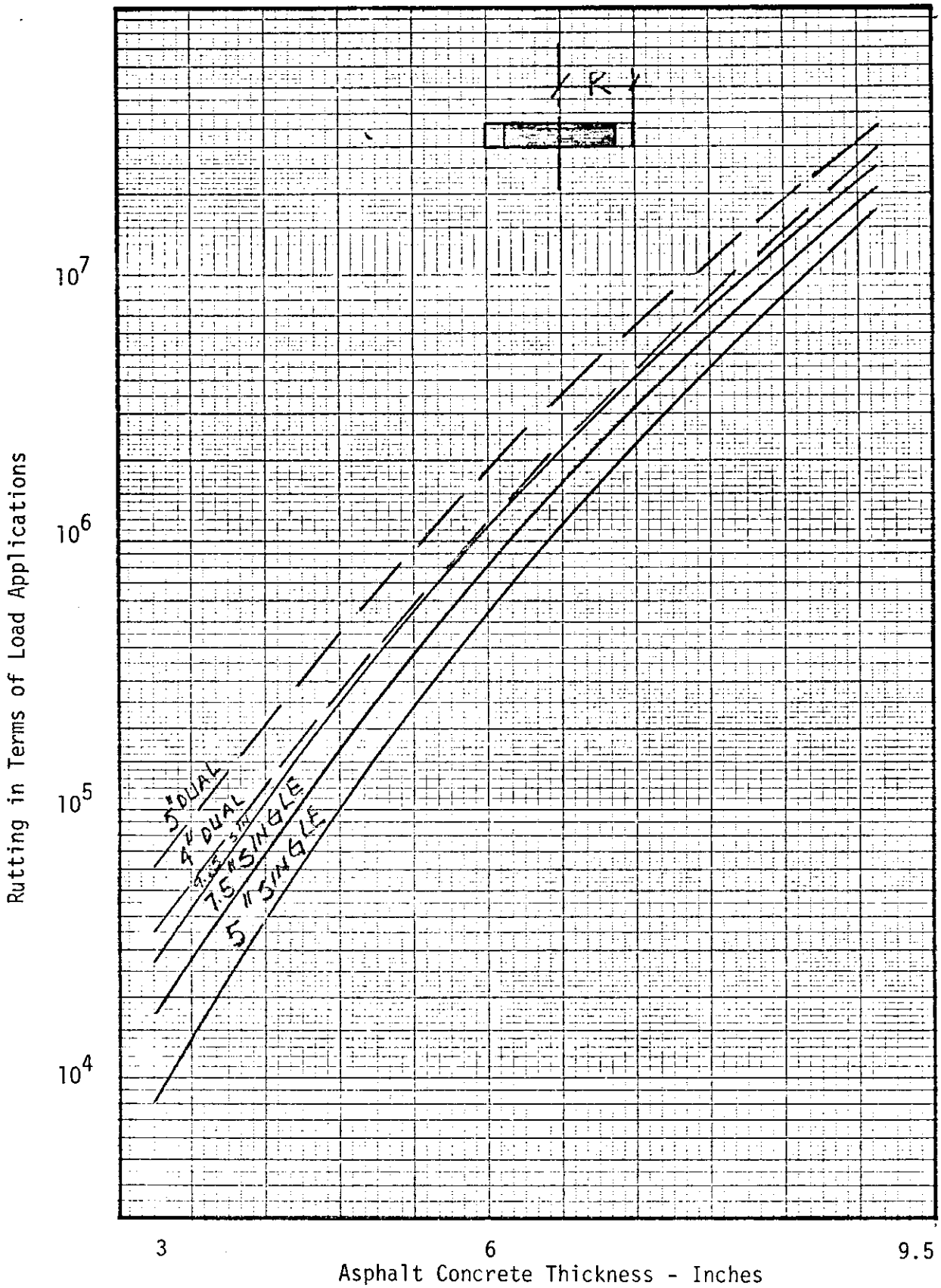

FIGURE D2 - MAXIMUM NUMBER OF 18 KIP AXLE LOAD APPLICATIONS ON SUBGRADE VS. ASPHALT CONCRETE THICKNESS RELATIONSHIPS FOR VARIOUS TIRE SIZES, SHOWN IN RADIUS, OF SINGLE AND DUAL TIRES

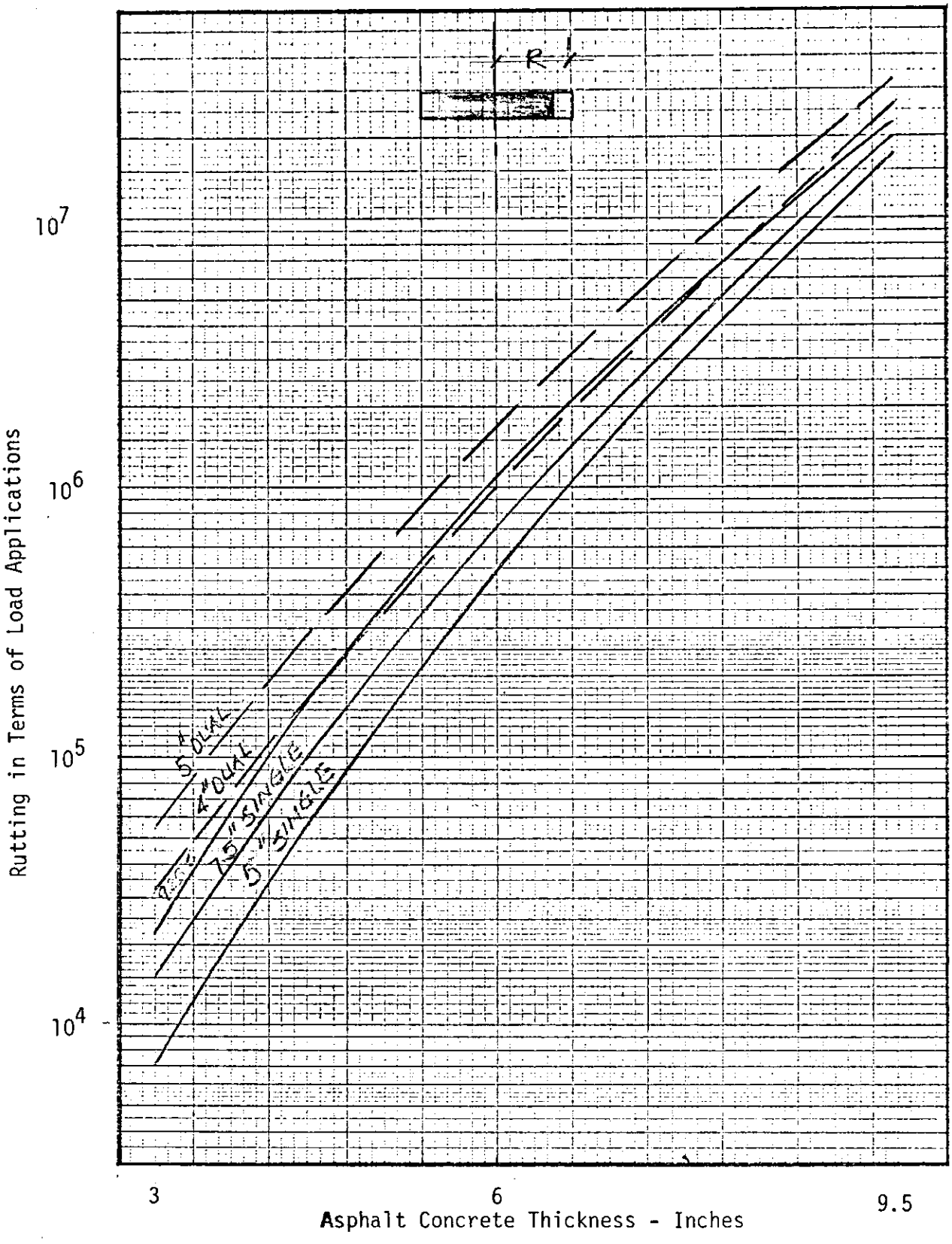

FIGURE D3 - MAXIMUM NUMBER OF 20 KIP AXLE LOAD APPLICATIONS IN SUBGRADE VS. ASPHALT CONCRETE THICKNESS RELATIONSHIPS FOR VARIOUS TIRE SIZES, SHOWN IN RADIUS, OF SINGLE AND DUAL TIRES

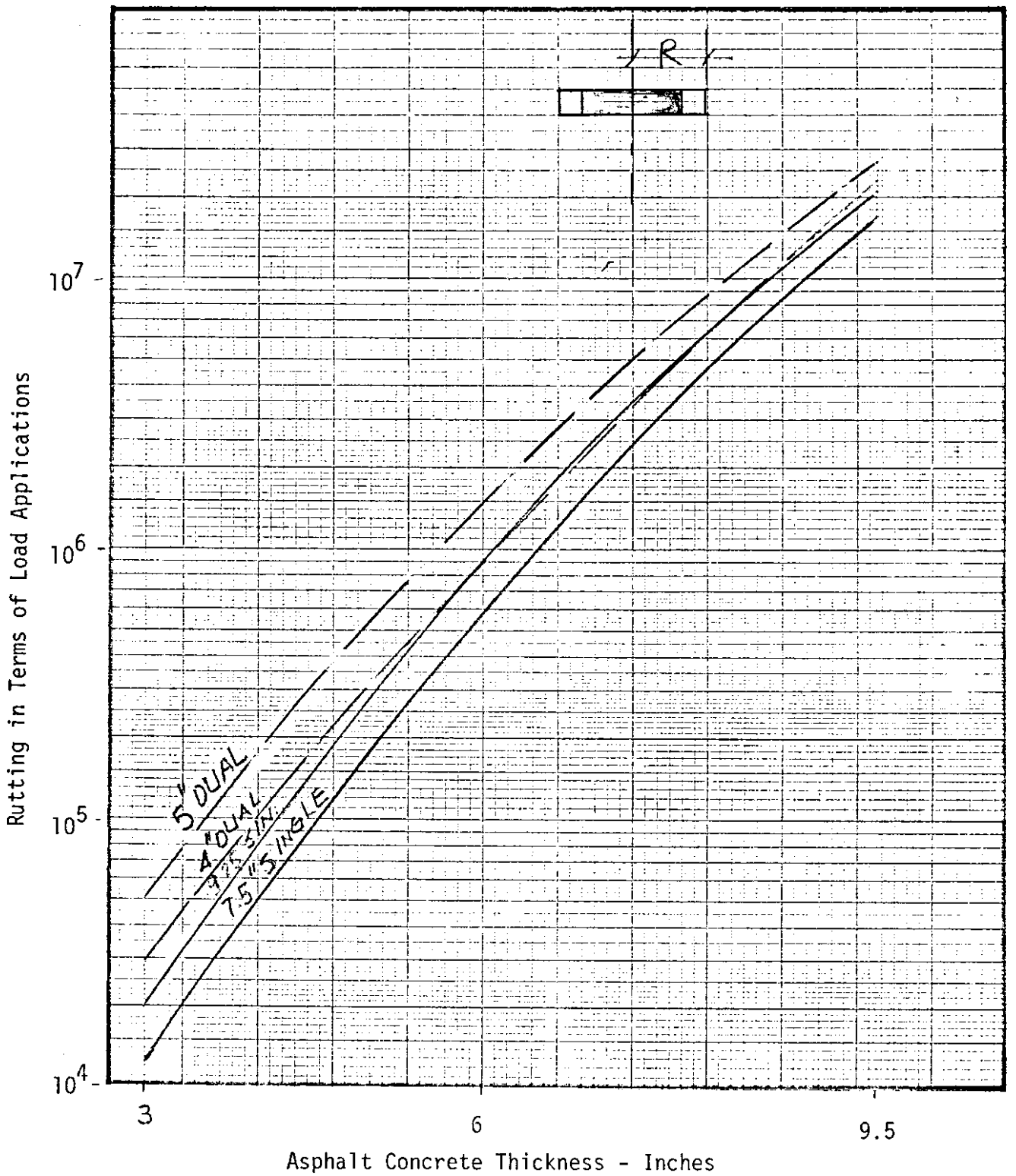

FIGURE D4 - MAXIMUM NUMBER OF 22 KIP AXLE LOAD APPLICATIONS ON SUBGRADE VS. ASPHALT CONCRETE THICKNESS RELATIONSHIPS FOR VARIOUS SIZES, SHOWN IN RADIUS, OF SINGLE AND DUAL TIRES

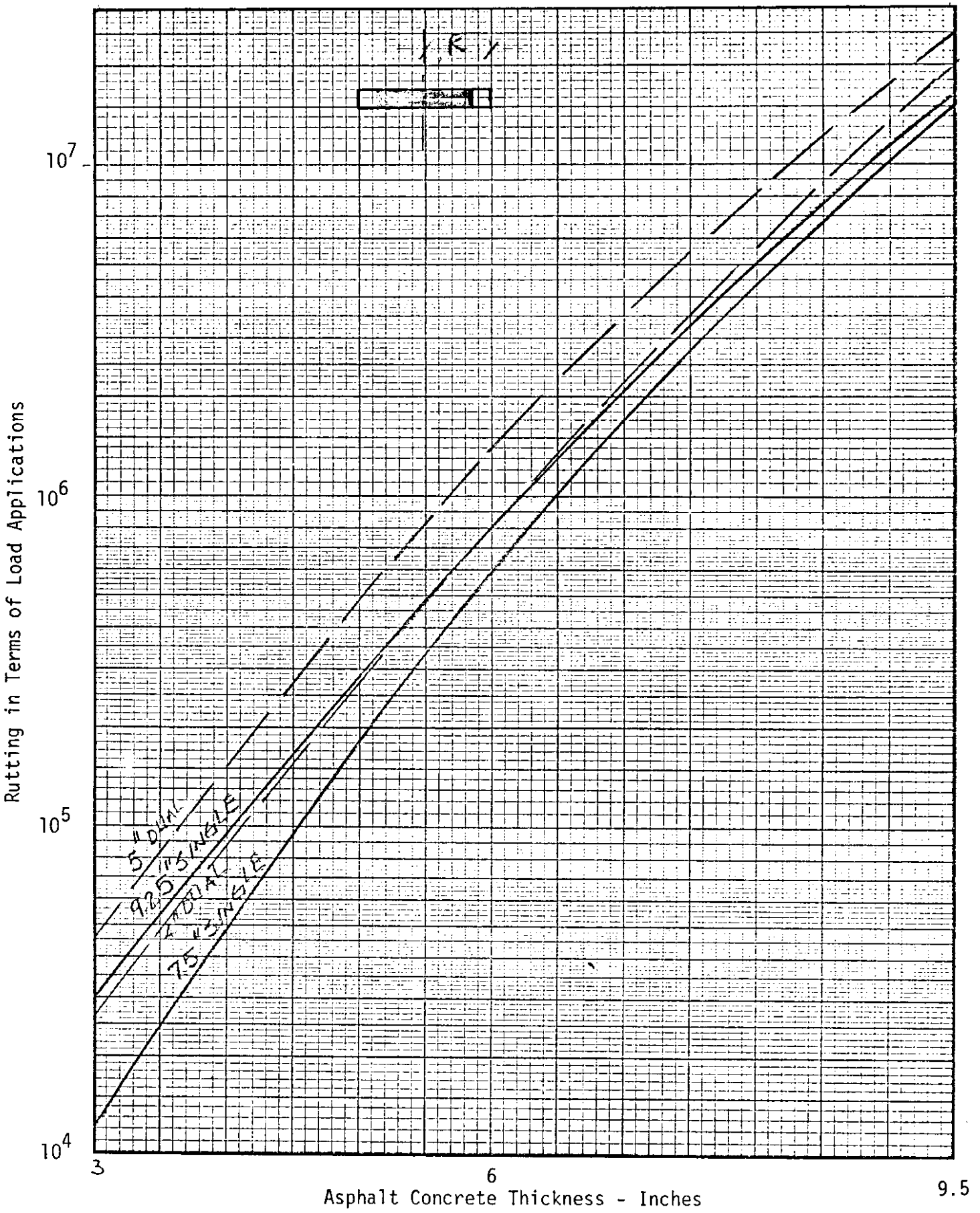

FIGURE D5 - MAXIMUM NUMBER OF 24 KIP AXLE LOAD APPLICATIONS ON SUBGRADE VS. ASPHALT CONCRETE THICKNESS RELATIONSHIPS FOR VARIOUS TIRE SIZES, SHOWN IN RADIUS, OF SINGLE AND DUAL TIRES

APPENDIX E

DEVELOPMENT OF DATA AND COMPUTATIONS FOR EFFECT OF TEMPERATURE CHANGE (CLIMATE) ON EQUIVALENCIES

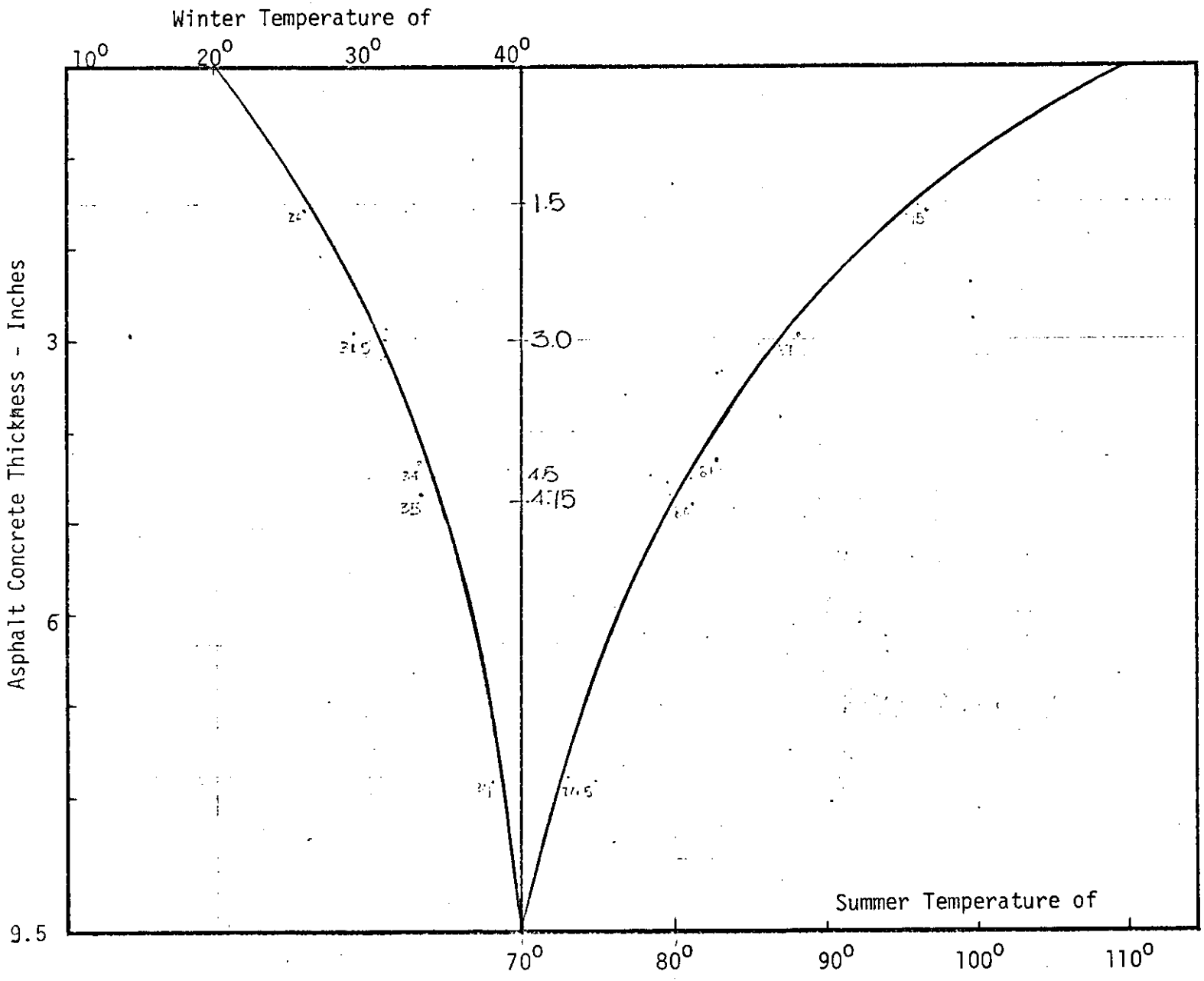

FIGURE E1 - ASSUMED TEMPERATURE PROFILE OF ASPHALT CONCRETE FOR SUMMER AND WINTER

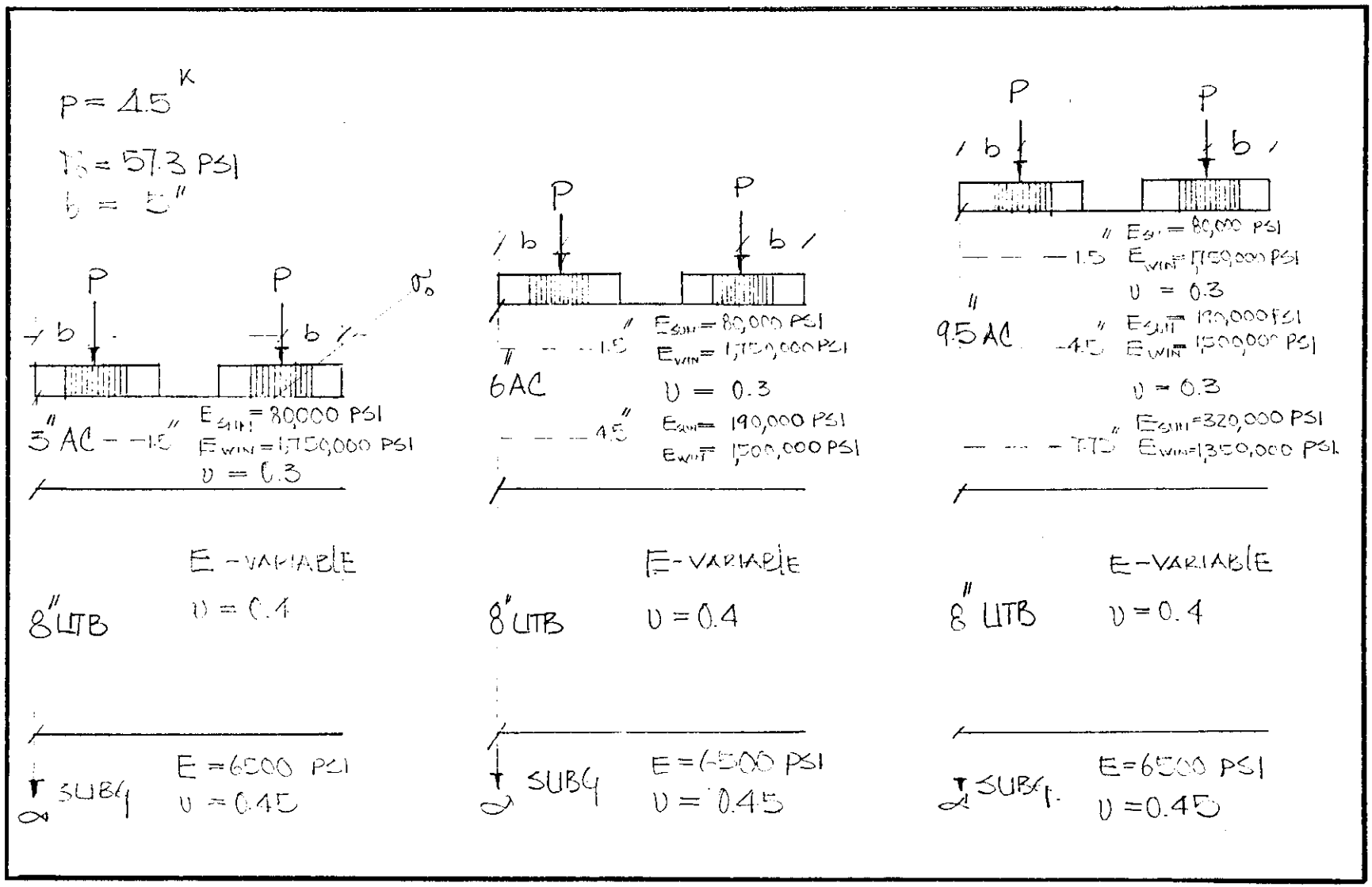

FIGURE E2 - PAVEMENT SECTIONS, AS USED IN COMPUTER ANALYSIS, SHOWN WITH ALL THE INPUT VARIABLES INCLUDING MATERIAL PARAMETERS

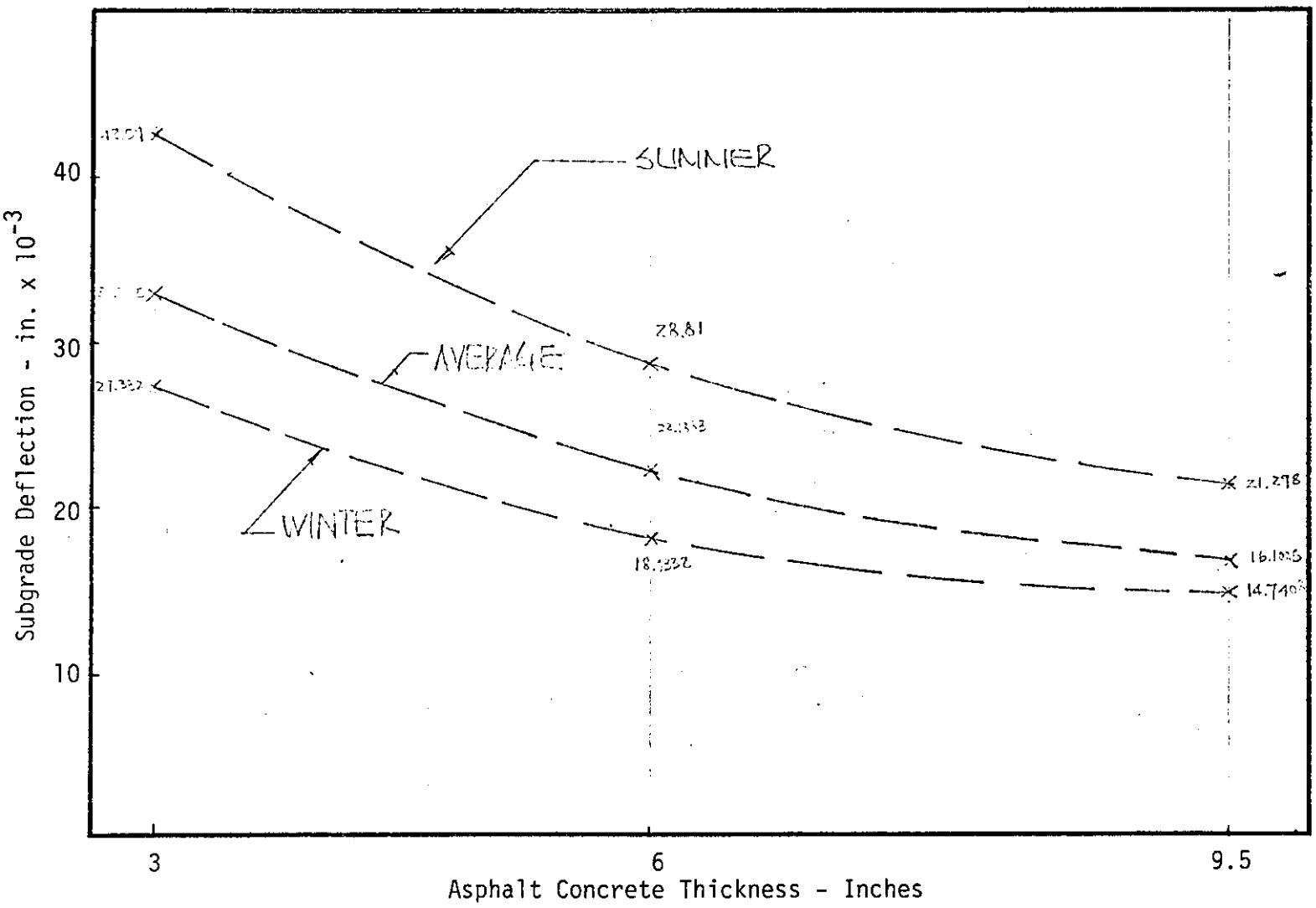

FIGURE E3 - MAXIMUM SUBGRADE DEFLECTION VS. ASPHALT CONCRETE THICKNESS RELATIONSHIPS FOR SUMMER, AVERAGE AND WINTER TEMPERATURES

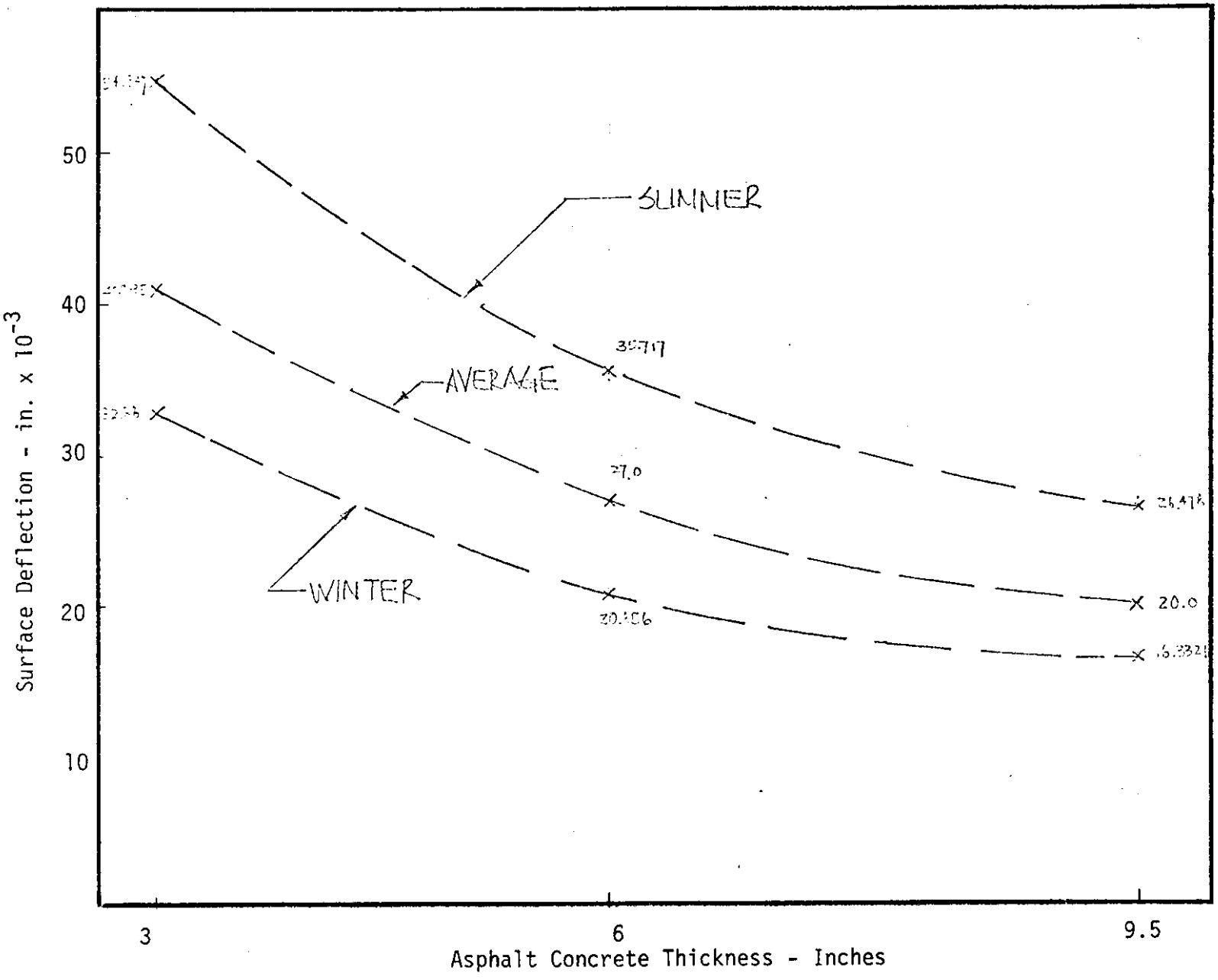

FIGURE E4 - MAXIMUM SURFACE DEFLECTION VS. ASPHALT CONCRETE THICKNESS RELATIONSHIPS FOR SUMMER, AVERAGE AND WINTER TEMPERATURES

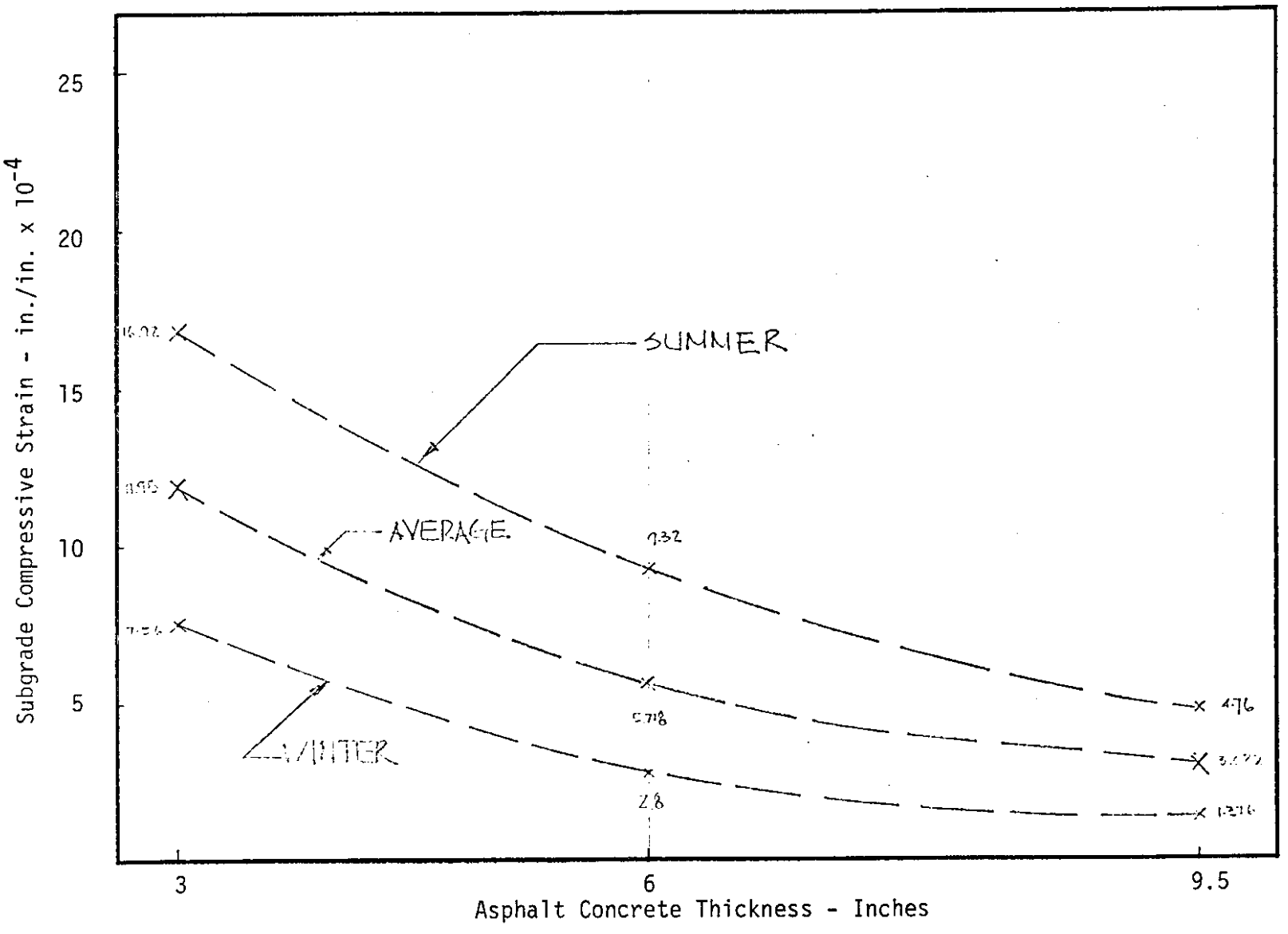

FIGURE E5 - MAXIMUM SUBGRADE COMPRESSIVE STRAIN VS. ASPHALT CONCRETE THICKNESS RELATIONSHIPS FOR SUMMER, AVERAGE AND WINTER TEMPERATURES

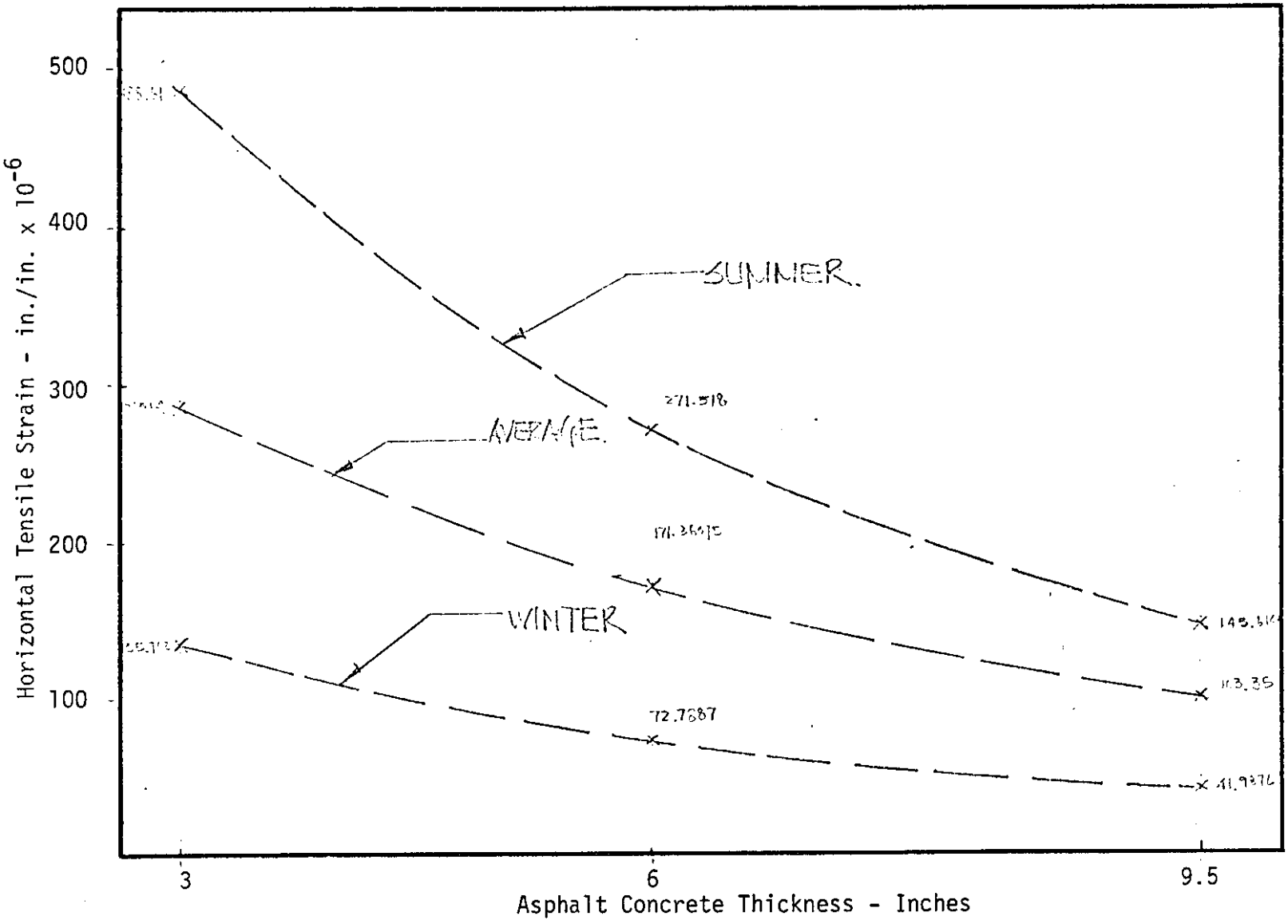

FIGURE E6 - MAXIMUM HORIZONTAL TENSILE STRAIN VS. ASPHALT CONCRETE THICKNESS RELATIONSHIPS FOR SUMMER, AVERAGE AND WINTER TEMPERATURES

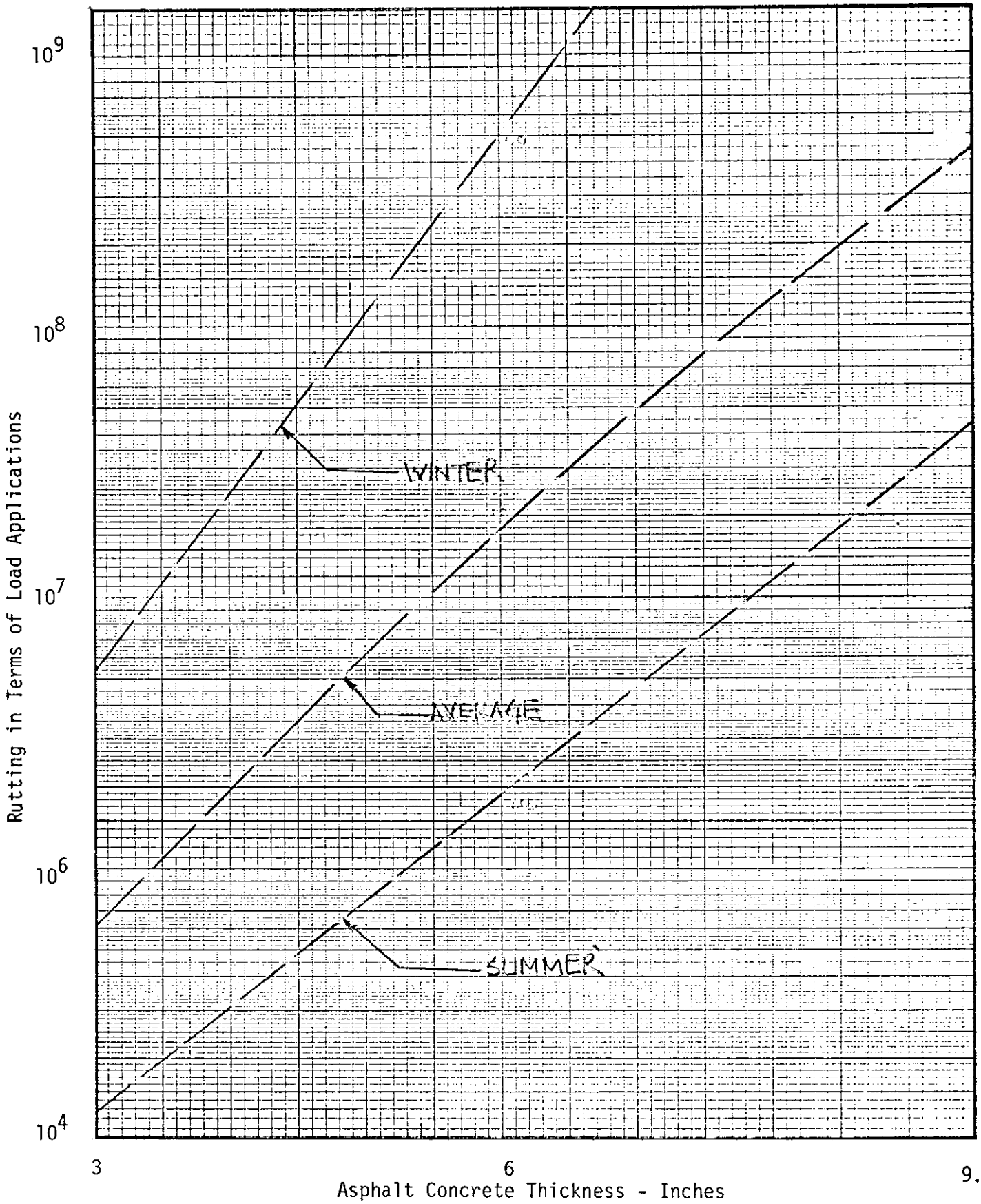

FIGURE E7 - MAXIMUM NUMBER OF 18^K AXLE LOAD APPLICATIONS ON SUBGRADE VS. ASPHALT CONCRETE THICKNESS RELATIONSHIPS FOR SUMMER, AVERAGE AND WINTER TEMPERATURES

APPENDIX F

DEVELOPMENT OF DATA AND COMPUTATIONS FOR EFFECT OF VEHICLE SPEED ON EQUIVALENCIES

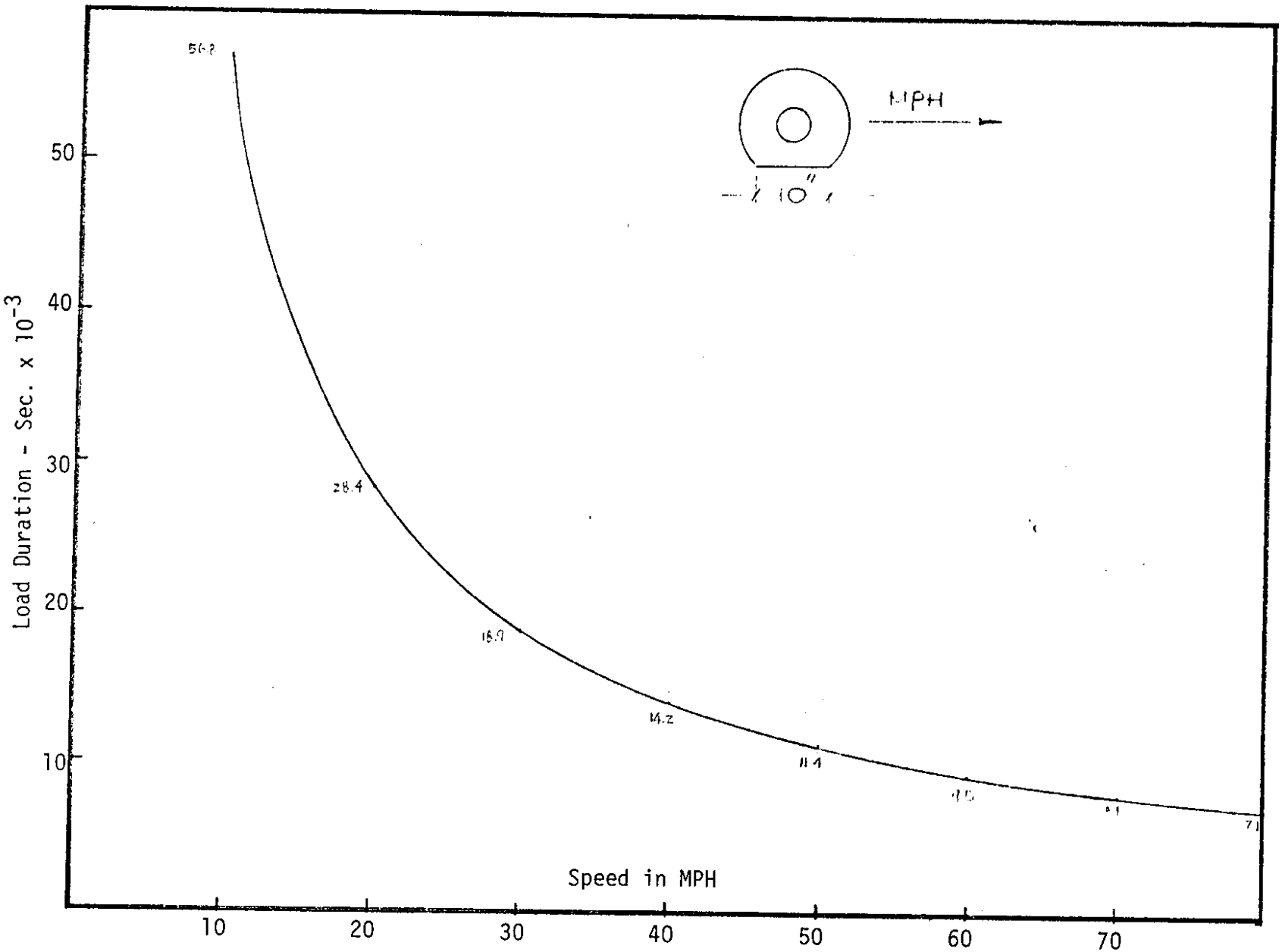

FIGURE F1 - RELATIONSHIPS BETWEEN LOAD DURATION AND SPEED

USED FOR
RISON WITH
MATED D/
FIGURE F

O 25°F (10, 30
△ 45°F (10, 30
□ 70°F (10, 30
* 90°F (10, 20

ON
ENT = 4.5 %

10 100
(sec.)

ration at Different Temperatures

$$\frac{S_{mix}}{S_{asphalt}} = (1 + \frac{2.5}{n} \cdot \frac{C_v}{1-C_v})^n$$

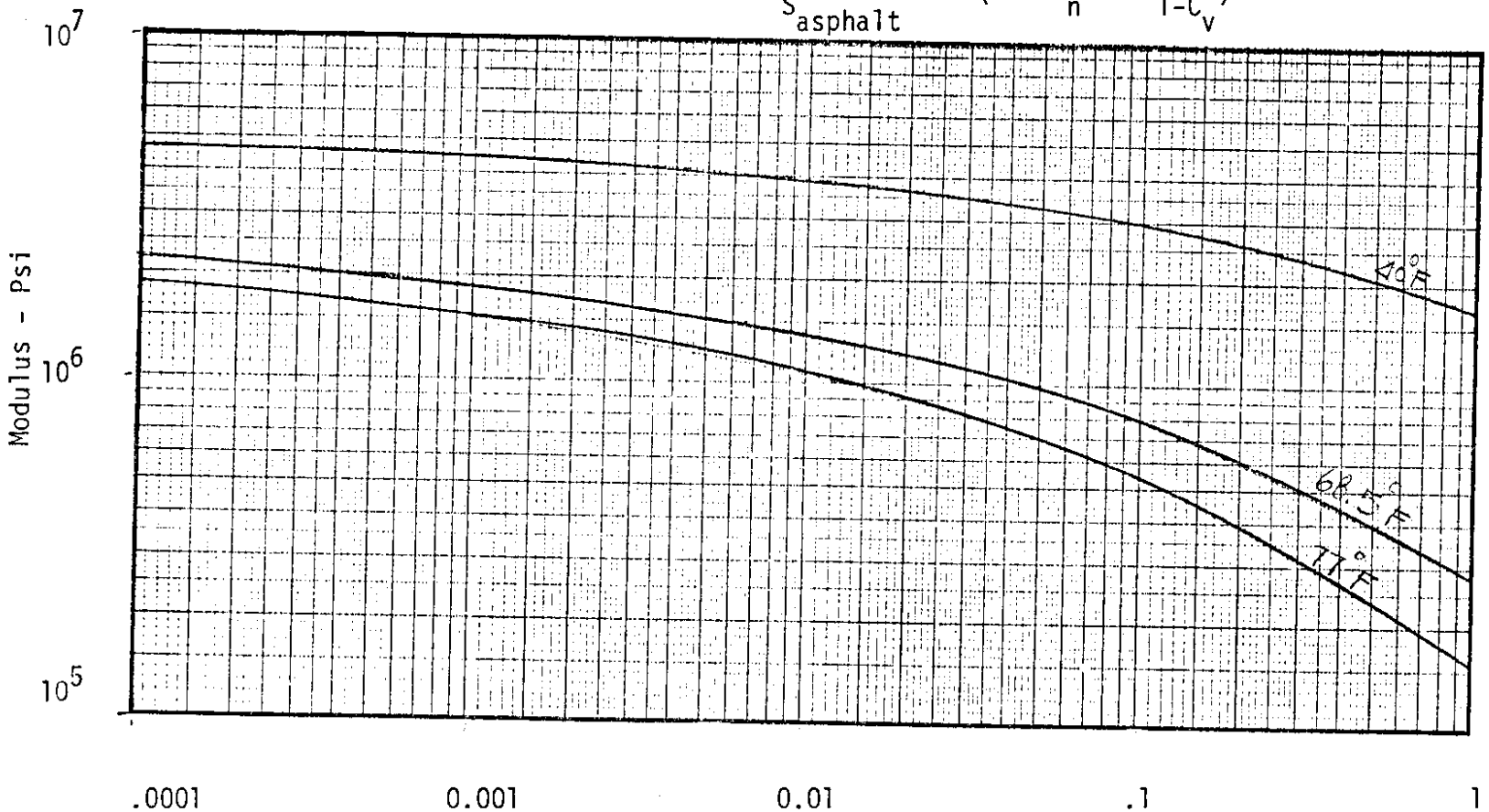

FIGURE F2 - MODULUS VS. LOAD DURATION RELATIONSHIPS FOR VARIOUS TEMPERATURES (23)

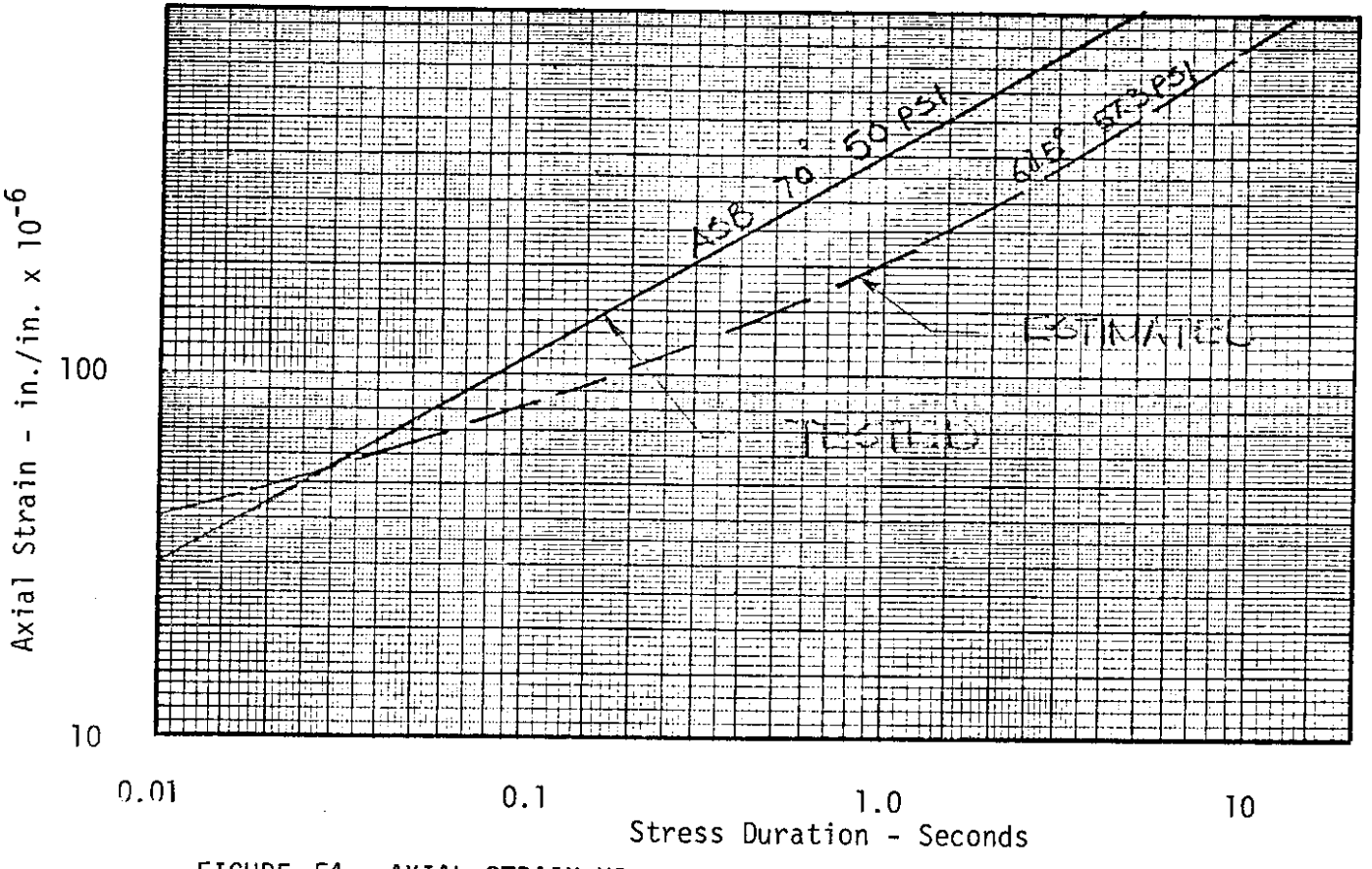

FIGURE F4 - AXIAL STRAIN VS. STRESS DURATION RELATIONSHIPS FOR TESTED AND ESTIMATED VALUES

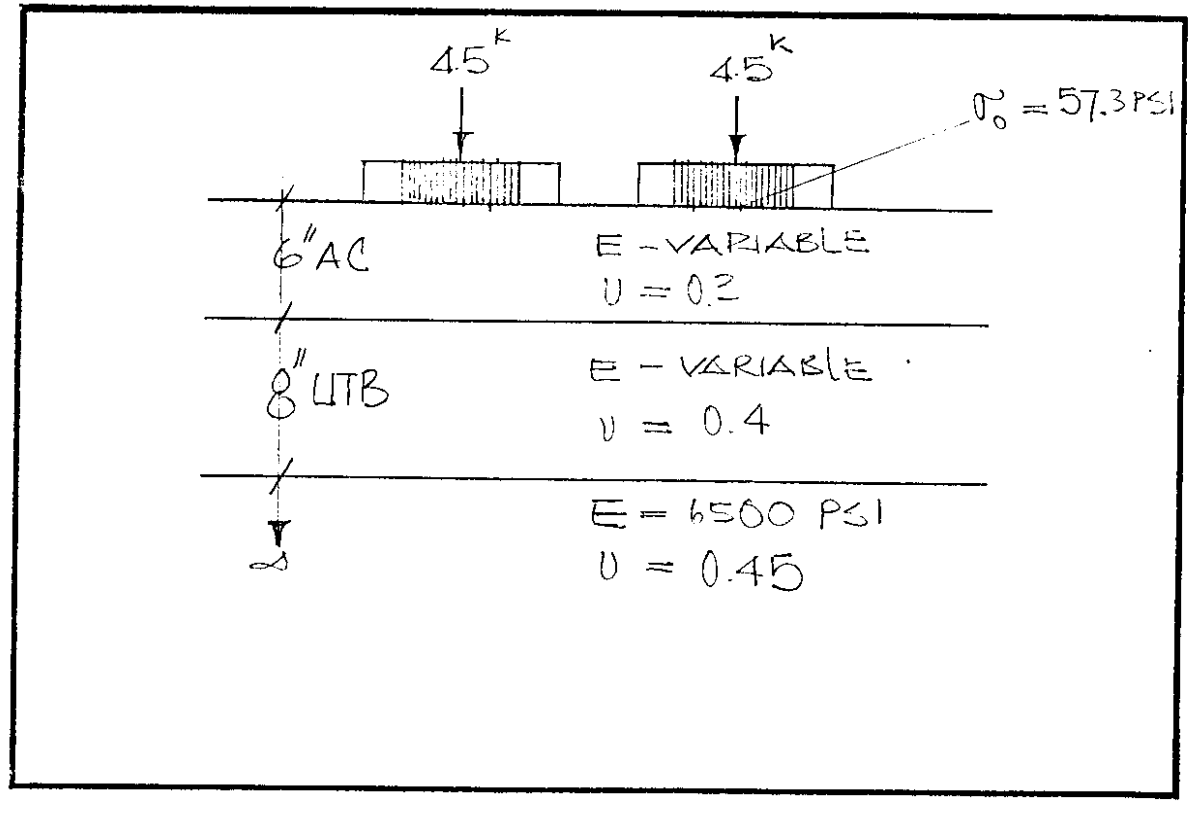

FIGURE F5 - PAVEMENT SECTION, AS USED IN COMPUTER ANALYSIS, SHOWN WITH INPUT VARIABLE INCLUDING MATERIAL PARAMETERS

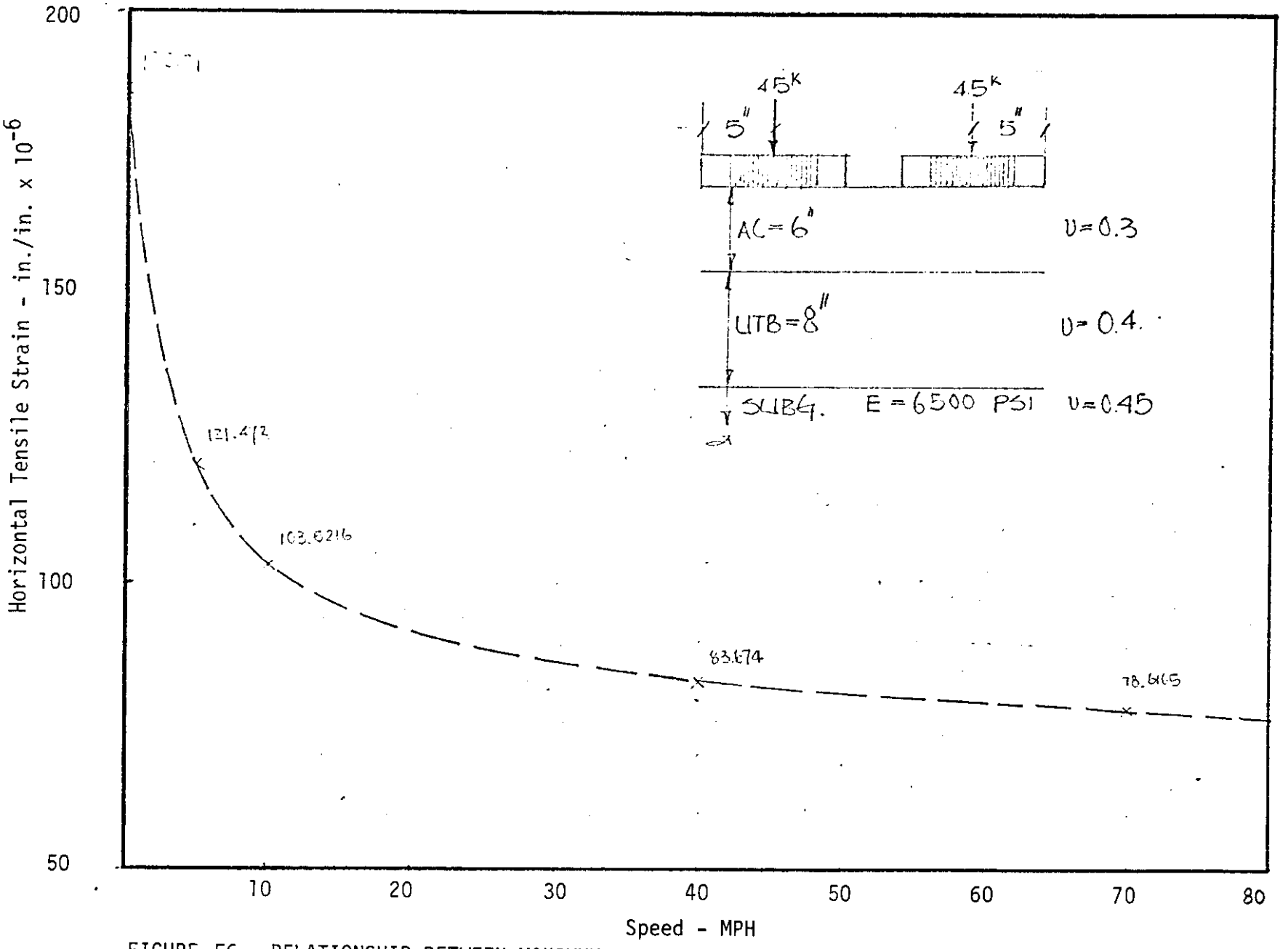

FIGURE F6 - RELATIONSHIP BETWEEN MAXIMUM HORIZONTAL TENSILE STRAIN AT BOTTOM OF ASPHALT CONCRETE LAYER AND VEHICLE SPEED

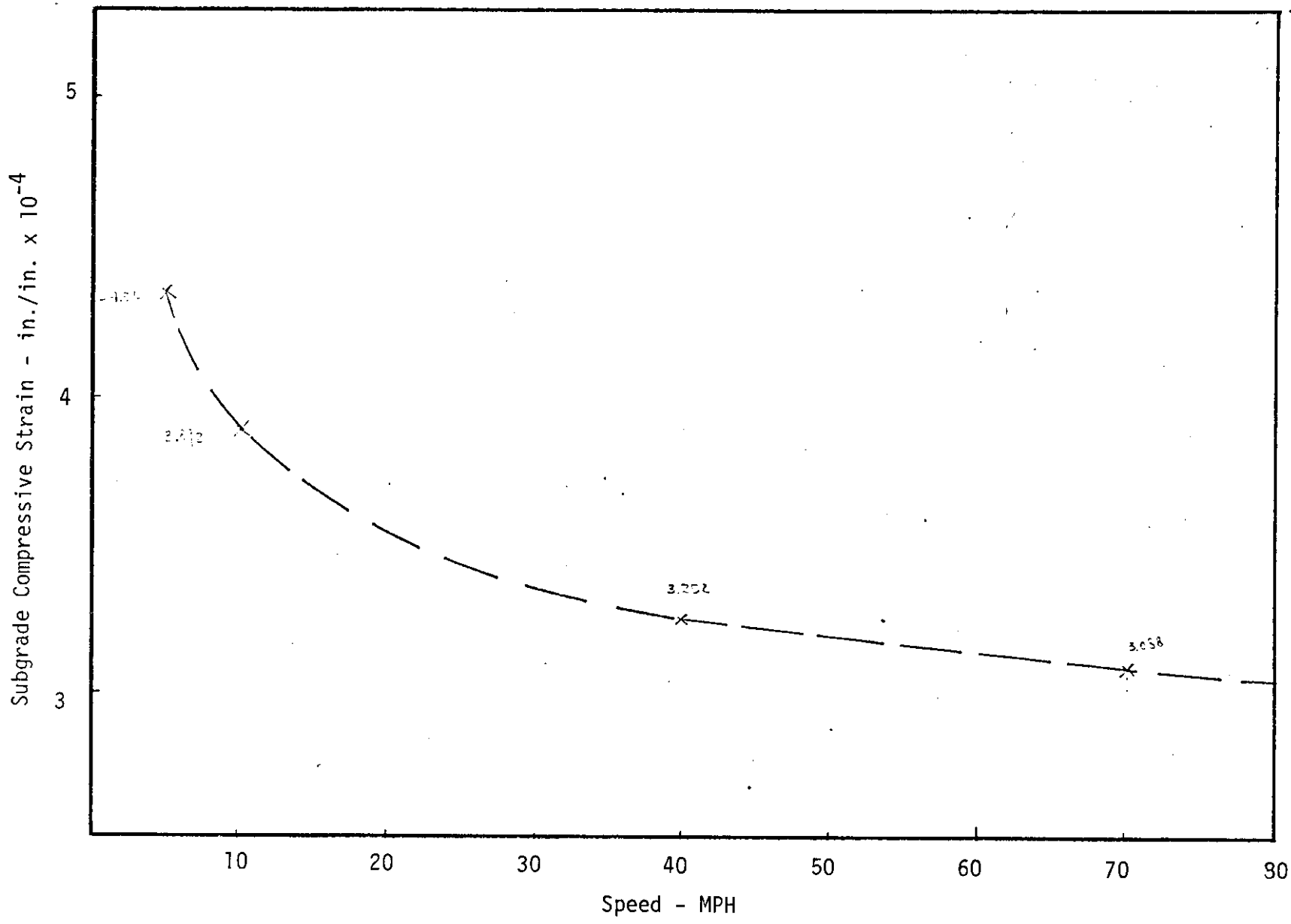

FIGURE F7 - RELATIONSHIP BETWEEN MAXIMUM COMPRESSIVE STRAIN AT TOP OF SUBGRADE AND VEHICLE SPEED

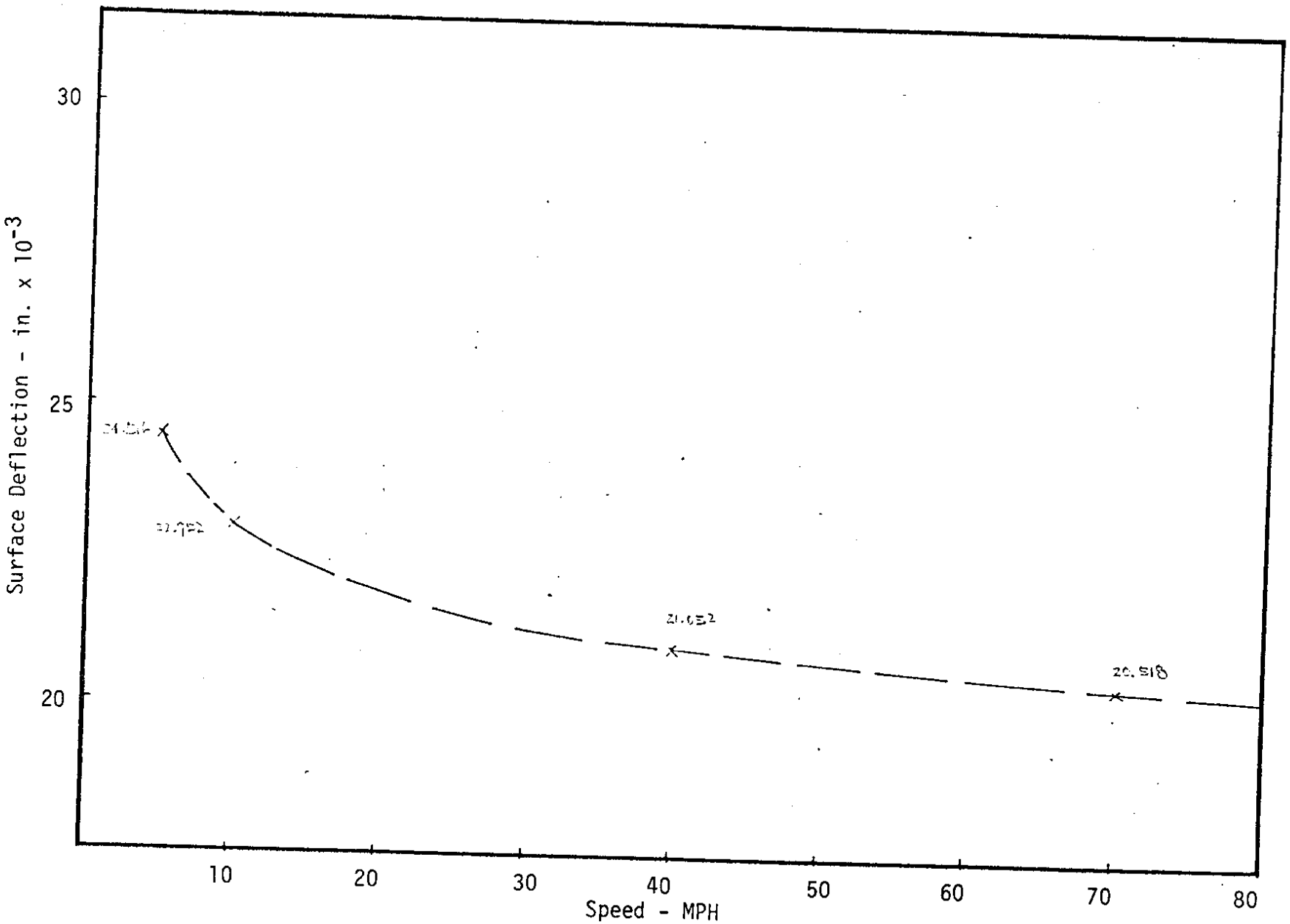

FIGURE F8 - RELATIONSHIP BETWEEN MAXIMUM SURFACE DEFLECTION AND VEHICLE SPEED

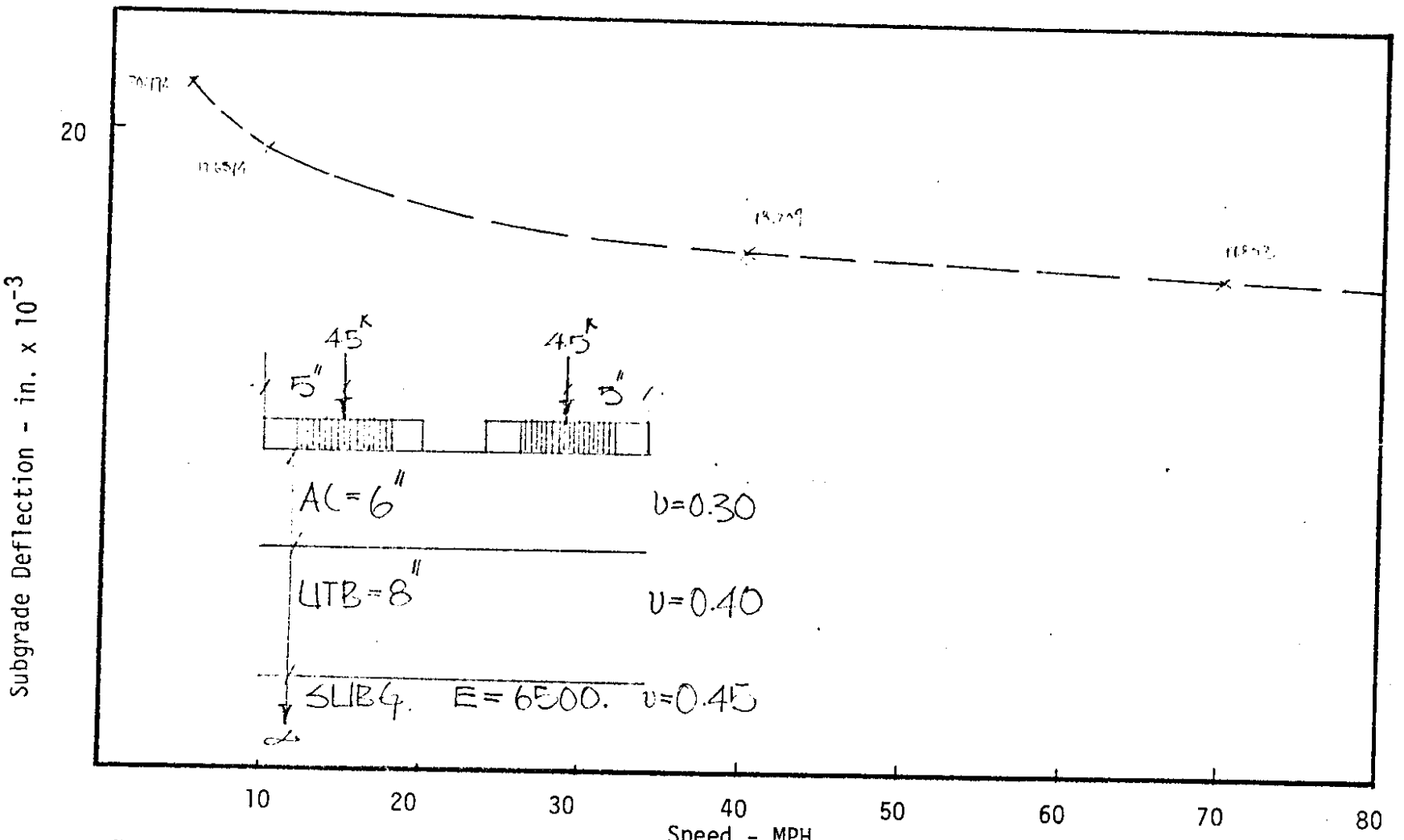

FIGURE F9 - RELATIONSHIP BETWEEN MAXIMUM SUBGRADE DEFLECTION AND VEHICLE SPEED

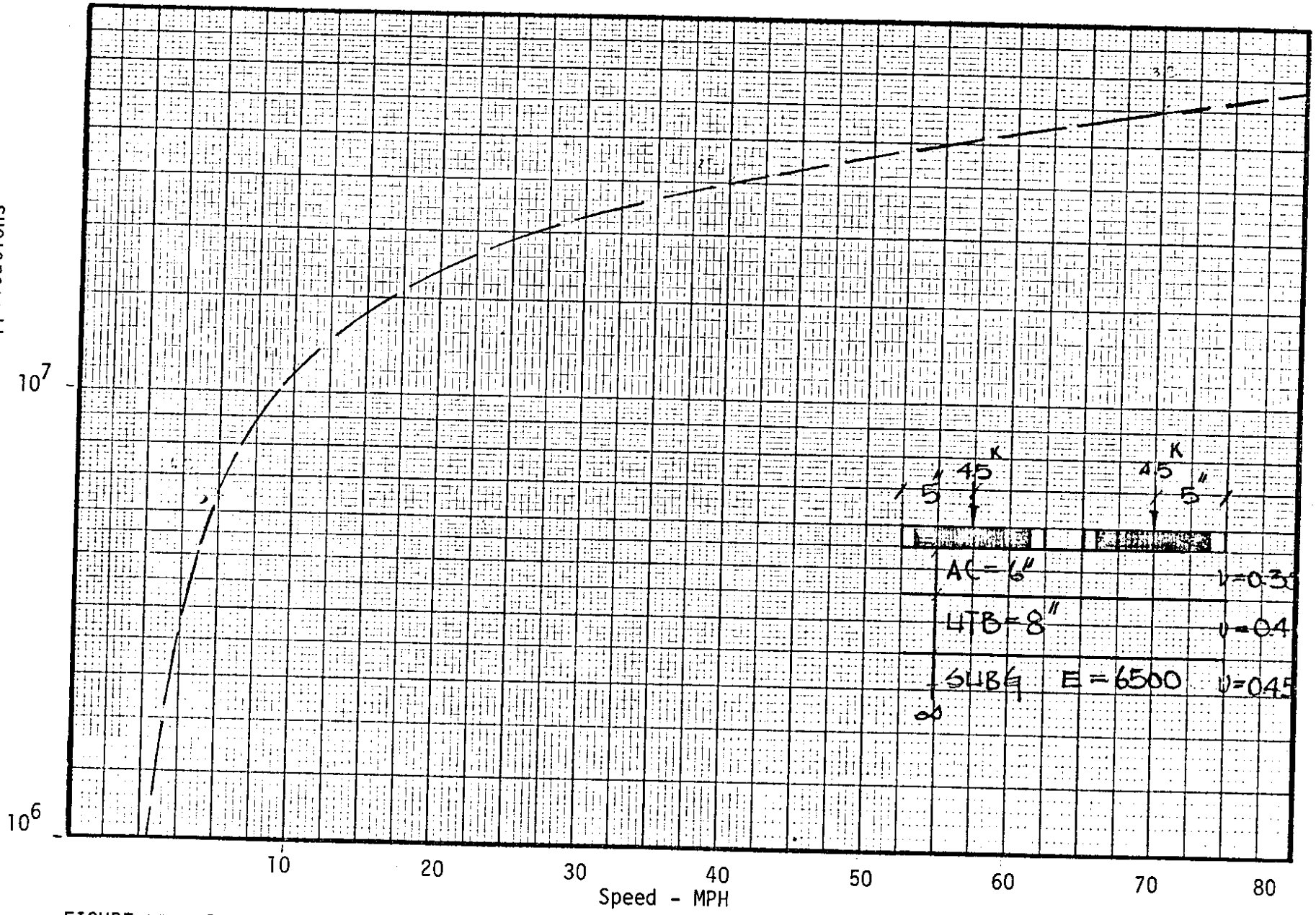

FIGURE F10- RELATIONSHIP BETWEEN MAXIMUM NUMBER OF 18 KIP AXLE LOAD APPLICATIONS ON SUBGRADE AND VEHICLE SPEED